DISSERTATION ZUR ERLANGUNG DES DOKTORGRADES
DER FAKULTÄT FÜR BIOLOGIE
DER LUDWIG-MAXIMILIANS-UNIVERSITÄT MÜNCHEN

Characterization of Dormant and Drug Resistant Stem Cells Using Xenograft Mouse Models of Patient-Derived Acute Leukemia Cells

---

SARAH EBINGER, geborene HUNTENBURG

2017

Completed at the Helmholtz Zentrum München

Date of submission: **26.10.2017**

First Examiner: **Prof. Dr. Dirk Eick**
Second Examiner: **Prof. Dr. Wolfgang Enard**

Date of the oral examination: **07.03.2018**

Eidesstattliche Erklärung

Ich versichere hiermit an Eides statt, dass die vorliegende Dissertation von mir selbstständig und ohne unerlaubte Hilfe angefertigt ist.

Erklärung

Hiermit erkläre ich, dass die Dissertation nicht ganz oder in wesentlichen Teilen einer anderen Prüfungskommission vorgelegt worden ist.
Ich erkläre weiter, dass ich mich anderweitig einer Doktorprüfung ohne Erfolg **nicht** unterzogen habe.

München, 26.10.2017

_____

Sarah Ebinger

Table of contents

List of abbreviations

AL	acute leukemias
ALL	acute lymphoblastic leukemia
AML	acute myeloid leukemia
AMSA	amsacrine
APC	allophycocyanin
Ara-C	cytarabine
BCP-ALL	B-cell precursor acute lymphoblastic leukemia
BrdU	5-Bromo-2'-desoxyuridine
BSA	bovine serum albumin
°C	degree Celsius
CFSE	5-(6)-Carboxyfluorescein-Succinimidyl Ester
CSC	cancer stem cell
CYCLO	cyclophosphamide
DAPI	4',6-diamidino-2-phenylindole
DAU	daunorubicine
DMSO	dimethyl sulfoxide
DNX	DaunoXome
DOX	doxorubicine
EDTA	Ethylenediaminetetraacetic acid
EPI	epirubicin
ETO	etoposide
ETP-ALL	early T-cell precursor acute lymphoblastic leukemia
FACS	fluorescence-activated cell sorting
FCS	fetal calf serum
FSC	forward scatter
g	earth‘s gravitational acceleration
h	hour
HSC	hematopoietic stem cell
i.p.	intraperitoneal
i.v.	intravenously
LDTA	limiting dilution transplantation assay
LIC	leukemia initiating cells

LRC	label retaining cells
LSC	leukemia stem cells
MACS	magnetic cell separation
MFI	mean fluorescence intensity
ml	milliliter
min	minutes
MITO	mitoxantrone
MRD	minimal residual disease
NOD	non-obese diabetic
non-LRC	non label retaining cells
NSG	non-obese diabetic/severe combined immunodeficiency/gamma chain depleted (NOD.Cg-Prkdc^{scid} IL2rg^{tm1Wjl}/SzJ)
PBS	phosphate buffered saline
PCA	principal component analysis
PDX	patient-derived xenograft
PE	phycoerythrin
PI	propidium iodide
RT	room temperature
SCID	severe combined immunodeficiency
SD	standard deviation
SSC	side scatter
TIC	tumor inducing cell
V	volume per volume
VCR	vincristine
v/v	volume percentage
µ	mikro (10^{-6})

List of figures

List of tables

1 Abstract

Acute leukemias (AL) are hematological malignancies with poor outcomes, and disease relapse represents a major challenge. Treatment resistant cells might persist for prolonged periods of time, might start proliferation and give rise to relapse. Novel treatment options are urgently needed to eradicate resistant cells and to prevent relapse in order to improve the prognosis and cure rate of AL patients. The aim of the present work was to identify and characterize the subpopulation of relapse-inducing cells in AL.

Towards this aim, a unique method was used which had been established shortly before in the hosting lab. Here, primary AL cells from patients are propagated in immunodeficient mice as patient-derived xenografts (PDX) cells. Using genetic engineering of PDX cells and a two-step enrichment protocol targeting the transgenes, minor numbers of PDX cells can be isolated from mouse bone marrow to near purity in an unbiased way. Using the proliferation-sensitive dye 5-(6)-Carboxyfluorescein-Succinimidyl Ester (CFSE) in mice, first hints had been generated that cells might exist in acute lymphoblastic leukemia (ALL) which reveal long term dormancy.

In this work, the present method was optimized and transferred to acute myeloid leukemia (AML). The study showed that 8 out of 8 tested ALL PDX samples and 8 out of 9 AML samples contained a rare subpopulation of long-term dormant cells indicating that long-term dormancy represents a frequent feature in PDX AL. Upon systemic treatment of mice with chemotherapeutic drugs, proliferating cells showed marked sensitivity, while long-term dormant cells remained resistant. Long-term dormant cells contained cancer stem cells as they were able to initiate leukemia in next recipient mice.

Thus, most patients' AL contains a rare subpopulation of dormant, treatment resistant cells with leukemia initiating properties which might represent a surrogate for relapse-inducing cells. Re-transplantation experiments indicated that dormant cells started proliferating in next recipient mice, while proliferating cells converted into long-term dormant cells indicating a major functional cell plasticity.

In conclusion, a rare cell population was identified that might serve as suitable surrogate to develop novel therapies against relapse in AL, targeting the challenging subpopulation of dormant, drug resistant, leukemia initiating cells. The transient nature of dormancy suggests that AL patients might profit from treatment strategies which release dormant, treatment resistant cells from their microenvironment in order to sensitize them towards treatment.

2 Introduction

2.1 Acute Leukemias (AL)

Acute leukemias (AL) belong to the ten most common cancers in the United States and Europe (Ferlay et al., 2013; Siegel et al., 2016). AL are hematologic malignancies with a rapid increase of immature blood cells. The accumulation of malignant, non-functional cells leads to an interference with healthy blood cells, and finally to bone marrow failure. Depending on the surface markers expressed on the tumor cells, AL is distinguished into two subtypes: acute myeloid leukemia (AML) and acute lymphoblastic leukemia (ALL) (Esparza and Sakamoto, 2005; Estey, 2014).

2.1.1 Acute myeloid leukemia (AML)

AML is the most common leukemia in adults. In the US there are around 20,000 new patients per year and around 10,000 patients die from AML each year (Siegel et al., 2016). The incidence rises with an increase in age; patients older than 65 years are over 10 times more frequently effected than patients younger than 65. The median age of patients diagnosed with AML is around 70 years (De Kouchkovsky and Abdul-Hay, 2016; Estey and Dohner, 2006). Environmental influences like ionizing radiation are known to have an influence on the development of AML. 10-15 % of AML patients underwent a previous cytotoxic chemotherapy, and cigarette smokers develop 1.2-2.3 times more often AML than non-smokers due to benzene exposure (Estey and Dohner, 2006). AML is a heterogeneous disease with many different subtypes due to different genetic mutations, epigenetic aberrations, and downstream abnormalities. More than 97 % of AML tumors reveal known genetic mutations. In addition, around 55 % of AML cases show cytogenetic abnormalities, like translocations, inversions, and chromosomal imbalances, or even complex karyotypes (Estey and Dohner, 2006).

The ancient French-American-British (FAB) classification system from 1976 uses cytomorphological and cytochemical characteristics of the myeloid blasts to group AML into eight AML subtypes. The World Health Organization released 2001 a new classification, which was revised 2008 and 2016 to incorporate genetic information, morphology, immunophenotype, and clinical presentation. Here, six AML subtypes are distinguished (De Kouchkovsky and Abdul-Hay, 2016; Estey and Dohner, 2006). The European Leukemia NET (ELN) classification incorporates cytogenetics and molecular genetic data, especially mutations in the NPM1, FLT3, and CEBPA genes, to define four risk groups. According to their

prognosis, the different groups are called favorable, intermediate-1, intermediate-2, and adverse which have in total 13 subsets (Estey, 2014; Roboz, 2012).

AML is diagnosed cytomorphologically by malignant blasts in bone marrow or peripheral blood of patients, and by positive testing of these cells for a myeloid origin by myeloperoxidase activity, or the presence of Auer rods (De Kouchkovsky and Abdul-Hay, 2016). Furthermore, myeloid blasts are identified immunophenotypically by the expression of typical myeloid surface markers, like CD33 and CD13 (Estey and Dohner, 2006; Estey, 2014). The accumulation of these malignant, undifferentiated myeloid blasts in the bone marrow leads to an interference with the normal hematological cells and eventually to bone marrow failure. In addition, myeloid blast can escape into the blood stream and spread to other organs of the body. Untreated, this cell accumulation leads to death within months (De Kouchkovsky and Abdul-Hay, 2016; Estey and Dohner, 2006). All patients are immediately treated by standard therapy, often even before the risk group is determined, which has the best outcomes for patients with a favorable or intermediate prognosis and a low risk of treatment-related mortality. The standard regimen includes two phases. The first phase, induction therapy, aims to achieve complete remission, which is defined by less than 5 % blasts in the bone marrow. Here, an anthracycline, like idarubicin or daunorubicin is given for three days, and in parallel a continuous administration of cytarabine is given for seven days. This so-called 3+7 scheme is repeated one to four times until complete remission is reached (De Kouchkovsky and Abdul-Hay, 2016; Estey and Dohner, 2006). After induction therapy stops, many patients develop relapse (Thol et al., 2015). In order to prevent relapse, the second phase, the consolidation therapy, starts to achieve lasting remission. If patients seem to not tolerate the intensive chemotherapy or chemotherapy alone is not effective, another possibility is allogeneic stem cell transplantation. Furthermore, for patients with a poor prognosis or a high risk of treatment-related mortality, investigational therapy, as part of a clinical trial, is an option (De Kouchkovsky and Abdul-Hay, 2016; Estey and Dohner, 2006).

Despite optimized chemotherapy and supportive care, the outcome for patients with AML is still poor. The long-term overall survival of younger patients is around 40-50 %. For patients older than 65, many of which also show a poor performance status, the prognosis is even worse, 70 % will die within one year (Estey, 2014; Roboz, 2012).

Besides age and performance status, the most relevant prognostic factor for chemotherapy response and outcome are the cytogenetic and molecular findings at diagnosis. Additionally, patients who suffer from a therapy-related AML or from AML after myelodysplastic syndrome are more resistant to chemotherapy and have a worse outcome. Therapeutic failure occurs due

to treatment resistance or due to treatment-related mortality. Treatment resistance is defined if complete remission cannot be achieved or maintained or if a relapse cannot be prevented or treated. Treatment-related mortality counts for patients who died from the adverse-effects of treatment (Estey, 2014). Prognostic markers for treatment-related mortality in patients are age and performance status at diagnosis, as well as platelet count, serum albumin, bilirubin and creatinine (De Kouchkovsky and Abdul-Hay, 2016; Estey and Dohner, 2006).

In summary, AML is associated with an overall poor prognosis, especially for elderly patients, certain adverse subgroups and upon relapse. Genome sequencing data revealed AML as a very heterogeneous disease regarding mutations and cytogenetic abnormalities, which are a reason for diverse treatment outcomes. As the main treatment still consists of cytotoxic chemotherapy, an urgent need for new treatment strategies, like targeted therapies, exists (Estey and Dohner, 2006). For the understanding of this complex biology, preclinical models are needed to finally develop new therapy strategies for a better prognosis of AML patients and to prevent AML relapse (Guzman and Allan, 2014).

2.1.2 Acute lymphoblastic leukemia (ALL)

ALL is the most common type of cancer in children. In the US are around 6,500 new cases per year (Siegel et al., 2016), hereof 60 % are persons younger than 20 years (Dores et al., 2012). The peak of incidence lies between the age of two and five (Hunger and Mullighan, 2015; Pui et al., 2008). However, also adults can develop the disease, but the incidence in adults is very low (Inaba et al., 2013; Pui et al., 2008).

Some genetic factors, like Down's syndrome, Blooms syndrome, ataxia-telangiectasia and Nijmegen breakage syndrome, are known to be associated with and leading to an increased risk of ALL (Hunger and Mullighan, 2015; Pui et al., 2008). In addition, some genetic alterations are associated with an increased risk for ALL or with a specific subtype of ALL. These include polymorphic variants in genes like *ARID5B*, *CDKN2A*, *CEBPE*, *GATA3* and *IKZF1*. Environmental exposures like radiation, some chemicals, and exposure to electromagnetic fields only have little influence on the development of ALL (Hunger and Mullighan, 2015; Inaba et al., 2013). In most patients, the first oncogenic mutation appears *in utero* and before birth (Schiffman, 2016).

The ancient French-American-British (FAB) classification divided ALL into three different subgroups by their morphological characterization. In 1997, and revised in 2008, the World Health organization combined morphological and cytogenetic criteria to divide ALL into three subtypes. The three main subtypes are mature B-cell, B-cell precursor (BCP-ALL) and T-cell

leukemia and have therapeutic implications. These subtypes can be further classified according to their specific genetic alterations (Pui et al., 2008; Terwilliger and Abdul-Hay, 2017). Besides karyotypic abnormalities, like aneuploidy or translocations, nowadays genome-wide analysis allows the genetic classification of all cases by the identification of genetic alterations, but is not yet used in clinical routine. Genes altered in ALL are often associated with hematopoietic differentiation, signaling or proliferation, and epigenetic regulation (Pui et al., 2012; Pui and Evans, 2013). A recently identified high risk immature subtype is early T-cell precursor (ETP) ALL, which is defined by specific immunological markers, characteristic gene expression profile, a mutational spectrum related to AML mutations, and transcriptional profile close to hematopoietic stem cells and granulocyte-macrophage precursors. These are hints for a stem cell disease of this subtype (Zhang et al., 2012).

ALL is diagnosed by morphological and immunophenotyping examinations of peripheral blood or bone marrow aspirates (Inaba et al., 2013; Pui et al., 2008). The further discrimination between T-cell, mature B-cell, BCP ALL, and ETP-ALL is subsequently important for therapeutic procedures (Pui et al., 2008). To identify chromosomal abnormalities like hyper- and hypodiploidies and leukemia-specific gene rearrangements, translocation-specific RT-PCR and fluorescence in-situ hybridization are used. Flow cytometry is performed to identify the cell linage and CRLF2 overexpression. Genome-wide analyses are not used in clinical routine yet, but have prognostic and therapeutic implications, too. As a consequence of these diagnostic measures combined with clinical data, children are stratified in several risk groups which receive different intensity of treatment. Tumor-specific molecular markers are further used to quantify tumor load repetitively in each patient in order to evaluate treatment effects and to recognize any putative tumor re-growth early (Inaba et al., 2013; Pui et al., 2008). Without treatment patients die of the disease. The malignant and undifferentiated lymphoid cells accumulate in the bone marrow, lead to interference with healthy hematopoietic cells and eventually to bone marrow failure. Malignant cells can invade into the blood stream and affect other organs of the body (Terwilliger and Abdul-Hay, 2017).

Treatment of all subtypes is divided into three phases: remission-induction therapy, consolidation therapy and maintenance therapy. Induction therapy, lasting for four to six weeks, includes a glucocorticoid, vincristine, and asparaginase or anthracycline. Standard risk children receive a combination of three chemotherapeutics, whereas high risk, very high risk, and adult patients receive a combination of four or more different chemotherapeutics. Patients with *BCR-ABL1* translocation benefit from tyrosine-kinase inhibitors, like Imatinib (Inaba et al., 2013; Pui et al., 2008).

Morphologic remission is defined by less than 1 % blasts in bone marrow; morphological remission is obtained in 96-99 % of children and in 78-92 % of adult patients (Inaba et al., 2013; Pui and Evans, 2006; Pui et al., 2008).

The consequent 20-30 weeks of consolidation therapy are used to target residual leukemic cells. Here, high-doses of methotrexate with mercaptopurine, frequent applications of vincristine and corticosteroid and repetitive applications of asparaginase, as well as drugs from induction therapy are used (Inaba et al., 2013; Pui et al., 2008).

The treatment phase of maintenance therapy lasts for around two years. This therapy phase shall prevent relapse and increase event-free and overall survival in patients. Here, daily mercaptopurine and weekly methotrexate is given with or without applications of vincristine and dexamethasone (Inaba et al., 2013; Pui et al., 2008).

For patients who did not response to initial treatment or have a high-risk ALL, like BCR/ABL-positive ALL, allogeneic hematopoietic stem cell transplantation or investigational therapy, as part of a clinical trial, are options (Inaba et al., 2013; Pui et al., 2008).

During the last decades, treatment optimization, increase in supportive care and risk assessment to use the best treatment strategy have been resulted in improvements, especially for children, from a former deadly disease in the 1950s to 5-year survival rates above 90 % (Inaba et al., 2013; Siegel et al., 2016). But survival rates for adults and infants remains little satisfactory with around 40 % survival rates for young adults and less than 10 % for adults older than 60 years (Dördelmann et al., 1999; Goldstone et al., 2008). The survival rates of BCR/ABL-positive ALL have improved through new treatment strategies including tyrosine kinase inhibitors from initial 10 % to around 40-60 % (Leoni and Biondi, 2015). Most ALL patients die from relapse and relapse occurs in 15-20 % of children and in 40-50 % of adult patients. The prognosis of relapsed patients is poor; in adults only less than 10 %, and in children 40-50 % can be cured, due to increased treatment resistance of relapsed ALL (Gokbuget et al., 2012a; Locatelli et al., 2013).

There are several factors besides the subtype and molecular alterations that are of prognostic relevance in ALL:

One is the age at diagnosis of the initial. Children between the age of 1 and 9 have better outcome than infants, adolescents, or adults (Hilden et al., 2006). Younger adults have a better prognosis than older ones.

Another prognostic factor is the race, with black and Hispanic patients have worse outcome compared to white people treated exactly the same (Inaba et al., 2013; Pui et al., 2008).

Furthermore, an increase in leucocyte count above $50x10^9$/L is associated with poorer outcome (Inaba et al., 2013; Pui et al., 2008).

The most important prognostic factor for children and adults and even for patients with low-risk disease at initial diagnosis is the determination of the minimal residual disease (MRD) levels during the induction therapy (Inaba et al., 2013). To determine and quantify these drug resistant MRD cells, morphological methods are recently replaced by the more sensitive methods of flow-cytometry and PCR amplifications. The advantage of PCR is the high sensitivity; here MRD levels around 0.001 % can be measured. With flow-cytometry MRD levels around 0.01 % can be determined, but this method is fast, less expensive and is applicable to a broad range of patients, allowing a fast treatment adjustment (Inaba et al., 2013).

Measurement of MRD levels three months after diagnosis is associated with following risk groups for outcome: No detectable MRD level is associated with low risk, MRD levels between 10^{-4} and $5x10^{-4}$ are associated with medium risk, and MRD levels above $5x10^{-4}$ are associated with high risk (van Dongen et al., 2015).

Taken together, although most ALL patients have a good prognosis, as survival rates are high, the prognosis for infants and adults is still poor due to frequent ALL relapse. Therefore, new treatment options are needed which target residual, treatment resistant cells and prevent ALL relapse.

2.2 Biology of AL cells

In order to prevent AL relapse by new treatment strategies, a deep knowledge of the biology of AL cells is necessary. The following chapter will give an overview about the most important adverse characteristics of AL cells, which make it difficult to treat and cure patients with AL and to prevent disease relapse.

2.2.1 Drug resistance

Drug resistant cells represent an important reason for treatment failure in AL. These cells are a major threat for ALL and AML patients as they survive initial chemotherapy, might persist in the patient at MRD levels, and are able to induce a tumor relapse with poor prognosis (Blatter and Rottenberg, 2015; Gokbuget et al., 2012b; Pettit et al., 2016). For example in childhood ALL resistance towards glucocorticoids is a major problem. ALL patients which are not responding toward glucocorticoid chemotherapy have in general a worse prognosis than patients with a response. The underlying mechanisms for resistance remain at least on part

elusive (Inaba and Pui, 2010). In general, despite their major clinical importance, the mechanisms leading to drug resistance and the basic biologic conditions of relapse are still poorly understood. For instance it is not known whether relapse-inducing cells exist before treatment or whether they develop due to treatment and it is unclear if constant or transient features determine relapse-inducing cells (Kunz et al., 2015). In addition, gained genetic alterations might increase the drug resistance of rare subclones. And even chemotherapy itself might pressure and select for the most aggressive and drug resistant cell clones. Besides drug resistant cells might be induced by a protective surrounding microenvironment, so that chemotherapeutics cannot reach these cells, or the microenvironmental conditions exert an impaired effect on these agents (Ishikawa et al., 2007).

Furthermore, drug resistance is closely associated with dormancy of cancer cells as conventional chemotherapy mainly interferes with cell cycle dependent processes which are not active in dormant cells (Clevers, 2011; Zhou et al., 2009).

Taken together the eradication of drug resistant cells is a major goal for new treatment strategies, as tumor relapse caused by drug resistant cells is associated with dismal prognosis.

2.2.2 Dormancy

In many tumors entities, relapse occurs after initial successful treatment and is associated with poor prognosis. Reasons for relapse are tumor cells that survived treatment and persist for longtime, sometimes even decades, as minimal residual disease (MRD) cells. One cause for their resistance and longtime persistence might be their dormant state (Aguirre-Ghiso, 2007; Essers and Trumpp, 2010; Schillert et al., 2013). As conventional chemotherapy is cell cycle dependent and mechanisms required for cell proliferation are not active in dormant cells, dormancy might be a reason for resistance to chemotherapy (Clevers, 2011; Zhou et al., 2009). Many different adult stem cells contain dormant cells and as cancer stem cells (CSC) share various characteristics of these cells, dormancy might be an important characteristic within CSC, too (Orford and Scadden, 2008; Schillert et al., 2013).

As mouse hematopoietic stem cells (HSC) represent the stem cells best characterized, many studies identified the existence of dormant cells within this population (Cheshier et al., 1999; Passegue et al., 2005; van der Wath et al., 2009; Wilson et al., 2008; Wilson et al., 2007; Yoshihara et al., 2007). In contrast, only few studies investigated dormancy in cancer cells so far, as (I) small subpopulations are difficult to identify due to detection limits, (II) lack of adequate markers to identify dormant tumor cells, and (III) lack of adequate model systems (Schillert et al., 2013). Some studies connected dormancy of CSC in a specific tissue with

increased drug resistance. For ovarian tumor cells, it has been shown that the $CD24^+$ stem cell population proliferates slower, is more tumorigenic and more resistant to cisplatin (Gao et al., 2010). With the help of the proliferating dependent dye 5-(6)-Carboxyfluorescein-Succinimidyl Ester (CFSE), a subpopulation of dormant cells, which is more resistant to chemotherapy and is able to start proliferation, was detected in a xenograft model of human primary breast cancer cells (Moore et al., 2012).

Even in BCR/ABL positive chronic myeloid leukemia, quiescent and Imatinib mesylate resistant stem cells have been identified (Essers and Trumpp, 2010). In addition, Guan and coworkers showed that most leukemia initiating cell (LIC) of primary AML cells were dormant, therefore mainly quiescent AML cells were able to induce a tumor in NOD/SCID mice (Guan et al., 2003). In a xenograft mouse model of AML, it has been shown that dormancy and chemotherapy resistance of $CD34^+CD38^-$ human AML leukemia stem cell (LSC) are connected. Here AML LSC are quiescent, chemotherapy resistant, and enriched in the mouse bone marrow endosteal niche (Ishikawa et al., 2007; Saito et al., 2010a; Saito et al., 2010b). The bone marrow endosteal niche is defined as the region around the bone matrix with a distance of less than 100 µm to the closest bone matrix (Nombela-Arrieta et al., 2013). The niche itself is an elusive structure within the bone marrow microenvironment. Several cellular components, like osteoblastic, endothelial, and mesenchymal cell, have been identified to contribute to the niche, as well as the signaling by molecular cross-talk and soluble factors provided by these cellular components and the HSC (Kiel and Morrison, 2008; Wilson and Trumpp, 2006).

Identifying dormant tumor cells in primary patients' samples is rather challenging (Essers and Trumpp, 2010), but feasible with Ki-67 staining in certain ALL subtypes where an accumulation of non-proliferating cells after chemotherapy has been described (Lutz et al., 2013). For these measurements, it remains unclear for how long dormancy persisted, as Ki-67 staining gives a snapshot of a given moment, but fails to distinguish between long-term and short-term dormancy.

Especially the localization and microenvironment of dormant hematopoietic and CSC are supposed to represent a cause for their dormancy (Ishikawa et al., 2007; Saito et al., 2010b; Zhou et al., 2009). Labeling with proliferation specific dyes enabled the localization of dormant HSC. These cells are mainly localized close to the bone surface, the endosteum (Arai et al., 2004; Fleming et al., 2008; Wilson et al., 2008; Wilson et al., 2007). These sites are assumed to be specialized niches and are called the endosteal bone marrow niches, where several studies showed an enrichment of HSC (Wilson and Trumpp, 2006). In addition for AML stem cells the

localization to the endosteal bone marrow niche has also been shown (Ishikawa et al., 2007; Saito et al., 2010b; Zhou et al., 2009).

Interaction and molecular crosstalk between niche and HSC, via cell-cell contacts and soluble factors, promote the localization and dormancy of HSC (Trumpp et al., 2010; Zhou et al., 2009). Several molecules have been identified which are associated with the regulation and activity of the bone marrow niche (Wilson 2006).

One approach to overcome chemotherapy resistance of CSC is to overcome their dormancy. Dormant HSC can be activated and start to proliferate after treatment with granulocyte colony-stimulating factor, interferon-α or arsenic trioxide. This activation sensitizes them toward chemotherapy treatment (Trumpp et al., 2010). Therefore the same has been proposed to overcome the dormancy and thus the resistance of LSC (Trumpp et al., 2010).

In an AML xenotransplantation model, treatment with the cytokine G-CSF induced proliferation of former dormant LSC; subsequent treatment with the chemotherapeutic drug cytarabine induced a decrease of LIC frequency and a longer survival of mice (Saito et al., 2010b).

In summary, the subpopulation of dormant cells represents a major challenge in the treatment of cancer patients, and reversing their dormancy represents an important goal to overcome drug resistance, to prevent relapse and to cure cancer patients. New treatment strategies should aim at targeting dormant tumor cells by bringing them back into proliferation (Essers and Trumpp, 2010; Saito et al., 2010b; Trumpp et al., 2010).

2.2.3 Stemness

In normal hematopoiesis, cells differentiate in several steps as a hierarchically organized differentiation tree from immature stem- and progenitor cells into specialized mature cells. Similarities between leukemia development and normal hematopoiesis led to the concept of cancer stem cells (CSC). The subpopulation of CSC differs from the bulk of tumor cells, as they represent a biologically distinct subpopulation, in AML with specific surface markers. CSC bear self-renewal properties, are responsible for tumor maintenance and relapse and they give rise to all tumor cells (Bonnet and Dick, 1997; Schillert et al., 2013; Visvader and Lindeman, 2008). CSC features are identical to those from adult stem cells. However, CSC might originate from more mature cells besides adult stem cells (Jordan et al., 2006).

The gold-standard method to prove the existence of CSC in a certain tumor sample is xenotransplantation into immunodeficient mice, as CSC are defined by and unique in their potential to initiate a new tumor. Due to this functional phenotype, CSC are also called tumor

initiating cells. In literature, both terms are used identically, without distinction and with a certain transition between both terms (Bansal and Banerjee, 2009; Zhou et al., 2009). In leukemia, the term leukemia initiating cell (LIC) is frequently used, but also replaced by the term leukemia stem cell (LSC) (Matsushita et al., 2014).

A CSC hierarchy has first been described in AML (Bonnet and Dick, 1997) and was also found in numerous solid tumors like breast cancer (Al-Hajj et al., 2003), pancreatic cancer (Hermann et al., 2007), and colorectal cancer (O'Brien et al., 2007).

Many studies exist on LSC in AML, which makes them the best characterized CSC between all different tumor entities (Pollyea et al., 2014; Wang and Dick, 2005). LSC are capable to give rise to identical daughter cells and to more differentiated cells, and can be identified by their immunophenotype (Lapidot et al., 1994; Pollyea et al., 2014). Thus LSC share many characteristics of hematopoietic stem cells (HSC) (Bhatia et al., 1997; Guenechea et al., 2001). First studies identified LSC as negative for the expression of lineage markers (lin^-), positive for CD34 ($CD34^+$), and negative for CD38 ($CD38^-$) (Bhatia et al., 1997; Bonnet and Dick, 1997; Reya et al., 2001). But recent studies showed that the phenotype of LSC is even more complex, with different expression of various markers appearing in individual patients or as a result of disease progression (Eppert et al., 2011; Sarry et al., 2011). In addition, it is proposed that LSC are mainly localized in specialized bone marrow niches, like it has been demonstrated for HSC (Ishikawa et al., 2007; Saito et al., 2010b; Wilson and Trumpp, 2006). These niches are necessary for the function of HSC, as they regulate the maintenance, self-renewal and differentiation of HSC.

Only a small frequency of all AML tumor cells are LSC (Bonnet, 2008; Bonnet and Dick, 1997). LSC is an operational term, as these cells sustain AML (Dick, 2008; Reya et al., 2001; Tan et al., 2006) and have been characterized by features like self-renewal, dormancy and treatment resistance. Therefore they are a clinically highly relevant subpopulation of challenging cells (Aguirre-Ghiso, 2007; Essers and Trumpp, 2010). These features are interdependent as, e.g., drug resistance might be a consequence of dormancy and temporary dormancy might represent a prerequisite for being a stem cell. If these features coexist in a given tumor cell, this cell is putatively able to induce relapse. In AML, it is difficult to eradicate LSC with standard chemotherapy as they have different characteristics compared to the bulk of tumor cells. Thus, LSC survive chemotherapy and might be responsible for tumor relapse (Schillert et al., 2013).

In contrast, in ALL, a defined stem cell hierarchy has not yet been identified and phenotypic markers are unable to characterize the population of stem cells or predict self-renewal potential

(Kong et al., 2008; le Viseur et al., 2008). Many ALL cells display CSC properties and initiate leukemia in mice (Morisot et al., 2010; Rehe et al., 2013). Therefore, stemness seems to be an insufficient characteristic to describe the subpopulation of relapse-inducing cells in ALL. Since leukemia initiating potential is a feature of nearly every single cell in samples from ALL patients, ALL might even be functionally homogeneous regarding stemness. Nevertheless, ALL behaves like a non-homogeneous disease regarding additional characteristics; seminal studies revealed a clear genetic heterogeneity in ALL (Anderson et al., 2011; Mullighan, 2013); and the existence of MRD after treatment argues in favor of functional heterogeneity in ALL from a clinical point of view.

In summary, many tumor entities, including AML contain a rare subpopulation of CSC which challenges tumor treatment, as cells differ from the bulk of tumor cells and often show treatment resistance. As these cells are able to induce a new tumor, relapse might occur due to the survival of only a few CSC. Even in ALL, where almost all cells seem to have tumor inducing potential, functionally heterogeneous subpopulations seem to exist, relapse occurs in many patients after initially successful treatment. For a final eradiation of the tumor, it is important to eradicate CSC (Wang, 2007).

2.2.4 Intra-tumor heterogeneity

The subpopulations within a tumor might differ regarding genetic, epigenetic and functional properties. The existence of MRD cells after treatment is a hallmark for the intra-tumor heterogeneity. Subpopulations with a survival benefit such as drug resistance or adverse genotype persist and represent a major problem for the cure of patients (Burrell et al., 2013; Marusyk et al., 2012; Metzeler and Herold, 2016).

Recent developments in genomic profiling through sequencing technologies have revealed extensive genetic diversity between different tumors types, between the same tumor types from different patients, and even within the tumor cells of one patient (Burrell et al., 2013; Greaves and Maley, 2012). Here, individual mutations or chromosomal aberrations define different subclones. These subclones within one tumor are related to each other in a complex clonal architecture (Anderson et al., 2011; Greaves and Maley, 2012). By sequencing or multiplex fluorescence in situ hybridization, this complex subclonal architecture can be followed up and thus give an insight into the cancer evolution. Thereby the amount of alteration, the types of genetic alterations, and the shared mutations between different clones expose the relationship within the different clones (Ding et al., 2012; Greaves and Maley, 2012). This diversity can be

seen in many tumor entities, including ALL, where an evolution with many branches has been detected (Burrell et al., 2013; Mullighan, 2013).

The development of the different cancer clones is considered as a Darwinian evolutionary process, meaning that the subclonal architecture develops during time. Selective pressure forms the different variants resulting in diverse functional characteristics for the individual clones (Ding et al., 2012).

The main reason for the different variants is genetic instability, with an increased mutation rate which leads to the genetic heterogeneity. This genetic diversity forms the evolution of the cancer genome and is one reason for the phenotypic variations of the different subclones (Burrell et al., 2013). As most tumors show a kind of genomic instability, this seems to have a benefit for the tumor evolution. Normally the replication of the genome occurs with high precision, as monitoring and repair mechanisms only lead to a low mutation rate and failures in chromosome segregation are rare. But errors in the mechanisms that maintain genome integrity or the exposure to exogenous mutagens lead to an increase in the mutation rate (Burrell et al., 2013). Different genomic instabilities lead to different genetic alterations, such as increased point mutations, small insertions and deletions, chromosomal rearrangements, and different chromosome numbers (Burrell et al., 2013).

A reason for selective pressure during cancer evolution might be chemotherapy, as it selects for clones with drug resistance which here have a survival advantages (Greaves and Maley, 2012). In addition chemotherapy itself can induce new mutations and thereby has a direct influence on the evolutionary process (Burrell et al., 2013; Greaves and Maley, 2012).

Often clonal evolution becomes noticeable when former effective treatment becomes later inefficient or is inefficient at relapse. This phenotypic evolution towards more aggressive clones can be explained by genotypic changes in the main tumor. These changes might result from additionally gained mutations, which lead to drug resistance or from former minor subclones with resistance, which than outcompete the other clones (Burrell et al., 2013; Marusyk et al., 2012). This phenomenon has also been detected in AL. In AML and ALL the clonal development from diagnosis and the corresponding relapse samples has been studied. Here, it has been shown that the clonal composition in the relapse samples differs from the corresponding one at diagnosis, suggesting a clonal evolution process from diagnosis to relapse. The clones found in the relapse sample had a survival advantage, which might be because of additionally gained mutations responsible for drug resistance (Anderson et al., 2011; Ding et al., 2012; Mullighan, 2013). In the majority of cases, the clones found in the relapse samples could be related to the clones at diagnosis. In only 6 % of the cases, the relapse was genetically

not related to the subclones at diagnosis. Often the major relapse clone was already present at diagnosis as a minor subclone. In general, at relapse more alterations were detected, which might be because of the mutagenic chemotherapy or because of spontaneous mutations which lead to a survival benefit. In addition certain pathways were often altered in relapse samples suggesting a survival benefit for these mutations.

In general, changes in the genotype of subclones are often associated with changes in the functional phenotype, like the patients' prognosis or response to therapy. But phenotypic heterogeneity is not always generated through genetic diversity, furthermore stochastic events in gene expression or protein stability, microenvironmental differences, and epigenetic alterations also have an influence on the functional phenotype of subclones (Burrell et al., 2013).

Especially epigenetic heterogeneity has been shown in recent studies to account for differences of genetically identical subclones. Gene expression can be influenced by different DNA methylation patterns at gene promoters, which might then influence the functional phenotype like proliferation or drug sensitivity (Burrell et al., 2013).

Some leukemia subtypes have a distinct epigenetic pattern such as an increased promoter methylation, which directly influences the corresponding gene expression levels. In AML and ALL several genes have been identified which are abnormally methylated (De Kouchkovsky and Abdul-Hay, 2016; Mullighan, 2013). But these findings also opened new perspectives for individual epigenetic treatment strategies. For leukemia the first epigenetic drugs, the DNA methyltransferase inhibitors 5-azacitidine and 5-aza-2′-deoxyazacytidine, are already in clinical use (Sato et al., 2017).

Taken together the intra- tumor heterogeneity of AL, which involves different genetic, epigenetic, and functional subpopulations, provides a survival benefit for the tumor during chemotherapy. The cancer evolution and the related clonal heterogeneity are an important element for relapse. Therefore an effective treatment is challenging, as it should target all different subclones, but could also exert selective pressure which might lead to new mutations. Novel treatment strategies are urgently needed to target all subpopulation in order to prevent relapse.

2.3 *In vivo* models for AL

As studies on the complex biology of AL cells cannot be performed directly in patients, suitable model systems have to be used. These model systems should mimic the situation in the patient in the best possible manner.

Primary AL cells have restrictions as they do not grow *in vitro*, disabling their amplification. Primary cell material is limited, especially in children, and often not enough material can be isolated for a single experiment and experiments cannot be reproduced. Furthermore, AL cell lines are not a suitable model for complex studies because they display continuous proliferation, clearly discriminating them from relapse-inducing cells. In addition, cell lines changed clonal composition during the process of immortalization and *in vitro* passaging alienating them from the original patients sample (Pan et al., 2009). Furthermore, the number of available AL cell lines is inadequate regarding the diversity of AL subtypes (Gillet et al., 2011; Hausser and Brenner, 2005).

Mouse models have the advantages to study leukemia cells within a complex living system including extrinsic factors like the microenvironment. They can be divided into syngeneic models, where a mouse leukemia is studied in the presence of a functional immune system, and xenograft models, where human leukemia cells are transplanted and studied in mice without functional immune system (Jacoby et al., 2014). For syngeneic mouse models, leukemia associated genes, which are known to be potential drivers of leukemogenesis, are modified, either through transgenic mice, or by genetic modification of primary HSC followed by transplantation into recipient mice, or by chemical carcinogens (Jacoby et al., 2014). To study human AML and ALL cells close to the patients', the currently best available model system is the patient-derived xenograft (PDX) mouse model of AL (Lee et al., 2007; Liem et al., 2004; Townsend et al., 2016).

2.3.1 Patient-derived xenograft (PDX) mouse model of AL

PDX are generated by the injection of primary AL cells derived from patients into immunodeficient mice. By serial re-passaging of leukemic cells from mouse to mouse, the PDX sample is amplified (Siolas and Hannon, 2013). The first immunodeficient mice which could be used for the engraftment of leukemic cell, were mice with a mutation leading to severe combined immunodeficiency (SCID) (Bosma et al., 1983). This mouse enabled the engraftment of human hematopoietic cells, leukemia cell lines, and primary patient cells (Kamel-Reid et al., 1989). But due to remaining immunity of the mice, engraftment rates were poor, which led to

the development of mouse strains with even stronger immunodeficiency. Here, the SCID mouse was backcrossed onto a nonobese diabetic (NOD) background, resulting in the NOD/SCID mouse with higher engraftment rates (Shultz et al., 1995). This mouse strain was further develop to generate mice with an almost completely absent immune system by additional mutation of the interleukin-2 receptor gamma chain. These NOD/SCID/gamma chain depleted (NSG) mice do virtually not have any mature T cells, B cells or natural killer cells, and an impaired innate immunity (Shultz et al., 2005), which leads to even increased engraftment rates of AML and ALL (Alruwetei et al., 2015; Schmitz et al., 2011; Terziyska et al., 2012; Townsend et al., 2016; Vick et al., 2015). In contrast to xenograft models of solid tumors, the development of the leukemia xenografts showed an orthotopic tumor distribution involving the bone marrow, blood, spleen and liver. Disease distribution is very similar to the situation in patients and the malignant cells reside in a similar microenvironment within the mouse bone marrow (Baersch et al., 1997; Liem et al., 2004; Lock et al., 2002; Townsend et al., 2016).

ALL PDX models have been used to model specific ALL subtypes. Engraftment and distribution levels correlate with the clinical outcome in patients. Additionally, the ALL PDX model is used to predict clinical chemotherapy response in patients (Liem et al., 2004; Woiterski et al., 2013) and to search for biomarkers that enable the prediction of response and resistance towards treatment (Townsend et al., 2016). Established ALL PDX samples are highly reliable, allowing the prediction of engraftment and the monitoring of the engraftment by blood analysis (Castro Alves et al., 2012; Lock et al., 2005; Terziyska et al., 2012). Especially in NSG mice, engraftment rates for different types of primary ALL samples are high. Townsend et al. reported engraftment rates of 67.5 % for B-ALL and even 46.7 % for the previous difficult to engraft T-ALL (Townsend et al., 2016).

AML PDX models have been used to identify specific immunophenotypes on leukemia initiating cells (LIC) and certain surface markers indicating LIC. Higher numbers of stem cells identified by appropriate markers in primary samples correlated with higher engraftment rates in mice (Bonnet and Dick, 1997; Hope et al., 2003; Lapidot et al., 1994). Surface markers are also used for the identification of biomarkers, to predict response and resistance after treatment and to predict the success of treatment for genetically different subtypes (Townsend et al., 2016). In addition AML PDX models are an attractive tool for the development of new treatment strategies targeting leukemia stem cells (LSC) (Hope et al., 2003). Compared to ALL PDX models, AML models are more difficult to handle, need longer engraftment times, and have a lower engraftment rate (Lee et al., 2007). In NSG mice, the engraftment rate for

repetitively transplantable primary AML samples is 23.2 %, which nowadays allowed the establishment of a large repository of established AML PDX samples (Townsend et al., 2016). PDX models of human AL provide an important tool to investigate numerous aspects of the complex biology of AL. They enable amplification of human leukemic cells and have been used for identify clinically relevant risk groups to evaluate new treatment strategies (Meyer and Debatin, 2011). AML PDX and ALL PDX cells have been shown to retain important characteristics of primary AL cells and to recapitulate most clinical aspects of the leukemia (Castro Alves et al., 2012; Meyer and Debatin, 2011; Schmitz et al., 2011; Terziyska et al., 2012; Vick et al., 2015).

In summary, the NSG PDX model represents an especially suitable model to study leukemic cells *in vivo*. PDX AL cells are very closely related to the primary patients' leukemia and represent an important tool to investigate questions on the complex biology of AL.

2.3.2 PDX model to identify a rare subpopulation of dormant ALL cells

The hosting lab where the current study was performed, established the PDX mouse model of AL for several years, both for acute myeloid (AML) and acute lymphoblastic leukemia (ALL) (Castro Alves et al., 2012; Terziyska et al., 2012; Vick et al., 2015). Before the study started, they had begun using the model to search for surrogates of relapse-inducing cells using dormancy as anchor. The underlying idea was that long-term dormant cells in the PDX AL model might represent relapse-inducing cells in patients, with the major advantage that PDX cells would allow repetitive and functional studies.

The study was started by Sebastian Tiedt. His first aim was to establish a method to isolate minute numbers of PDX cells from bone marrow. Towards this aim, he chose a molecular approach and expressed three different marker transgenes in PDX cells by lentiviral transduction (Figure 1). The advantage of the molecular approach was that it allowed an unbiased isolation of entirely all human PDX cells independent from the expression of endogenous surface antigens, which might be restricted to yet undefined leukemia subpopulations.

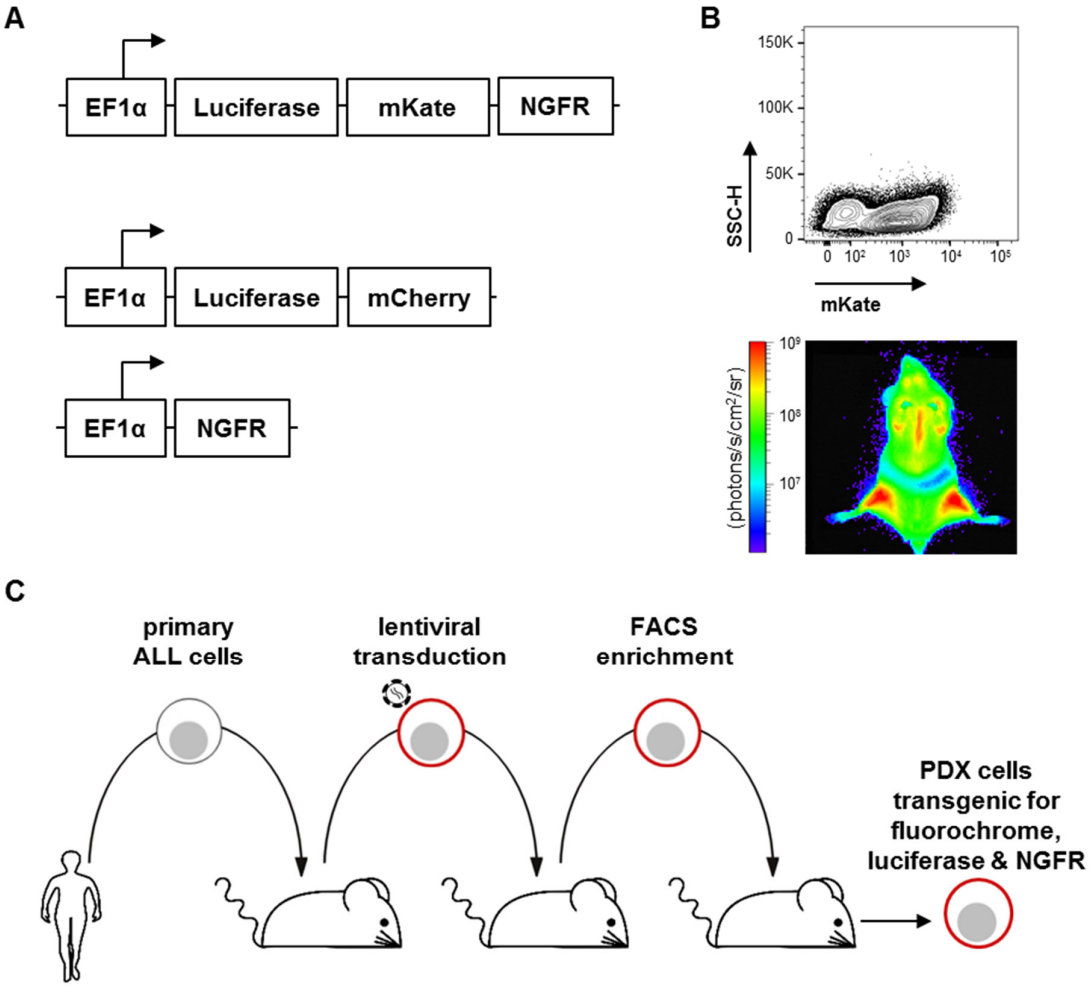

Figure 1: Generation of transgenic PDX ALL with high expression of artificial transgenes
A Scheme of the lentiviral constructs applied for expression of transgenes; arrow indicates start of transcription; EF1α = elongation factor 1-alpha promoter; mKate = red fluorescent protein cloned from sea anemone Entacmaea quadricolor; mCherry = red fluorescent protein cloned from Discosoma sp.; NGFR = a truncated form of the human low affinity nerve growth factor receptor lacking the intracellular signaling domain.
B Exemplary FACS blot (upper panel) and bioluminescence *in vivo* imaging (lower panel) of enriched transgenic PDX ALL-199 cells (upper panel) and PDX ALL-265 cells (lower panel).
C Schematic workflow for the generation of genetically engineered PDX ALL cells. Primary patients ALL cell were injected i.v. into immunodeficient NSG mice. After engraftment and proliferation, PDX cells were serially passaged in further recipient mice. Furthermore, PDX cells were transduced with lentiviral constructs as depicted in B. PDX cells expressing the transgenes were enriched by FACS sorting and amplified.

As transgenic markers, he decided for expressing (i) the fluorescent protein mKate or mCherry for cell tracking and enriching by flow cytometry (Fehse et al., 1997); (ii) the artificial antigen NGFR for cell enrichment by magnetic cell sorting; and (iii) luciferase for repetitively monitoring disease progression in the same mouse (Figure 1A, B) (Rabinovich et al., 2008; Terziyska et al., 2012). A schematic workflow how transgenic PDX samples were generated is depicted in Figure 1C. In brief, PDX cells were lentivirally transduced *ex vivo* either with just one construct containing mCherry and the luciferase or with two constructs, one containing the

red fluorescent protein mCherry and a luciferase and the other containing the truncated extracellular receptor nerve growth factor receptor (NGFR) (Figure 1A). As transduction efficiencies in PDX cells are often low, in average around 30 %, but sometimes even less than 5 %, flow cytometry was used to enrich transduced PDX cells to more than 95 % purity.

Sebastian Tiedt next transplanted PDX ALL cells expressing all three transgenes into NSG mice and re-isolated them back again from mouse bone marrow at early time points in the leukemic disease when only very low numbers of PDX cells were yet present. He isolated mouse bone marrow and enriched human PDX ALL cells in a first step by magnetic beads coupled with an antibody directed against NGFR. In a second step, he enriched PDX ALL cells further by sorting fluorochrome positive cells by flow cytometry. Using this approach, he enriched low numbers of PDX cells from mouse bone marrow by a factor well above 10.000 (Tiedt, 2014).

Once the method was established, Sebastian Tiedt started to search for long-term dormant PDX ALL cells using stainings with the proliferation-dependent dye Carboxyfluorescein-Succinimidyl Ester (CFSE) (Tiedt, 2014).

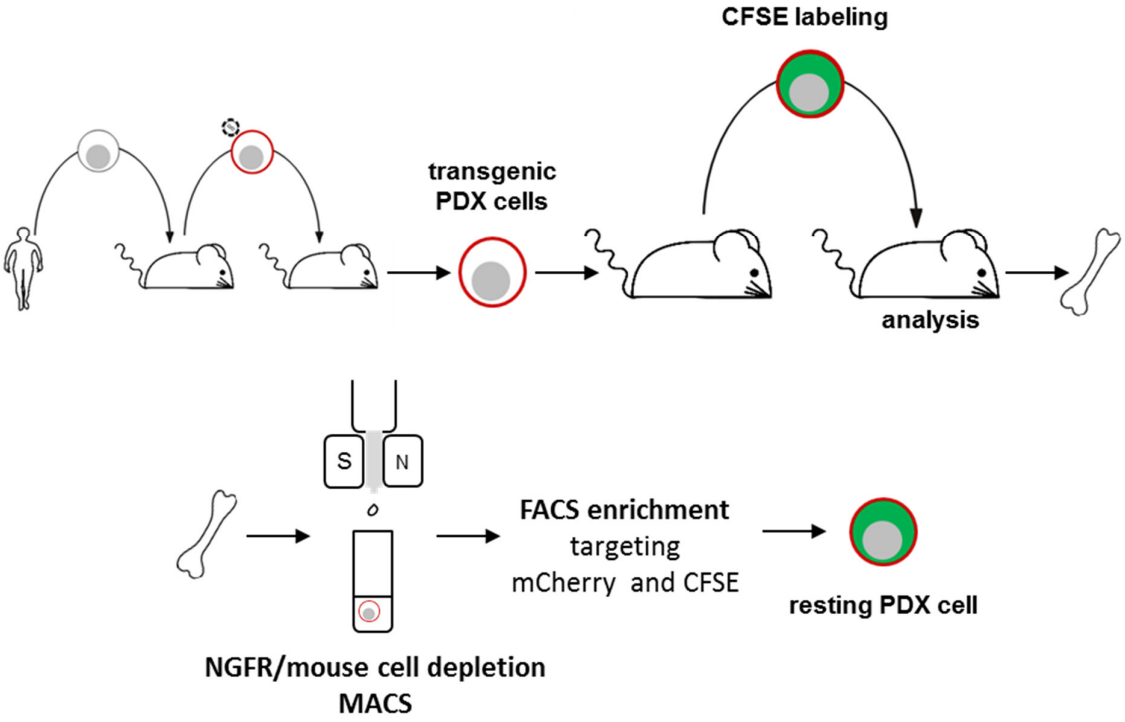

Figure 2: Schematic workflow of staining with CFSE and enriching rare transgenic, CFSE stained PDX cells from mouse bone marrow

CFSE remains covalently bound inside of cells *in vivo* over several months (Takizawa et al., 2011) and is distributed onto daughter cells upon cell division. Figure 2 shows the staining and detection workflow for CFSE.

Using CFSE as label and a first kinetic, Sebastian Tiedt indeed found a rare subpopulation of PDX ALL cells that did not participate in tumor growth, but instead remained dormant over prolonged periods of time (Tiedt, 2014) – which represented the starting point of my work described below.

Taken together, the working group of the hosting laboratory for this study had generated tools and techniques which enables re-isolating minute numbers of PDX cells from mouse bone marrow using molecular markers as anchors and has established CFSE staining in the PDX model for identifying long-term dormant ALL cells.

2.4 Aim of this work

In acute leukemias, treatment resistant cells, which might persist as minimal residual disease (MRD), might later be responsible for relapse and thereby determine the prognosis of patients. Chemotherapy resistance is considered to be closely related to dormancy, but the responsible biological mechanisms are still unclear. To prevent relapse and improve the outcome in patients, new treatment strategies for elimination of chemotherapy resistant cells are urgently needed. However until now technical limitations impede the isolation and detailed investigations on relapse-inducing cells in AML and ALL.

The first aim of the present work was to develop the individualized patient-derived xenograft (PDX) model further by optimizing the isolation of minimal human PDX cells from mouse bone marrow.

This technique together with the label retaining dye CFSE was then used to evaluate the *in vivo* growth behavior of ALL and AML PDX in the bone marrow of NSG mice.

The study aimed to investigate, whether PDX samples derived from different patients with ALL or AML would frequently contain a subpopulation of dormant cells. To characterize dormant cells on a functional level, the study investigated, whether dormant PDX ALL and AML cells displayed a behavior that challenges current anti-leukemia treatment, such as drug resistance, stem cell properties and relapse-inducing potential. Furthermore, the study addressed the question whether adverse characteristics of the dormant subpopulation were transient or constant and which influence the bone marrow environment might have on growth behavior of PDX AL cells.

The developed model and the consequent findings will be of translational importance as they establish a basis to develop new treatment strategies to eradicate relapse-inducing cells.

3 Material

3.1 Mice

NOD.Cg-Prkdc^{scid} IL2rg^{tm1Wjl}/SzJ (NSG) (Shultz et al., 2005)

NSG mice have a severe combined immunodeficiency/non-obese diabetic (NOD/SCID) background with an interleukin-2 receptor gamma chain knockout. As a result mice are immunodeficient; they have no mature T cells, B cells or natural killer cells and are deficient in cytokine signaling. Mice were obtained from the Jackson Laboratory (Charles River Laboratories France).

3.2 Cell lines

HEK-293T (SV40 large T-antigen expressing human embryonic kidney cells)	DSMZ, Braunschweig, Germany
Nalm-6 (B cell precursor leukemia cells)	DSMZ, Braunschweig, Germany

3.3 Plasmids and primer

Plasmid

pRSV-Rev (392)	Addgene, Cambridge, MA, USA
pMDLg/pRRE (393)	Addgene, Cambridge, MA, USA
pMD2.G	Addgene, Cambridge, MA, USA
pCDH-EF1α-extGlucT2A-mCherry	cloned by Michela Carlet
pCDH-EF1α- NGFR	cloned by Michela Carlet

Primer for finger printing of mitochondrial DNA

Primer 456	5'TCCACCATTAGCACCCAAAGC3'
Primer 457	5'TCGGATACAGTTCACTTTAGC3'

3.4 Antibodies

CD33hu-PE,	BD Bioscience, Heidelberg, Germany

clone: WM-53, #555450	
CD38hu-PE, clone: HB7, #345806	BD Bioscience, Heidelberg, Germany
CD45hu-APC, clone: HI30, #555485	BD Bioscience, Heidelberg, Germany
CD45mu-APC, clone: 30-F11,#103112	Biolegend, San Diego, CA, USA
CD45mu-APC-Cy7, clone: 30-F11, #103115	Biolegend, San Diego, CA, USA
CD271hu-PerCP/Cy5.5 (NGFR) clone: ME20.4, #345111	Biolegend, San Diego, CA, USA
Mouse IgG1 APC Isotype Control, clone: MOPC-21, #555751	BD Bioscience, Heidelberg, Germany
Mouse IgG1 APC Isotype Control, clone: MOPC-21, #400119	Biolegend, San Diego, CA, USA
Mouse IgG1 PE Isotype Control, clone: MOPC-21, #559320	BD Bioscience, Heidelberg, Germany
Mouse IgG1 PE Isotype Control, clone: MOPC-21, #400140	Biolegend, San Diego, CA, USA
Mouse cell depletion kit	Miltenyi, Bergisch Gladbach, Germany
NGFR Beads	Miltenyi, Bergisch Gladbach, Germany

3.5 Buffer and media

DMEM medium for cultivation of AL cell line cells

DMEM (Gibco, San Diego, USA), 10 % FCS (Biochrome, Berlin, Germany), 1 % glutamine (Gibco, San Diego, USA)

Glucose-containing Hepes buffer

H_2O, 5 % Glucose (Braun, Melsungen, Germany), 20 mM Hepes pH 7.1 (Gibco, San Diego, USA)

Medium for cultivation of ALL PDX cells

RPMI-1640 (Gibco, San Diego, USA), 20 % FCS (Biochrome, Berlin, Germany), 2 mM glutamine (Gibco, San Diego, USA), 1 % penicillin-streptomycin (Gibco, San Diego, USA), 1 % gentamicin (Lonza, Allendale, USA), ITS-G (=6 mg/l insulin, 3 mg/l transferrin, 4 µg/l selenium) (Gibco, San Diego, USA), 1 mM sodium pyruvate (Sigma-Aldrich, St. Louis, USA), 50 µM α-thioglycerol (Sigma-Aldrich, St. Louis, USA)

Medium for cultivation of AML PDX cells

StemPro-34 medium (Thermo Fischer Scientific, Waltham, USA), 1 % penicillin-streptomycin (Gibco, San Diego, USA), 1 % glutamine (Gibco, San Diego, USA), 2 % FCS (Biochrome, Berlin, Germany), 10 µg/l recombinant human Flt-3 Ligand (R&D Systems, Minneapolis, USA), 10 µg/l Recombinant human SCF (PeproTech, Rocky Hill, USA), 10 µg/l Recombinant human TPO (PeproTech, Rocky Hill, USA), 10 µg/l Recombinant human IL-3 (PeproTech, Rocky Hill, USA)

PDX short-term storage medium

RPMI-1640 (Gibco, San Diego, USA), 20 % FCS (Biochrome, Berlin, Germany), 1 % penicillin-streptomycin (Gibco, San Diego, USA), 1 % gentamicin (Lonza, Allendale, USA), 2 mM glutamine (Gibco, San Diego, USA)

Phosphate-buffered saline (PBS)

H_2O, 137 mM NaCl (Carl Roth, Karlsruhe, Germany), 2.7 mM KCl (Merck Milipore, Darmstadt, Germany), 10 mM Na_2HPO_4 (Sigma-Aldrich, St. Louis, USA), 1.8 mM KH_2PO_4 (Merck Milipore, Darmstadt, Germany)

Phosphate-buffered saline with EDTA (PBE)

PBS, 0.5 % BSA, 5 mM EDTA (Lonza, Allendale, USA)

3.6 Kits

BrdU APC Flow Kit	BD Bioscience, Heidelberg, Germany
CellTrace CFSE Cell Proliferation Kit for flow cytometry	Life Technologies, Carlsbad, CA, USA
MinElute PCR Purification kit	Qiagen, Venlo, NL
QIAamp DNA Blood Mini Kit	Qiagen, Venlo, NL

3.7 Chemotherapeutics

Cytarabine	cell pharm GmbH, Bad Vilbel, Germany
Daunorubicine	PFIZER PHARMA GmbH, Berlin, Germany

DaunoXome	Galen, Craigavon, UK
Doxorubicine	Accord Healthcare GmbH, Freilassing, Germany
Epirubicine	TEVA GmbH, Ulm/Donau, Germany
Etoposide	TEVA GmbH, Ulm/Donau, Germany
Mitoxantrone	TEVA GmbH, Ulm/Donau, Germany
Vincristine	cell pharm GmbH, Bad Vilbel, Germany

3.8 Reagents and chemicals

α-thioglycerol	Sigma-Aldrich, St.Louis, USA
Baytril (2.5 %)	Bayer, Leverkusen, Germany
BrdU	VWR, Radnor, USA
BSA	Carl Roth, Karlsruhe, Germany
Coelenterazine	Synchem OHG, Felsberg, Germany
DAPI (4',6-diamidino-2-phenylindole) (1mg/ml)	Sigma-Aldrich, St. Louis, USA
D-Luciferin	BIOMOL GmbH, Hamburg, Germany
DMSO	Sigma-Aldrich, St. Louis, USA
DNase I	Roche, Mannheim, Germany
DNase I buffer	Roche, Mannheim, Germany
dNTPs (10 mM each)	Biozym, Hessisch Oldendorf, Germany
EDTA (0.5 M)	Lonza, Allendale, USA
FACS Lysing Solution 10x	BD Bioscience, Heidelberg, Germany
FCS	Biochrome, Berlin, Germany
Ficoll	GE Healthcare, Freiburg, Germany
Gentamicin	Lonza, Allendale, USA
Glucose (20 %)	Braun, Melsungen, Germany
Glutamine	Gibco, San Diego, USA
GoTaq G2 DNA Polymerase + Reaction Buffer (5x)	Promega, Madison, USA
Heparin	Ratiopharm, Ulm, Germany
Hepes (1 M)	Gibco, San Diego, USA
Isopropyl alcohol	Merck Milipore, Darmstadt, Germany
ITS-G (insulin-transferrin-selenium; 100x)	Gibco, San Diego, USA

KCl	Merck Milipore, Darmstadt, Germany
KH_2PO_4	Merck Milipore, Darmstadt, Germany
NaCl	Carl Roth, Karlsruhe, Germany
Na_2HPO_4	Sigma-Aldrich, St. Louis, USA
Penicillin-Streptomycin (5000 U/ml)	Gibco, San Diego, USA
Polybrene (2 mg/ml)	Sigma-Aldrich, St. Louis, USA
Recombinant human Flt-3 Ligand	R&D Systems, Minneapolis, USA
Recombinant human IL-3	PeproTech, Rocky Hill, USA
Recombinant human SCF	PeproTech, Rocky Hill, USA
Recombinant human TPO	PeproTech, Rocky Hill, USA
Sodium pyruvate (100 mM)	Sigma-Aldrich, St. Louis, USA
Turbofect	Thermo Fischer Scientific, Waltham, USA
Trypsin (1x)	Invitrogen, Karlsruhe, Germany
Trypan blue	Sigma-Aldrich, St. Louis, USA

3.9 Consumables

Amicon-Ultra 15 centrifugal filter units	Merck Millipore, Darmstadt, Germany
Cell strainer	Greiner bio-one, Frickenhausen, Germany
Centrifuge tubes (15 ml and 50 ml)	Greiner bio-one, Frickenhausen, Germany
Cryotubes	Thermo Fischer Scientific, Waltham, USA
Disposable serological pipettes (5 ml, 10 ml, 25 ml, 50 ml)	Greiner bio-one, Frickenhausen, Germany
LS columns	Miltenyi, Bergisch Gladbach, Germany
Microvette, Lithium-Heparin (100 µl)	Sarstedt, Nümbrecht, Germany
Needles RN G32 PST3 51MM	Hamilton, Reno, USA
Petri dishes	Greiner bio-one, Frickenhausen, Germany
Pipette filter tips TipOne (10, 20, 200, 1000)	Starlab, Hamburg, Germany
Well-Plates for tissue culture (6-well, 12-well, 24-well)	Corning, Corning, USA

3.10 Equipment

Biological safety cabinet Safe 2020	Thermo Fisher Scientific, Langenselbold, Germany
Cell sorter BD FACSAriaIII	BD Bioscience, Heidelberg, Germany
Centrifuge Rotanta 460R	Andreas Hettich GmbH & Co. KG, Tuttlingen, Germany
Quietek CO_2 Induction Systems	Next Advance, Averill Park, USA
Flow cytometry BD Calibur	BD Bioscience, Heidelberg, Germany
Flow cytometry BD LSRFortessa	BD Bioscience, Heidelberg, Germany
Incubator HERA CELL 150i	Thermo Fisher Scientific, Langenselbold, Germany
In vivo Imager IVIS Lumina II Imaging System	Caliper Life Sciences, Mainz, Germany
Light microscope 550 1317	Zeiss, Jena, Germany
Micro Scales Sartorius 2001 MP2	Sartorius AG, Göttingen, Germany
NanoDrop ND-1000	Thermo Fisher Scientific, Langenselbold, Germany
Table Centrifuge mini Spin	Eppendorf, Hamburg, Germany
Thermocycler Primus 25 advanced	Peqlab, Erlangen, Germany

3.11 Software

Name	Application
FlowJo V10	Analysis of flow cytometry
GraphPad Prism 6	Drawing of graphs, statistical analysis
Living Image software 4.4	Analysis of *in vivo* imaging
Microsoft Office	Figure drawing, calculations, writing

4 Methods

4.1 Ethical statements

4.1.1 Patient material

Patients' acute leukemic cells were collected from peripheral blood or bone marrow aspirates that had been obtained from leftovers of clinical routine sampling before onset of therapy. Written informed consent was obtained from all patients and from parents/carers in the cases where patients were minors.

For AML, primary AML blasts were obtained from patients treated at the Department of Internal Medicine III, Ludwig-Maximilians-Universität, Munich.

For ALL, primary ALL blasts were obtained from children treated at the Dr. von Haunersches Kinderspital, Ludwig-Maximilians-Universität, Munich or for one sample from a child treated at the University Children's Hospital in Zurich.

The study was performed in accordance with the ethical standards of the responsible committee on human experimentation (written approval by Ethikkommission des Klinikums der Ludwig-Maximilians-Universität München, Ethikkommission@med.uni-muenchen.de, April 2008 (068-08) and September 2010 (222-10)) and with the Helsinki Declaration of 1975, as revised in 2000.

4.1.2 Animal work

All animal trials were performed in accordance with the current ethical standards of the official committee on animal experimentation (written approval by Regierung von Oberbayern, poststelle@reg-ob.bayern.de; July 2010, number 55.2-1-54-2531-95-10; July 2010, number 55.2-1-54-2531.6-10-10; January 2016, number 55.2-1-54-2532-193-2015; May 2010, number 55.2-1-54-2532-193-2015 and August 2016, number 55.2-1-54-2532.0-56-2016).

4.2 The NSG mouse model of individual acute leukemias

For amplification of patients' acute leukemias cells, the previously described NSG (see 3.1 Mice) mouse model was used, which had been established in the hosting laboratory (Shultz et al., 2005; Terziyska et al., 2012; Vick et al., 2015).

NSG mice were maintained under specific pathogen-free conditions in the research animal facility of the Helmholtz Zentrum München, Munich, Germany. Animals had free access to

food and water, and were housed with a 12-hour light-dark cycle and constant temperature. After injection, mice were treated with Baytril to prevent infections. Therefore 1 ml of 2.5 % Baytril solution was added to 250 ml drinking water.

4.2.1 Expansion of primary patient cells and PDX cells

For amplification of leukemic blast from acute leukemia patients, up to 10^7 cells from peripheral blood or bone marrow aspirates were re-suspended in 100 µl autoclaved and filtered PBS and injected into 6-16 weeks old NSG mice via the tail vein.
For amplification of PDX cells, 10^2 - 10^7 cells were injected.
Engraftment was monitored by up to 2-weekly flow cytometry measurement of human cells in peripheral blood (see 4.2.3 Flow cytometry of human cells in mouse peripheral blood). Mice were sacrificed (see 4.2.4 Sacrificing mice by CO_2 exposure) at (i) defined days post-injection for specific experiments, (ii) first clinical signs of disease (rough fur, hunchback, or reduced motility) or (iii) at signs of advanced leukemia, as measured by quantification of human cells in peripheral blood or by *in vivo* imaging. If leukemia became not apparent, mice were killed and analyzed 25 weeks after cell injection by latest. From engrafted mice, leukemic cells were harvested from enlarged spleens (see 4.2.5 Isolation of PDX cells from mouse spleen) or from bone marrow (see 4.2.6 Isolation of PDX cells from mouse bone marrow). Re-passaging was successful in all engrafted samples. Accuracy of sample identity was verified by repetitive finger printing using PCR of mitochondrial DNA (see 4.2.2 Repetitive finger printing using PCR of mitochondrial DNA) (Hutter et al., 2004).

4.2.2 Repetitive finger printing using PCR of mitochondrial DNA

For early detecting putative, involuntary sample mix-ups and for a regular authentication of PDX samples, distinct areas of mitochondrial DNA was routinely sequenced and analyzed for sample-specific single nucleotide variants (Hutter et al., 2004).
DNA was prepared of 10^7 PDX cells with the Qiagen QIAamp DNA Blood Mini Kit according to manufacturer's instructions. DNA concentration was measured at the NanoDrop and DNA was stored at -80 °C.
The following 50 µl reaction mixture was used for Polymerase Chain Reaction (PCR):

Table 1: PCR reaction mix

reagent	[µl]
5x reaction buffer	10
300 ng DNA	1
10 pmol primer 456	2.5
10 pmol primer 457	2.5
dNTPs	1
GoTaq	0.25
H_2O	32,75

PCR was run Thermocycler with following program:

Table 2: PCR reaction cycle

cycles	time	temperature [°C]
1	2 min	95
	30 sec	94
35	30 sec	60
	30 sec	72
1	5 min	72

PCR products were purified using the Qiagen MinElute 70-7000 bp according to manufacturer's instructions. 100 ng/µl of purified PCR products were sent for Sanger sequencing to GATC (Biotech, Konstanz, Germany) using primer 456 and primer 457.

Results from sequencing were analyzed by comparing them to the reference sequence of each patient sample. If the sequence was correct, the sample could be used for experiments; if the sequence was incorrect, cells were trashed and cells from earlier passages were sequenced and used.

4.2.3 Flow cytometry of human cells in mouse peripheral blood

For quantification of human cells in mouse peripheral mouse blood, 50 µl blood from the tail vein was collected with a heparin coated glass capillary and pour into a lithium-heparin Microvette.

The blood was incubated with 0.5 µl hCD38-PE and 0.5 µl mCD45-APC (ALL samples) or with 5 µl hCD45-APC and 3 µl hCD33-PE (AML samples) for 30 min in the dark at room temperature.

1 ml FACS Lysing Solution was added to the stained blood samples and incubated for 15 min at room temperature for lysing the erythrocytes. The blood sample was washed twice with 3 ml FACS buffer at room temperature, and centrifuged at 300 g for 5 min. Afterwards flow cytometry analyses were performed with a FACSCalibur (see 4.4.7 Flow cytometry analysis) and the results were analyzed using the FlowJo software. If more than 1 % of human cells were detected, the sample was classified as engrafted.

4.2.4 Sacrificing mice by CO_2 exposure

Mice were sacrificed by CO_2 asphyxiation by the Quietek CO_2 Induction Systems. The mouse to be sacrificed was placed in a CO_2 empty cage (V = 7.67 l). The cage was closed with a Quietek lid, which was connected with the house CO_2 system (100 % CO_2) via a hose. Afterwards the Quietek CO_2 Induction Systems was started. First the mouse/mice was/were anesthetized by a gas flow rate of 10 % of the chamber volume per minute (750 ml/min) for one minute. Afterwards the mouse/mice was/were sacrificed by a gas flow rate of 30 % of the chamber volume per minute (2250 ml/min) for four minutes. Before organs were removed, the clinical death of the mouse/mice was/were verified.

4.2.5 Isolation of PDX cells from mouse spleen

To isolate PDX cells from mouse spleen, the spleen was homogenized by smashing the organ through a 70 µm cell strainer with 10 ml PBS into a 50 ml Falcon tube, and filled up with PBS to 30 ml. Afterwards the cell suspension was under-laid with 10 ml Ficoll by a 51 mm needle and centrifuged (400 g, 30 min, RT, without rotor brake). After Ficoll gradient centrifugation mononuclear cells could be harvested as a layer at the interphase. The cells were washed twice with PBS (400 g, 5 min, RT). After washing, the cells were re-suspended in required buffer or PDX short-term storage medium depending on further use and counted using a Neubauer chamber (see 4.4.1 Determination of cell numbers).

4.2.6 Isolation of PDX cells from mouse bone marrow

For isolation of PDX cells from mouse bone marrow, the isolated two femura, two tibiae, two hips, backbone and sternum were crushed using a mortar and pestle. The cells were suspended in PBS and filtered through a 70 µm cell strainer. The cells were washed twice with 10 ml PBS (400 g, 5 min, RT). After washing, the cells were re-suspended in required buffer or PDX short-term storage medium depending on further use and counted using a Neubauer chamber (see 4.4.1 Determination of cell numbers).

4.2.7 Enrichment of PDX cells by magnetic cell separation (MACS)

For enrichment of PDX cells from mouse bone marrow magnetic cell separation (MACS) was used.

The isolated bone marrow cells from one mouse (see 4.2.6 Isolation of PDX cells from mouse bone marrow) harboring PDX cells transgenic for NGFR, were incubated with 200 µl anti-human NGFR MicroBeads for 10 minutes at 4 °C. Cell suspension was divided onto two LS columns, prepared according to manufacturer's instructions. Cells were recovered from the column according to manufacturer's instructions and washed with PBS.

The isolated bone marrow cells from one mouse (see 4.2.6 Isolation of PDX cells from mouse bone marrow) harboring PDX cells not transgenic for NGFR, were incubated with 100 µl mouse cell depletion kit MicroBeads for 20 minutes at 4 °C. Cell suspension was divided onto two LS columns, prepared according to manufacturer's instructions. Cells were recovered from the column according to manufacturer's instructions and washed with PBS.

4.2.8 Enrichment of PDX cells by fluorescence-activated cell sorting (FACS)

mCherry positive PDX cells from mouse bone marrow cell suspensions were enriched by flow cytometry. Cells obtained after MACS enrichment (see 4.2.7 Enrichment of PDX cells by magnetic cell separation (MACS)) were stained with 10 µg/ml DAPI to exclude dead cells. Cells were sorted using a BD FACSAriaIII, gating on lymphocytes in forward/side scatter, the gate negative for DAPI and positive for expression of mCherry (Figure 3).

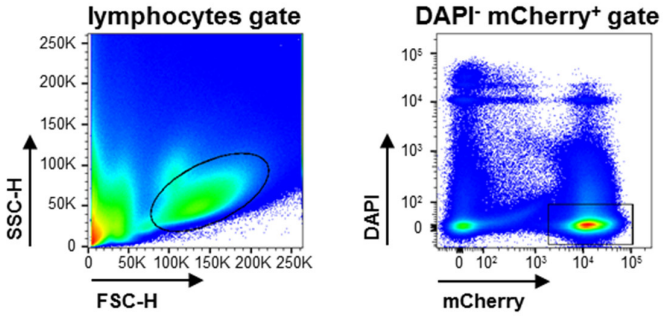

Figure 3: Gating strategy to sort mCherry⁺ PDX cells from mouse bone marrow

Alternatively, 10 % of the entire bone marrow cell suspension without prior MACS enrichment step was directly analyzed by flow cytometry with the identical staining and gating procedure. The entire cell suspension was recorded for quantifications. Depending on further use, sorted cells were either frozen (see 4.4.2 Freezing viable cells), re-injected into mice or used for different experiments.

4.2.9 Isolation of dormant and proliferating cells

Separating PDX cells into dormant label retaining cells (LRC) and fast proliferating non-LRC was performed within the FACS enrichment step (see 4.2.8 Enrichment of PDX cells by fluorescence-activated cell sorting (FACS)) by using two additional gates on CFSE positive or negative cells. To set the gate, CFSE intensity of CFSE labeled PDX cells either incubated for two to three days *ex vivo* or isolated from a mouse two to three days after injection was measured. Here major bleaching of CFSE was complete while a decisive CFSE indicated that proliferation was only minor or did not start yet. At day two or three the CFSE mean fluorescence intensity (MFI) was measured and defined as the absence of cell proliferation ("0 divisions"). Day three CFSE MFI was divided by factor two to calculate CFSE bisections mimicking cell divisions (Figure 4).

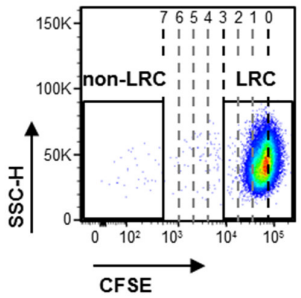

Figure 4: Gating strategy to define LRC and non-LRC gate

According to literature (Takizawa et al., 2011), seven CFSE MFI bisections were defined to correspond to the entire loss of the CFSE signal. Non-LRC were defined as all cells harboring CFSE content below seven CFSE MFI bisections. The LRC gate was set including all cells harboring high CFSE signal of below three CFSE MFI bisections so that a maximum of 3 cell divisions was allowed in LRC.

4.2.10 Calculation of cell number doubling times *in vivo*

For calculation of cell number doubling times *in vivo*, first absolute numbers of PDX cells re-isolated from bone marrow after at least three different days after cell injection were determined according to 4.2.8 Enrichment of PDX cells by fluorescence-activated cell sorting (FACS). Then, growing curves with a logarithmic y-axis for isolated PDX cells were calculated in GraphPad Prism 6. From the linear range of these curves linear regression lines were calculated in GraphPad Prism 6. With help of the linear regression lines, exact y values were calculated for day 3 and day 7. Afterward the growth rate μ was calculated by following formula:

$$\mu = \frac{(\ln y_7 - \ln y_3)}{(t_7 - t_3)}$$

y_7 = calculated y-value for day 7

y_3= calculated y-value for day 3

$t_7 = 7$

$t_3 = 3$

Finally the doubling time in days was calculated by following formula:

$$doubling\ time = \frac{\ln 2}{\mu}$$

4.2.11 Bioluminescence *in vivo* imaging

In vivo imaging was used to detect and follow up leukemia in mice. *In vivo* imaging is based on the bioluminescence through the oxidation of substrates by luciferase enzymes. Cells can be tracked by cloning luciferase systems into these cells, the application of the respective substrates and the follow up detection of the emitted light by ultra-sensitive cameras (Kim et al., 2015).

The gaussia luciferase gene was originally cloned from the marine copepod *Gaussia prince*. It catalyzes the oxidation of coelenterazine in the present of oxygen. The light emission through the reaction ranges from 480 to 600 nm (Kim et al., 2015).
The firefly luciferase gene was originally cloned from the North American firefly *Photinus pyralis*. It catalyzes the oxidation of D-luciferin in the presence of ATP, Mg^{2+} and oxygen and thereby emits light with a peak at 562 nm (Kim et al., 2015; Rabinovich et al., 2008).

For *in vivo* imaging of NSG mice engrafted with PDX cells expressing gaussia or a recombinant codon-optimized form of firefly luciferase (effluc), the IVIS Lumina II Imaging System was used as previously described (Barrett et al., 2011; Bomken et al., 2013; Terziyska et al., 2012). Mice were anesthetized with isoflurane and immobilized in the imaging chamber.
For imaging of PDX cells expressing gaussia luciferase, coelenterazine, dissolved in acidified methanol to a final concentration of 10 mg/ml, was used. Shortly before injection, 10 µl (= 100 µg coelenterazine) was diluted in 200 µl sterile glucose-containing Hepes buffer and injected into the tail vein. Immediately after injection, mice were imaged for 15 seconds using a field of view of 12.5 cm with binning 8, f/stop 1 and open filter setting. Depending on imaging signal binning and f-stop were adjusted.
For imaging of PDX cells expressing effluc (Rabinovich et al., 2008), D-Luciferin dissolved in sterile PBS to a final concentration of 30 mg/ml was injected at 150 mg/kg into the tail vein. Pictures were taken immediately for 15 sec or up to two minutes using a field of view of 12.5 cm with binning 8, f/stop 1 and open filter setting. Depending on imaging signal binning and f-stop were adjusted.
The Living Image software 4.4 was used for data acquisition and quantification of light emission.

4.2.12 *In vivo* treatment of mice

NSG mice were injected intravenously (i.v.) with $1x10^7$ PDX cells and were treated once or daily for three adjacent days starting on day seven after cell injection.
Drug concentrations for treatment of mice were calculated from clinically relevant concentrations converting the human doses to mouse equivalent doses based on body surface area (Sharma and McNeill, 2009). Therefore first the human dose in mg/m^2 was converted into the human dose in mg/kg using the human k_m factor of 37:

$$human\ dose\ in\ \frac{mg}{kg} = \frac{human\ dose\ in\ \frac{mg}{m^2}}{37}$$

Next the human dose in mg/kg was converted into the mouse equivalent dose in mg/kg using the conversion factor 12.3:

$$murine\ dose\ in\ \frac{mg}{kg} = human\ dose\ in\ \frac{mg}{kg}\ x\ 12.3$$

Control animals received PBS intraperitoneal (i.p.) or i.v. and all cytotoxic drugs were diluted in sterile PBS. Vincristine (VCR), etoposide (ETO), cyclophosphamide (CYCLO), cytarabine (ARA-C), amsacrine (AMSA), epirubicin (EPI), and DaunoXome (DNX) were used for treatment of mice depending on injected sample. Unless otherwise noted, the treatment scheme listed in Table 3 were applied.

Mice were taken down 3 days after treatment start, bone marrow was collected, and PDX cells were isolated (4.2.6 Isolation of PDX cells from mouse bone marrow) and analyzed (4.4.7 Flow cytometry analysis).

Table 3: Treatment scheme of mice injected with PDX samples

sample	drug	concentration [mg/kg]	application
ALL-199	VCR	2	once, i.v.
	ETO	75	once, i.p.
ALL-265	CYCLO	150	once, i.p
	ETO	75	once, i.p
ALL-50	ETO	33	daily over 3 days, i.p.
	ARA-C	150	daily over 3 days, i.p.
	AMSA	25	daily over 3 days, i.p.
	EPI	25	once, i.p
ALL-435	ETO	33	daily over 3 days, i.p.
	AMSA	15	daily over 3 days, i.p.
	EPI	20	daily over 3 days, i.p.
all AML	combination treatment DNX & ARA-C	DNX: 20 ARA-C: 150	DNX: once, i.v. ARA-C: daily over 3 days, i.p.

4.2.13 Limiting dilutions transplantation assay (LDTA)

NSG mice were injected i.v. with limiting numbers of PDX cells. Development of leukemia was monitored by bioluminescence *in vivo* imaging (see 4.2.11 Bioluminescence *in vivo* imaging) every 7 to 14 days after cell injection or by quantification of human cells in peripheral mouse blood (see 4.2.3 Flow cytometry of human cells in mouse peripheral blood) every second week. Here, first the mice with the highest amount of injected cells were analyzed. When these mice showed a positive engraftment, mice who received the next dilution were analyzed too. Leukemia initiating cells (LIC) frequencies were determined according to Poisson statistics, using the ELDA software application (http://bioinf.wehi.edu.au/software/elda/) (Hu and Smyth, 2009).

4.2.14 5-Bromo-2'-desoxyuridine (BrdU) labeling of proliferating PDX DNA

To label DNA of proliferating PDX cells with BrdU, mice engrafted with PDX cells were fed with BrdU-containing drinking water (0.8 mg/ml) during the last seven days before cell isolation. BrdU was dissolved in H_2O to a concentration of 12 mg/ml and stored at 4 °C. BrdU solution was diluted in drinking water of mice to a final concentration of 0.8 mg/ml every day, as BrdU is unstable at room temperature.

4.3 Genetic engineering of PDX cells

All genetic engineering procedures and constructs were approved by the Regierung von Oberbayern (written approvals September 2008, number 55-8791-8.549.1460, January 2010, number 55-8791-8.549.1562, and June 2016, number 55.1-8791-8.549.2261. All work with lentiviruses was performed under S2 conditions.
For genetic engineering of PDX cells, a third generation lentivirus system was used (Dull et al., 1998; Zufferey et al., 1999).

4.3.1 Lentivirus production in HEK-293T cells

For production of lentiviruses, the adherent cell line HEK-293T was used as packaging cell line. HEK-293T cells were grown in DMEM medium in a 75 cm^2 culture flask. When cells reached 50-80 % confluency, medium was exchanged and transfection solution was prepared. For this purpose the packaging plasmids 392 (2.5 µg), 393 (5 µg) and pMD2.G (1.25 µg) and the respective transfer vector (2.5 µg) were mixed with 24 µl Turbofect and filled up with DMEM to a final volume of 1 ml. The solution was incubated for 20 min at RT and afterwards added dropwise to the cells in one culture flask. After incubation for three days cell suspension was transferred into a Falcon tube and centrifuged (400 g, 5 min, RT). Supernatant was filtered through a 0.45 µm filter and concentrated by centrifugation (2000 g, 30 min, RT) using Amicon-Ultra 15 centrifugal filter units until a remaining volume of 200-250µl. The concentrated virus was frozen in aliquots of 10 µl and stored at -80 °C.

4.3.2 Determination of lentivirus titer

For quality monitoring, the virus titer of the produced lentiviruses (see 4.3.1 Lentivirus production in HEK-293T cells) was determined on Nalm-6 cells. 0.5 x 10^6 cells in 0.5 ml RPMI were plated in 5 wells of a 24-well plate. Increasing amounts of virus (control, 1 µl, 3 µl, 10 µl,

25 µl) and 8 µg/ml polybrene were added to the cells. 4 days after transduction, cells were washed three times with PBS (400 g, 5 min, RT) and the percentage of positive transduced Nalm-6 cells was determined by flow cytometry (see 4.4.7 Flow cytometry analysis) for each virus concentration. The virus titer was calculated by following formula:

$$virus\ titer = \left(\frac{F \cdot Z}{V}\right) TU/ml$$

F = % of transduced cells
Z = number of cells at infection
V = Volume of virus in ml

For this study virus titer between 10^8 TU/ml and $3x10^8$ TU/ml were used.

4.3.3 Lentiviral transduction of PDX cells

10^7 freshly re-isolated PDX cells were resuspended in 1 ml of medium for cultivation of ALL PDX cells or medium for cultivation of AML PDX cells were plated in a 6-well plate. 20 µl of virus (see 4.3.1 Lentivirus production in HEK-293T cells) containing the required transgene(s) and 8 µg/ml polybrene were added to the cells. 24 h after transduction, cells were washed three times with PBS (400 g, 5 min, RT), re-suspended in 100 µl PBS and injected into a mouse. Transduction rate was assessed by determining percentage of transgene expression by flow cytometry (see 4.4.7 Flow cytometry analysis).

4.3.4 FACS sorting to enrich genetically engineered cells

For enrichment of transgene expressing cells (see 4.3.3 Lentiviral transduction of PDX cells) sorting via a BD FACSAriaIII was performed. Freshly isolated (see 4.2.5 Isolation of PDX cells from mouse spleen or 4.2.6 Isolation of PDX cells from mouse bone marrow) or thawed (see 4.4.3 Thawing cells) PDX cells were filtered through a 70 µm cell strainer. PDX cells which were transfected with pCDH-EF1α-NGFR were stained for NGFR (see 4.4.6 Antibody staining of cells and staining of dead cells). Afterwards cells were washed with PBS (400 g, 5 min, RT). PDX cells were re-suspended in PBS or PDX short-term storage medium to a concentration of 10^7 cells/ml. Cells were stained with DAPI to exclude dead cells (see 4.4.6 Antibody staining of cells and staining of dead cells). For sorting a 100 µm nozzle and the adjustment “purity”

was used. The cells were sorted into medium for cultivation of ALL PDX cells or PBS supplemented with 10 % FCS.

4.4 *Ex vivo* methods

4.4.1 Determination of cell numbers

Cell numbers were determined by a "Neubauer" counting chamber.
From cell solutions a suitable concentration from 0.25 x 10^6 cells/ml to 1 x 10^6 cells/ml was prepared and 10 µl were filled into the counting chamber covered with a glass cover. Using a light microscope, cells in all 4 squares were counted. Here cells touching the lower and right limits were included, unlike cells touching the upper and left limit. If number of counted cells in all 4 squared was below 100, the cell concentration was too low. If number of counted cells in all 4 squared was above 400, the concentration was too high.
For counting living cell, cell dilutions were mixed 1:1 (v/v) with 0.4 % trypan blue (w/v) before filling them into the counting chamber. Under the microscope living cells appear colorless and bright whereas dead cells were stained blue.
Cell concentration was calculated as follows:

$$cell\ concentration = (mean\ of\ counted\ cells)\ x\ (dilution\ factor)\ x\ 10^4\ cells/ml$$

4.4.2 Freezing viable cells

Cells for later sorting (see 4.3.4 FACS sorting to enrich genetically engineered cells) were frozen at 5 x 10^7 cells/ml and all other cells were frozen at 10^7 cells/ml. Cell pellets were re-suspended in 0.5 ml FCS per cryotube. Afterwards 0.5 ml freezing medium (80 % FCS + 20 % DMSO v/v) per cryotube were prepared and added dropwise to the cell suspension. 1 ml of the cell suspension was transferred into each cryotube. For a cooling rate of 1°C/min, cryotubes were placed into a freezing container, filled with isopropyl alcohol and stored at -80 °C. After 24 h cryotubes were removed from freezing container and either stored at -80 °C for short term storage or in liquid nitrogen at -196 °C for long-term storage.

4.4.3 Thawing cells

To obtain cells with high viability, they were thawed by the thawing protocol of Dominique Bonnet (Bonnet, 2008).

Frozen cells (see 4.4.2 Freezing viable cells) were rapidly thawed in a 37 °C water bath. 100 µl DNase (1 mg/ml) were added dropwise to the thawed cells and mixed. Cells were transferred into a 50 ml tube and 1 ml FCS was added dropwise. After waiting for 1 min 10 ml PBS supplemented with 2 % FCS was added slowly. After waiting for 1 min cell suspension was slowly filled up to 30 ml with PBS + 2 % FCS. Afterwards cells were centrifuged (200 g, 4 min, RT).

4.4.4 *Ex vivo* culture of PDX cells

For *ex vivo* culture, PDX cells were diluted in medium at a concentration of 10^6 cells/ml. ALL PDX cells were incubated in medium for cultivation of ALL PDX cells and AML PDX cells in medium for cultivation of AML PDX cells. Cells were transferred into well plates and incubated at 37 °C, 5 % CO_2.
Ex vivo culture of PDX cells did not exceed three days, therefore no medium change was necessary.

4.4.5 5-(6)-Carboxyfluorescein-Succinimidyl Ester (CFSE) staining of cells

For labeling cells with 5-(6)-Carboxyfluorescein-Succinimidyl Ester (CFSE), freshly isolated PDX cells were suspended in pre-warmed (37 °C) PBS supplemented with 0.1 % BSA at a concentration of 10^6 cells/ml. Carboxyfluorescein diacetate succinimidyl ester (CFDASE) was suspended in DMSO to a concentration of 5 mM. Afterwards the diluted CFDASE was added to the cell suspension to a final concentration of 10 µM and incubated for 10 minutes at 37 °C. After incubation the staining was stopped by adding five times the original staining volume of cold RPMI supplemented with 10 % FCS and incubation for 5 min on ice. This step removes any free dye. Cells were centrifuged (400 g, 5 min, RT) and re-suspended in PBS for direct injection into recipient mice, or in appropriate medium.

4.4.6 Antibody staining of cells and staining of dead cells

A NGFR staining

PDX cells transfected with pCDH-EF1α-NGFR, were stained with 5 µl/100 µl CD271hu-PerCP/Cy5.5 (NGFR) antibody for 30 min at 4 °C.

B muCD45 staining

Bone marrow suspension (4.2.6 Isolation of PDX cells from mouse bone marrow) was diluted in PBS to a concentration of 4 x 10^8 cells/ml, stained 1:100 (v/v) with CD45mu-APC-Cy7 antibody and incubated for 30 min at 4 °C.

C 5-Bromo-2'-desoxyuridine (BrdU) staining

The detection of BrdU incorporation was performed according to maufacturer's instructions of the BrdU Flow Kit (3.6 Kits).

D 4',6-diamidino-2-phenylindole (DAPI) staining

To exclude dead cells 10 µg/ml DAPI was added to the cell suspension immediately prior to measurement.

After incubation time cells were washed with PBS (400 g, 5 min, RT) and re-suspended in PBS to a final concentration of 10^7 cells/ml.
Stained cells where analyzed by flow cytometry, using either a BD LSRFortessa or a BD FACSAriaIII (see 4.4.7 Flow cytometry analysis).

4.4.7 Flow cytometry analysis

Flow cytometry analyses were performed using a BD LSRFortessa, a BD FACSAriaIII, or a BD FACSCalibur. Fluorescent proteins (mKate, mCherry) and other fluorochromes (APC-Cy7, PerCP-Cy5.5, DAPI,) were measured using the laser and filter settings indicated in Table 4. PDX samples were gated for living cells in FSC/SSC and for respective fluorochromes.

Table 4: Filter settings of flow cytometry

Laser [nm]	Longpass Filter [nm]	Bandpass Filter [nm]	Parameter
LSRFortessa			
355	505	525/50	Indo-1
		450/50	DAPI
405	595	605/12	Qdot 605
	475	525/50	Qdot 525
		450/50	Pacific Blue
488	600	695/40	PerCP-Cy5.5

	505	530/30	FITC, CFSE
		499/10	SSC
561	750	780/60	PE-Cy7
	685	710/50	PE-Cy5.5
	635	670/30	PE-Cy5
	600	610/20	mCherry
	570	585/15	PE
640	750	780/60	APC-Cy7
	710	730/45	Alexa Fluor 700
		670/14	APC-Cy7
FACSAriaIII			
375/405	735	780/60	Qdot710
	610	616/23	Qdot605
	556	584//42	PacOrange
	502	530/30	Cerulan
		450/40	DAPI
488	655	695/40	PerCP-Cy5.5
	502	530/30	FITC, CFSE
		488/10	SSC
561	735	780/60	PE-Cy7
	630	670/14	PE-Cy5
	600	610/20	mCherry, mKate
		582/15	PE
633	735	780/60	APC-Cy7
		660/20	APC
FACSCalibur			
488		488/10	SSC
		530/30	FL1 FITC
		585/42	FL2 PE
		>670	FL3 PerCP
635		661/16	FL4 APC

4.5 Statistics

Two-tailed unpaired t-test was applied to determine the significance of relative reduction rates upon drug stimulation. F-test was applied to compare variances and in cases in which variances differed significantly, Welch's correction was employed. All statistical analyses were calculated using GraphPad Prism 6 software.

LIC frequencies were calculated according to Poisson statistics using the ELDA software application (http://bioinf.wehi.edu.au/software/elda) (Hu and Smyth, 2009).

5 Results

Drug resistant cells that survive treatment might induce relapse in acute leukemias (AL) patients and therefore represent a major obstacle for curing AL. It remains a major challenge to isolate high numbers of drug resistant cells directly from patients as these cells are very rare; therefore, data on the functional characteristics of these important cells does not exist in the literature.
To overcome this obstacle, the patient-derived xenograft (PDX) model was used to study patients' tumor cells *in vivo* (Kamel-Reid et al., 1989; Liem et al., 2004; Shultz et al., 2005). The aim was to identify, isolate and characterize drug resistant cells with relapse-inducing potential from patients' AL samples, using their *in vivo* resting phenotype as anchor.
The following result section is divided into three parts; first, the optimization and the establishment of two methods to isolate minute amounts of PDX cells out of mouse bone marrow is described. Second, data are presented which reveal the presence of long-term resting PDX cells in patient samples of diverse leukemia subtypes. Third and last, certain functional properties of long-term resting PDX cells are described.
These results will help to understand relapse-inducing cells in more detail and to ultimately develop treatment strategies to target relapse-inducing cells for a better prognosis of AL patients.

5.1 Pool of transfected AL samples

The overall study on dormant ALL cells was started by Sebastian Tiedt who mainly worked with two high risk relapse samples ALL-199 and ALL-265 (Tiedt, 2014). Therefore the current work was started by establishing a broader pool of PDX AL cells with the aim to be more representative for the heterogeneity within AL. Cells from different patients, with different AL subtypes and at different stages of disease were chosen for the experiments. Table 6 and Table 5 show the five AML and the four ALL PDX samples that were used for the main experiments within this study. Information on all further samples that were used in this study is shown in Table S 2 and Table S 1.

Table 5: Clinical data of AML patients and sample characteristics of AML PDX samples used for main experiments.

sample	ELN classification	disease stage*	age* [years]	sex	passaging time§ [days]	transgenic for
AML-346	adverse	1st relapse	1	f	47	mCherry, luciferase
AML-372	adverse (complex karyotype)	1st relapse	42	m	87	mCherry, luciferase, NGFR
AML-388	adverse (MLL rearranged)	initial diagnosis	57	m	43	mCherry, luciferase
AML-393	adverse (MLL rearranged)	1st relapse	47	f	39	mCherry, luciferase
AML-491	cytogenetic abnormalities not classified as favorable or adverse	1st relapse	53	f	47	mCherry, luciferase

*when the primary AML sample was obtained; §time of passaging through mice refers to the time from injection of the sample until mice had to be sacrificed due to end stage leukemia; ELN = European Leukemia Net; MLL = mixed lineage leukemia; f = female; m = male

The passaging time in mice, defined as the days from injection of around 10^7 cells per mouse until mice had to be sacrificed due to end stage leukemia, was between 30 and 130 days with an average of 66 days for AML and 59 days for ALL samples. Furthermore and for time saving reasons, all but one sample had passaging times below 50 days limiting the aim to represent the heterogeneity of AL.

For the main experiments in AML, samples expressed mCherry and luciferase were used to facilitate enrichment from mouse bone marrow. The transgenes had already been expressed in the PDX cells by other laboratory group members before. For the main experiments in ALL, samples expressing mCherry, luciferase and/or NGFR were used. mCherry transfection was performed for these samples within this study.

Table 6: Clinical data of ALL patients and sample characteristics of ALL PDX samples used for main experiments.

sample	type of ALL	disease stage*	age* [years]	sex	passaging time§ [days]	transgenic for
ALL-50	BCP-ALL pediatric	initial diagnosis	7	f	45	mCherry, luciferase
ALL-199	BCP-ALL pediatric	2nd relapse	8	f	42	mCherry, luciferase, NGFR
ALL-265	BCP-ALL pediatric	1st relapse	5	f	30	mCherry, luciferase, NGFR
ALL-435	BCP-ALL pediatric	initial diagnosis	<1	m	40	mCherry, luciferase

*when the primary ALL sample was obtained; §time of passaging through mice refers to the time from injection of the sample until mice had to be sacrificed due to end stage leukemia; BCP = B-cell precursor; f = female; m = male;

5.2 Isolation of minute numbers of PDX cells from mouse bone marrow

Minute numbers of treatment resistant cells might be responsible for relapse in patients. To improve treatment and prognosis of patients, investigations on these cells are necessary, but technical limitation hampered functional characterization of these challenging cells so far. The present study used the PDX AL model and concentrated on the first 3 weeks of AL growth in mice. Here, the low tumor burden is mainly restricted to bone marrow without major involvement of further organs (Barrett et al., 2011; Bomken et al., 2013) and reliable isolation, enrichment and detection of very low numbers of PDX cells from mouse bone marrow was necessary (Figure 5).

When 10^7 ALL-199 PDX cells were injected into two mice and re-isolated after two or 42 days from mouse bone marrow, huge differences in the number of PDX cells became visible. After two days, human cells were measured which had successfully homed to the bone marrow which were only a 0.21 % of all living mononuclear cells in mouse bone marrow after transplantation

of ALL-199, whereas after 42 days 91.6 % of all living mononuclear cells in mouse bone marrow were human (Figure 5).

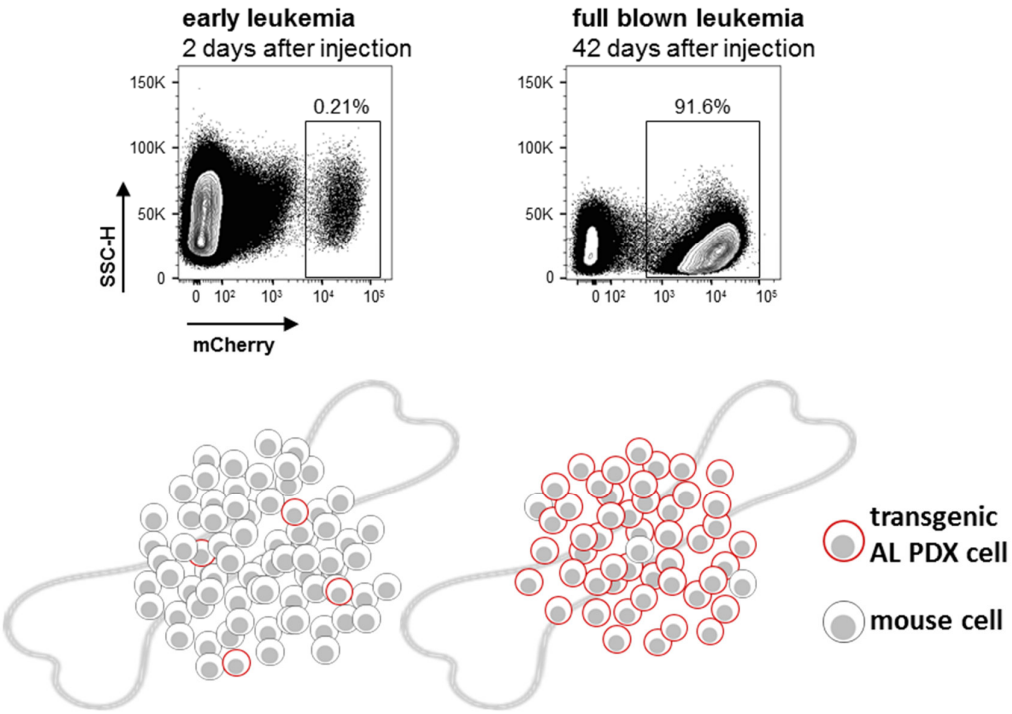

Figure 5: Minute numbers of PDX cells exist at early time points in the mouse bone marrow
Upper panel: original FACS data of mouse bone marrow cells, gated on the living lymphocyte population ($DAPI^-$) two and 42 days after injection of 10^7 ALL-199 PDX cells. Lower panel: scheme indicating that at early time points after injection of AL PDX only minute numbers of human PDX can be detected in the mouse bone marrow, whereas full blown leukemia consist of nearly 100 % human PDX cells in mouse bone marrow.

For isolation and enrichment of low numbers of PDX cells from mouse bone marrow, cells transgenic for NGFR and a fluorochrome were used in the enrichment method established by Sebastian Tiedt (Tiedt, 2014).

Transgenes allowed the effective enrichment of PDX cells from mouse bone marrow in a twostep procedure. A first enrichment step consisted in magnetic cell separation (MACS) of NGFR-expressing PDX ALL cells from the entire mouse bone marrow isolated. The second consecutive enrichment step consisted in flow cytometry enrichment of red fluorescent protein mKate expressing cells out of the cell suspension obtained after MACS enrichment. Here cells obtained after MACS enrichment were stained with DAPI to exclude dead cells and with anti-muCD45 antibody to exclude mouse hematopoietic cells (see 4.2.7 Enrichment of PDX cells by magnetic cell separation (MACS) and 4.2.8 Enrichment of PDX cells by fluorescence-activated cell sorting (FACS)).

Within this work the NGFR MACS FACS procedure was optimized to save time and material. As the red fluorescent protein mKate used by Sebastian Tiedt was not bright enough to clearly discriminate between transfected and non-transfected cells, cells were transfected with mCherry, as this fluorochrome has higher mean fluorescent intensity (MFI) (Figure 6).

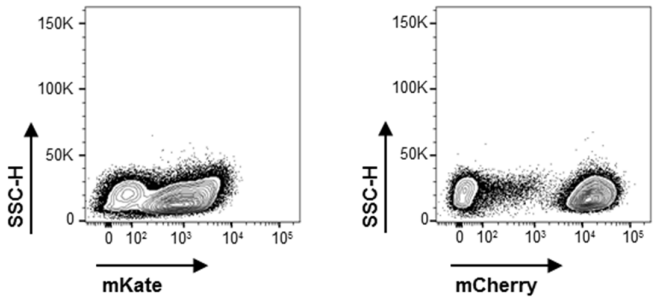

Figure 6: The red fluorescent protein mCherry has higher MFI than the red fluorescent protein mKate
10^7 ALL-199 PDX cells expressing mKate or mCherry were injected i.v. into mice, and after 10 days re-isolated from mouse bone marrow and analyzed for red fluorescent color.

For mKate alone it was not possible to clearly separate the positive PDX population from the negative mouse population by FACS. PDX cells expressing mCherry could be reliably identified in flow cytometry, and no additional anti-muCD45 staining was necessary to discriminate human from mouse cells (Figure 6). In addition, a titration of the magnetic anti-NGFR beads was performed, to reduce cost. $4x10^8$ whole bone marrow cells isolated from leukemia-free NSG mice were mixed with $8x10^5$ ALL-199 PDX cells expressing mCherry and NGFR, and with different amounts of magnetic anti-NGFR beads. As highest amount of beads the company instruction (800µl) was used. For titration steps different amounts of beads until 1/80 of company instructions (10µl) were added to the cell suspension.

Afterwards MACS-based enrichment was performed on the mixtures, and collected cells were measured and quantified by flow cytometry gating (i) on the lymphocyte gate in forward/side scatter and (ii) the gate negative for DAPI and positive for mCherry (Figure 7).

The graph in Figure 7 shows clearly that no cell loss was obtained if at least 100 µl of beads were used. When less beads were used the amount of isolated PDX cells decreased. To avoid cell loss during the enrichment steps, 200 µl of anti-NGFR beads were used for all further experiments. By reducing the amount of required beads by factor 4, the cost for beads could be reduced by factor 4 and thus substantially.

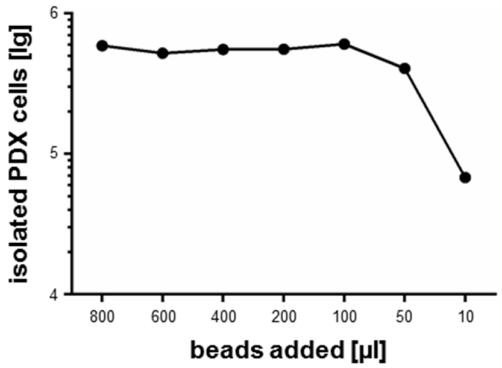

Figure 7: Optimization of NGFR MACS procedure
$4x10^8$ mouse bone marrow cells were mixed with $8x10^5$ ALL-199 PDX cells expressing mCherry and different amounts of magnetic anti-NGFR beads; MACS-based enrichment by NGFR was performed and collected cells were measured by flow cytometry. Total amount of mCherry positive cells was quantified by flow cytometry.

As a second approach and to spare the second lentiviral transduction step for the expression of recombinant NGFR, a MACS based enrichment method which was independent of NGFR expression and instead used a newly commercially available so called "mouse cell depletion kit, which came on the market 2014. Here mouse cells from the bone marrow were captured by a commercial available mix of mouse antibody beads. During magnetic separation labeled mouse cells are captured in the columns and unlabeled cells were directly collected (Agorku et al., 2014). After this altered MACS enrichment step 1, further enrichment was performed by flow cytometry targeting on the transgenic mCherry identically as described above. To establish this enrichment method, the required amount of mouse cell depletion beads were determined by titration: $4x10^8$ mouse bone marrow cells were mixed with $8x10^5$ mCherry expressing PDX cells and different amounts of magnetic beads. Theoretically, if lower amounts of beads are used, lower amounts of mouse cells are captured and therefore the negative fraction including the human PDX cells would increase. Therefore here the read out was the measurement time at the flow cytometer for the negative fraction. To perform experiments with four mice on one day, measurement time of one mouse should not exceed one hour (Table 7).
Table 7 shows that all tested amounts of beads lead to measurement times below one hour. To save material the lowest amount of beads (100µl) was used for all further experiments.

Table 7: Optimization of mouse cell depletion MACS to enrich minute numbers of PDX cells from mouse bone marrow cells

mixed			*read out by flow cytometry*		
number of mouse bone marrow cells	PDX in mouse bone marrow cells [%]	beads added [µl]	number of cells DAPI$^-$ mCherry$^+$	events measured	time for measurement [min]
4x10^8	0.2	600	77,891	0.23x10^7	5
4x10^8	0.2	400	142,034	2.06x10^7	45
4x10^8	0.2	200	216,709	2.86x10^7	55
4x10^8	0.2	100	247,049	1.67x10^7	35

Next, the mouse cell depletion method was validated, to ensure that it can isolate minute numbers of PDX cells from mouse bone marrow. Different numbers of mCherry expressing PDX cells were mixed with mouse bone marrow cells followed by the new enrichment procedure to quantify recovered PDX cell (Table 8).

Table 8: Twostep procedure with mouse cell depletion MACS allows enrichment of minute numbers of PDX cells from mouse bone marrow

mixed			*recovered*		
number of mouse bone marrow cells	number of PDX cells	PDX in mouse bone marrow cells [%]	number of cells (DAPI$^-$ mCherry$^+$)	recovery [%]	enrichment factor
4x10^8	0	0	6	-	-
2x10^8	300	0.00015	174	51	1,149,425
2x10^8	1,000	0.00050	324	29	617,283
2x10^8	3,000	0.00150	817	26	244,798
2x10^8	10,000	0.00500	3,492	32	57,273

A mouse bone marrow from a mouse without injected or mixed in PDX cells only showed 6 false positive events in the DAPI$^-$ mCherry$^+$ population. This background amount was always subtracted from all measured mCherry positive PDX samples to determine the absolute amount of PDX cells. Using the new enrichment protocol, as few as 174 PDX cells could be re-isolated out of 2x10^8 normal mouse bone marrow cells and therefore enabled cell enrichment of a factor well above 10^6 with little cell losses. This enrichment procedure could reliably be used for

further experiments to detect and isolate very few PDX cells in mouse bone marrow. The two enrichment protocols will referred to as NGFR MACS and MCD (mouse cell depletion) MACS throughout the text.

Next both enrichment techniques were compared to ensure that they do enrich and isolated PDX cells from mouse bone marrow with similar efficiency. $1x10^8$ mouse bone marrow cells were mixed with $4.2x10^4$ mCherry and NGFR expressing PDX cells. Duplicates were either enriched by NGFR MACS or by MCD MACS and total amount of PDX cells were determined using flow cytometry targeting mCherry expressing cells (Table 9).

Table 9: MCD MACS can substitute NGFR MACS

mixed				*recovered by flow cytometry*	
method	**mouse bone marrow cells**	**PDX cells added**	**PDX in mouse bone marrow cells [%]**	**number of cells $DAPI^-$ $mCherry^+$**	**recovery [%]**
NGFR MACS	$1x10^8$	42,000	0.42	34,016	81
NGFR MACS	$1x10^8$	42,000	0.42	33,217	79
MCD MACS	$1x10^8$	42,000	0.42	30,187	72
MCD MACS	$1x10^8$	42,000	0.42	28,169	67

Table 9 shows that both methods can recover between 67 % and 81 % of added PDX cells. Therefore, MCD MACS was used for all further experiments in NGFR negative PDX samples. Taken together, two different techniques to isolate minute numbers of transgenic PDX cells from mouse bone marrow were established or optimized and serve as basis for further isolation and characterization of challenging subpopulations in AL.

5.3 Growth behavior of PDX cells in mice

The established procedures enabled addressing basic questions with translational potential in AL biology. Investigations on leukemia biology were performed at diagnosis, meaning at late

time points of the disease, during treatment process or at relapse (De Kouchkovsky and Abdul-Hay, 2016; Pui et al., 2015). Investigations on early leukemia development are missing. As a consequence little is known about the growth of leukemia in patients. But knowledge about the early growth, detailed kinetic and relapse of the leukemia would increase the understanding of the disease and would help to improve or develop new treatment strategies. Therefore, the *in vivo* growth behavior of different AL samples in mouse bone marrow was studied regarding homing and spontaneous growth.

5.3.1 Homing of PDX samples to mouse bone marrow

Homing is the process in which cells, systemically injected into the blood stream of animals, travel to their most appropriate niche. This process, intensively studied in normal hematopoiesis, elucidates rolling, adhesion, migration and the tumor-stroma interaction. As the hosting laboratory had reproduced that the bone marrow is the first site of homing for PDX AL cells in NSG mice (Terziyska et al., 2012; Vick et al., 2015), here the homing to mouse bone marrow was studied.

10^7 fresh ALL or AML cells from mice with advanced leukemia sacrificed on the same day were injected into the tail veins of next recipient mice and re-isolated three days later by applying one of the established enrichment methods. The time point of three days was chosen as the current study could show that cells did not proliferate within the first three days (see below Figure 13 and Figure 18), while removal of non-homed cells by the mouse phagocyte system should be completed by then.
In samples that did not express any transgenes, an alternative protocol was used; PDX AL cells were stained with CFSE (see 4.4.5 5-(6)-Carboxyfluorescein-Succinimidyl Ester (CFSE) staining of cells) before injection and analyzed directly by flow cytometry for CFSE positive cells. As cells could not be enriched by NGFR MACS prior to FACS analysis and FACS analysis was unfeasible for larger cell numbers, a portion of the bone marrow suspension was directly analyzed and absolute numbers of PDX cells were calculated thereof (Figure 8). However, after the MCD kit had been established this drawback was solved and mouse cells were removed by MACS before FACS measurement for samples not expressing transgenes (Agorku et al., 2014).

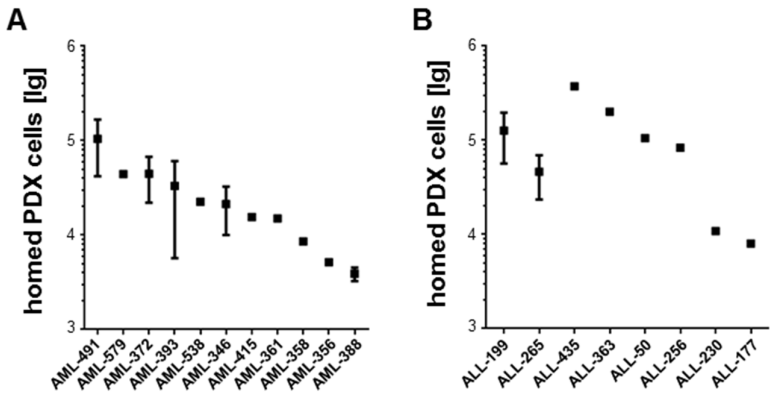

Figure 8: PDX samples differ broadly in their homing capacity to mouse bone marrow
10^7 AML (**A**) or ALL (**B**) PDX cells were injected i.v. into mice and re-isolated from the bone marrow three days later, and absolute cell number was measured; each dot represents data from one mouse, except that a mean of six mice plus standard error is shown for samples ALL-199 and ALL-265 and mean of up to three mice plus standard error is shown for samples AML-491, AML-372, AML-393, and AML-346.

Homing of 19 different PDX AL samples was measured and a maximum of 4 % of the injected PDX cells could be re-isolated from mouse bone marrow three days after injection (Figure 8). The eight different ALL samples and eleven AML samples showed highly different cell recruitment to bone marrow differing by more than two orders of magnitude with a minimum efficiency of only 0.01 % of injected cells homing to bone marrow in AML-388 and a maximum of 1.05 % in AML-491.

These data indicate that homing of fresh PDX AL samples to mouse bone marrow is an overall highly inefficient process, but similar between ALL and AML. Differences between the samples suggest that homing might depend on specific, yet undefined characteristics of individual samples.

Next, it was studied how the number of injected PDX cells might influence homing. Between 10^7 and 10^5 ALL-199 cells were injected i.v. into mice and re-isolated by NGFR MACS three days later (Figure 9). A maximum 10^7 cells were chosen for injection, as former experiments in the laboratory showed that injection of more than 10^7 cells lead to severe agglutination in mice.

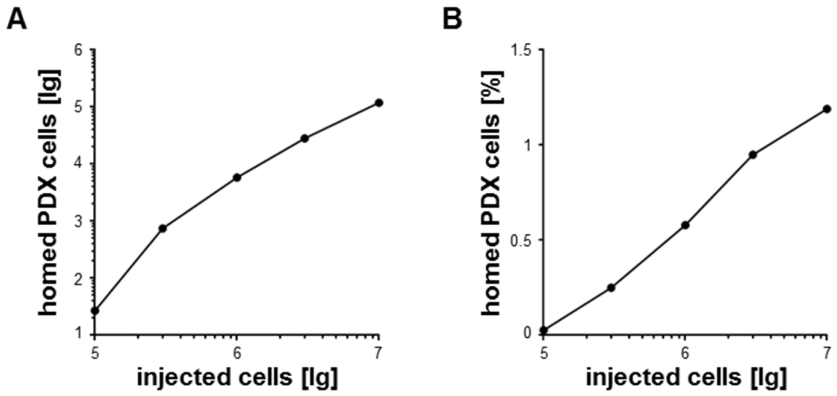

Figure 9: Homing to mouse bone marrow depends on the cell number injected
ALL-199 cells were injected i.v. into mice at different cell numbers and re-isolated by NGFR MACS after three days; each dot indicates data from one animal.
A Absolute number of homed PDX cells.
B Percentage of homed PDX cells.

The homing capacity into the mouse bone marrow strictly depended on the cell numbers injected. Surprisingly, when higher cell numbers were injected, homing efficiency increased. Injection of 10^7 cell lead to homing of 1.2 % of the injected cells, whereas the injection of 10^5 cells lead to a homing of 0.03 % of cells (Figure 9B).
To work with a maximum number of homed PDX AL cells per sample, 10^7 freshly isolated cells/mouse were injected in all further experiments.

These data argue against the existence of a preformed, fixed number of niche places present in the bone marrow of each NSG mouse, which are able to house PDX cells. These data strengthen the assumption, that specific characteristics of the individual leukemia sample and the cell number injected determine the ability of the cells to home to bone marrow.

5.3.2 *In vivo* growth of PDX cells in mouse bone marrow over time

For a more detailed knowledge about the growth of leukemia, the *in vivo* growth of PDX cells in mice was studied over time. Therefore, 10^7 PDX cells were injected i.v. into mice and followed by quantifying absolute numbers (Figure 10) or relative amount (Figure 11) of PDX cells in mouse bone marrow at different time upon *ex vivo* cell enrichments.

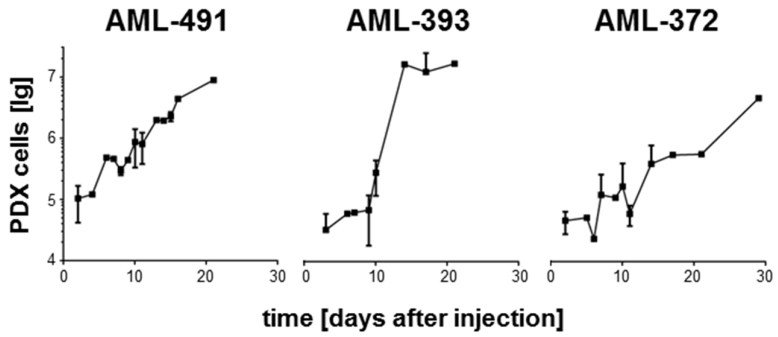

Figure 10: Growth curves of AML-PDX cells *in vivo* show early logarithmic growth in mouse bone marrow
10^7 CFSE stained PDX cells were injected i.v. at different time points up to five mice were analyzed and PDX cells were quantified; shown is mean +/- standard error.

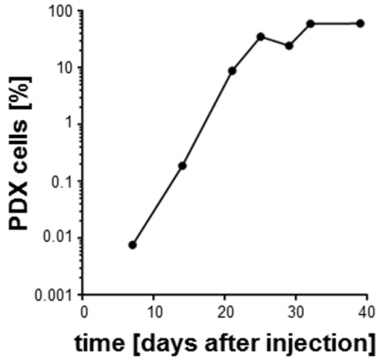

Figure 11: Percentage of PDX in bone marrow shows early logarithmic growth in mouse bone marrow
10^7 ALL-199 PDX cells were injected i.v. At different time points 10 % of mouse bone marrow was analyzed and percentage of PDX cells was calculated.

The growth of PDX AL cells in mouse bone marrow was logarithmic over the first weeks of *in vivo* growth, and growth slowed down thereafter when PDX cells reached only 10 % of total cells in mouse bone marrow. This growth behavior is called logistic growth (Araujo and McElwain, 2004; Schacht, 1980) and the same results had also been obtained for absolute numbers of ALL samples (Tiedt, 2014).

From samples which were isolated at least at three different time points, absolute PDX numbers were determined and doubling times were calculated thereof (see 4.2.10 Calculation of cell number doubling times *in vivo*) (Figure 12).

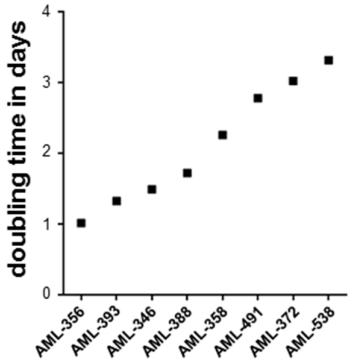

Figure 12: AML PDX samples differ broadly in their doubling times *in vivo*
10^7 AML PDX cells were injected i.v. into at least three mice and re-isolated from the bone marrow at different time points. From absolute numbers of re-isolated PDX cells doubling time in days per sample was calculated.

Doubling times were analyzed in eight different AML PDX samples and varied widely. The shortest time for a single duplication was one day, whereas the maximum time was 3.5 days in the eight samples studied.

Taken together new insights about leukemic growth were gained. PDX AL cells show sample-specific homing and doubling times followed by early logistic growth in mouse bone marrow.

5.4 A rare long-term dormant subpopulation exists in PDX cells

Surviving malignant cells after therapy are a major obstacle in the cure of ALL and AML as they might induce deadly relapse (Blatter and Rottenberg, 2015; Gokbuget et al., 2012b; Ommen, 2016). A reason for therapy resistant cells might be their dormant state (Aguirre-Ghiso, 2007; Essers and Trumpp, 2010; Schillert et al., 2013). The hosting laboratory decided using long-term dormancy as an anchor to get their hands onto relapse-inducing cells before this study started. Towards this aim, Sebastian Tiedt had established a method using the proliferation-sensitive dye 5-(6)-Carboxyfluorescein-Succinimidyl Ester (CFSE) which had already been used in mouse model studies on healthy hematopoiesis or AML, e.g., to characterize heterogeneous growth pattern and to identify dormant HSC (Takizawa et al., 2011; van der Wath et al., 2009). Sebastian Tiedt adapted the use of CFSE to studies on PDX ALL cells. Using three different samples, Sebastian Tiedt found for the first time that a rare subpopulation of long-term dormant cells exists in PDX ALL (Tiedt, 2014). The present work aimed next at broadening the existing data and studied additional PDX ALL samples for the existence of the long-term dormant subpopulation, including further ALL subtypes and PDX AML samples.

5.4.1 Establishing CFSE staining to follow up PDX AML proliferation *in vivo*

With the aim of optimizing the established protocol from Sebastian Tiedt and transferring it to PDX AML, 10^7 AML-491 cells were stained *ex vivo* with CFSE (see 4.4.5 5-(6)-Carboxyfluorescein-Succinimidyl Ester (CFSE) staining of cells) and were re-injected into next recipient mice. After 2, 10 and 16 days mouse bone marrow was collected from one mouse per time point and PDX cells were enriched by MCD MACS. Afterwards, PDX cells were analyzed targeting transgenic mCherry and the green CFSE dye to follow up proliferation in flow cytometry (Figure 13).

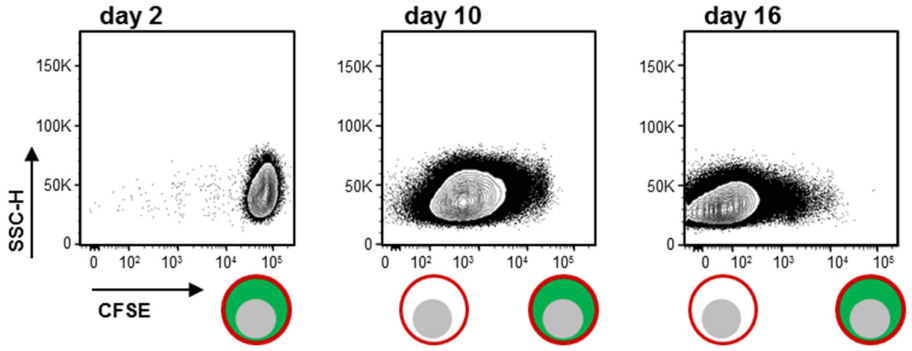

Figure 13: Loss of CFSE signal over time
10^7 AML-491 cells were injected into 3 mice and re-isolated by MCD MACS and analyzed by flow cytometry for the green CFSE dye at day 2, 10, and 14 after cell injection.

Two days after cell injection, all PDX cells in the mouse bone marrow were still CFSE positive. At later time points cells were slowly losing their CFSE label. The CFSE MFI was drifting from right to left. The distribution of the CFSE signal at later time points was broad, showing that not all cells participated identically in proliferation (Figure 13).

As BrdU incorporation is commonly used as proliferation marker and might be considered as "gold standard" to measure proliferation, CFSE labeling was validated as readout for measuring *in vivo* proliferation using a parallel BrdU staining (Figure 14).

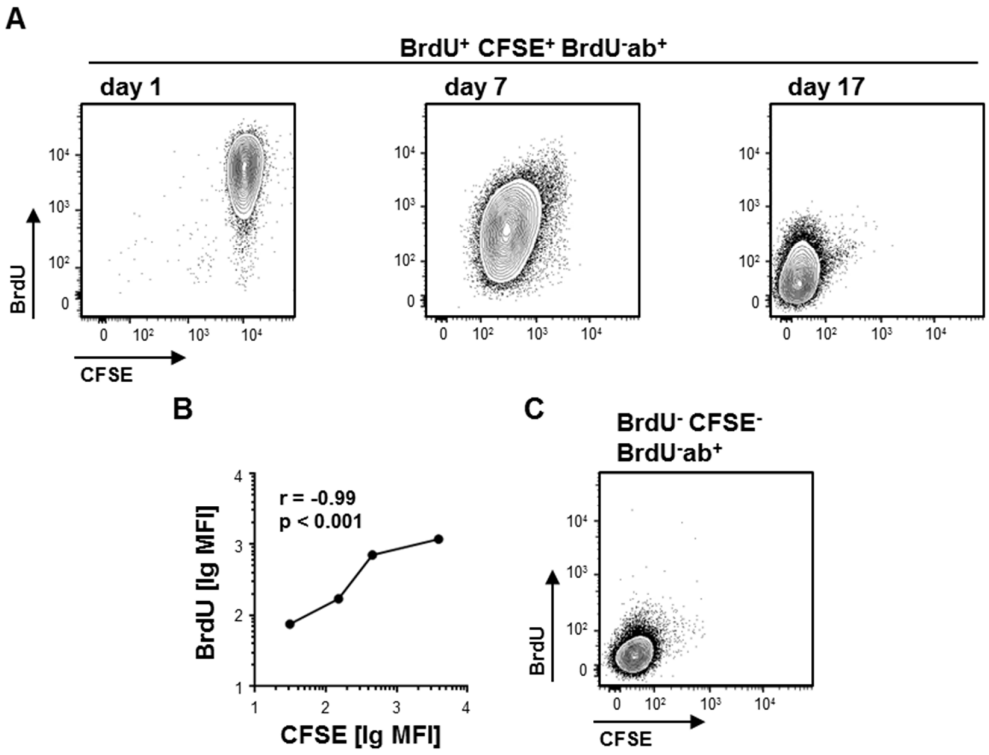

Figure 14: Loss of CFSE correlates with loss of BrdU
Donor mouse engrafted with ALL-265 was fed with drinking water containing BrdU (0.8 mg/ml) within the last seven days before cell harvesting. After re-isolation 10^7 cells were stained *ex vivo* with CFSE and were injected into four recipient mice. At days 1, 7, 10 and 17 mice were sscrified and PDX cells were isolated and quantified. "BrdU-ab" indicates that cells were stained with the anti-BrdU antibody; "+" and "-" indicate that the procedures were performed or not, respectively.
A Raw FACS data of three time points for BrdU and CFSE stainings.
B Correlation of BrdU positive and CFSE positive cells. Each dot represents data from one mouse.
C Exemplary FACS blots of control cells which were negative for BrdU and CFSE but stained with the BrdU antibody.

To stain leukemia cells with BrdU, a donor mouse was fed with BrdU the last 7 days before mice had to be taken down due to advanced leukemia. All leukemia cells re-isolated from the mouse spleen were BrdU positive, indicating strong proliferation in spleen at late time points. These cells were then stained *ex vivo* with CFSE, and 10^7 $CFSE^+$ and $BrdU^+$ PDX cells were injected i.v. into four mice. At different time points, mice were taken down and PDX cells were isolated and analyzed concerning BrdU and CFSE intensity. One day after cell isolation BrdU and CFSE signal are high. 7 and 17 days after cell injection both dyes lost the same amount of signal and the cell population is shifting from the right upper corner towards the left lower corner. The BrdU signal was from beginning on more egg shaped, most probably due to different BrdU take of in the donor mice before, and stays egg shaped for all time points (Figure 14A). When CFSE and BrdU negative control cells were stained with BrdU antibody, the cell population was still negative for both signals, indicating no false positive staining by the

antibody (Figure 14C). Graphical analysis of the BrdU and CFSE MFI shows tight correlation of the loss of CFSE with the loss of BrdU signal (Figure 14B). Therefore CFSE can substitute BrdU as proliferation marker for further experiments.

As additional quality control, loss of CFSE signal was correlated with cell quantity upon cell isolation (Figure 15).

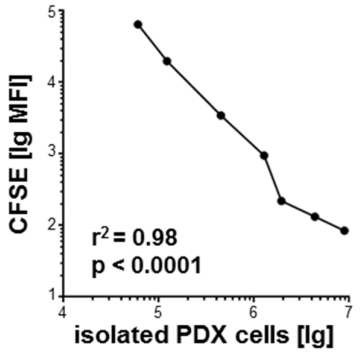

Figure 15: Loss of CFSE correlates to gain in cell numbers
10^7 CFSE stained PDX AML-491 cells were injected i.v. into mice and PDX cells were re-isolated and quantified from the bone marrow after 2, 4, 7, 10, 14, 16 and 21 days; each dot represents data from one mouse.

Here 10^7 CFSE stained PDX cells were injected i.v. into seven mice. PDX cells were re-isolated at different time points from day two on, quantified and analyzed for CFSE content. Figure 15 shows that increase in PDX cell numbers closely correlated with loss of CFSE signal.

As loss of CFSE staining closely correlates with both loss of BrdU staining and increase in absolute cell numbers, CFSE staining represents a reliable approach to monitor proliferation of PDX AML and ALL cells in mice.

5.4.2 Analyzing CFSE staining to detect dormant cells

Next, loss of CFSE was used to distinguish subpopulations of slowly and rapidly growing cells in AML and ALL. Therefore, gates for slowly and rapidly growing cells were defined as established by Sebastian Tiedt for ALL (Figure 16).

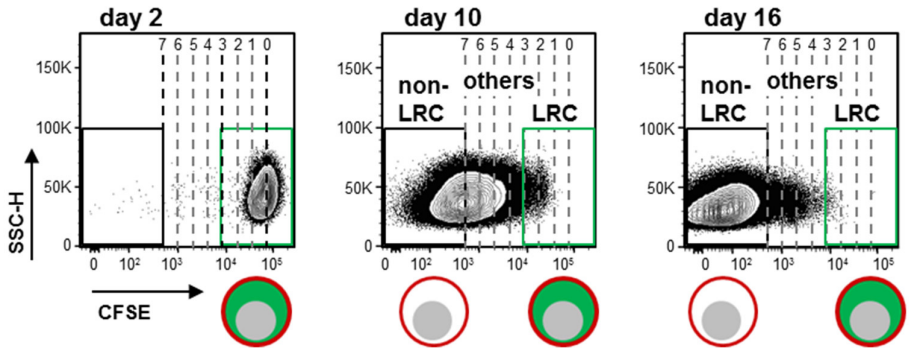

Figure 16: Gates defining label retaining cells (LRC) and non-label retaining cells (non-LRC)
MFI of CFSE at start of the experiment (2 or 3 days after cell injection) was divided by factor 2 to model bisections; upon less than 3 bisections, cells were considered as LRC, upon more than 7 bisections as non-LRC; intermediate cells were considered as "others". Shown are exemplary FACS blots with the calculated bisection lines of AML-491 at day 2, 10, and 14 after cell injection.

To set these gates and measure maximum CFSE mean fluorescence intensity (MFI), maximum CFSE intensity was measured at day 2 or 3 after injection. CFSE MFI was used to define start of any cell proliferation ("0 divisions"). CFSE bisections were calculated as surrogates for cell divisions by dividing CFSE MFI by factor 2. According to the use of the term in work on normal mouse hematopoiesis, cells were called label-retaining cells (LRC), if they had undergone less than 3 bisections of maximum CFSE MFI indicating dormant cells (Schillert et al., 2013). Cells that entirely lost CFSE and contained less CFSE than 7 bisections of maximum CFSE MFI were called non-LRC, indicating proliferating cells (Figure 16).

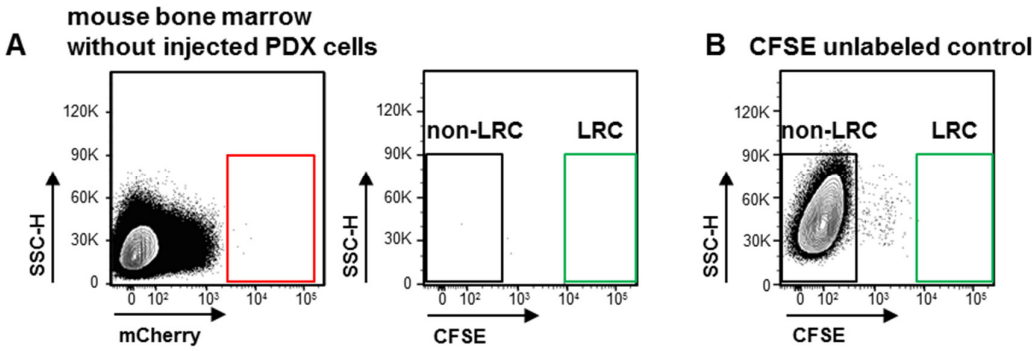

Figure 17: Controls for enrichment method with MCD MACS and CFSE staining
A MCD MACS was performed with a mouse bone marrow without prior application of PDX cells. Only six cells were detected in the mCherry gate but no cells in the LRC gate.
B MCD MACS was performed with a femur of a fully engrafted mouse without prior CFSE labeling of AML-491 PDX cells. No cells were found in the LRC gate**.**

Additional quality controls were performed and background green fluorescence after MCD MACS in (i) a mouse with advanced leukemia containing PDX cells never labeled with CFSE; and (ii) a mouse which never received PDX cells were determined (Figure 17).

In both controls, no cells were found in the LRC gate, indicating that all cells that are detected in the LRC gate during experiments truly derive from CFSE labeled PDX AL cells.

For each *in vivo* experiment a day 2 or day 3 mouse was required as control to set the LRC gate. To save resources, it was tested if CFSE stained PDX cells cultured *ex vivo* could be used for the LRC gate settings (Figure 18).

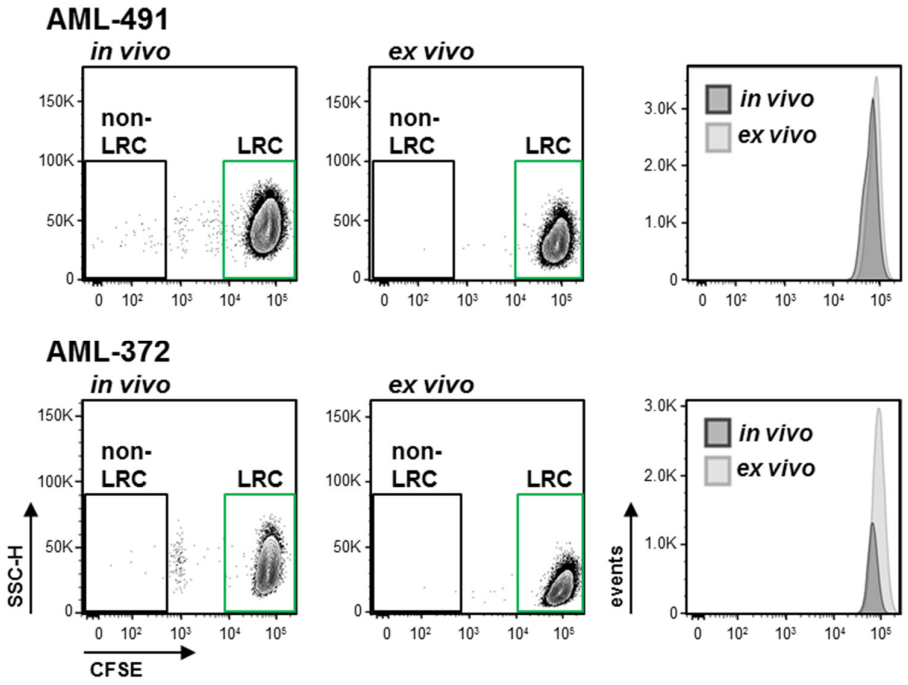

Figure 18: CFSE stained cells have similar MFI after 2 days *in vivo* and *ex vivo* consequently giving raise to same LRC and non-LRC gates
10^7 CFSE stained AML-491 or AML-372 PDX cells were injected i.v. into one mouse and re-isolated from the bone marrow 2 days later (left panel); 10^6 CFSE stained AML-491 or AML-372 PDX cells were cultured *ex vivo* for 2 days (middle panel); CFSE MFI signals of *in vivo* and *ex vivo* cultured PDX cells were compared by histogram (right panel).

For two different samples, 10^7 CFSE stained PDX cells were injected into one mouse and re-isolated and analyzed 2 days later. In parallel 10^6 CFSE stained PDX cells were cultured *ex vivo* for 2 days (see 4.4.4 *Ex vivo* culture of PDX cells). For both approaches CFSE MFI was determined and LRC and non-LRC gates were calculated thereof. As shown in Figure 18, CFSE MFI for both approaches and in both samples was similar and therefore gave rise to the same LRC and non-LRC gates. Thus, in further experiments, CFSE stained PDX cells cultured *ex vivo* for 2 or 3 days were used to set LRC gate.

In summary, as Sebastian Tiedt established before for ALL, CFSE labeling and analyzing was established to study PDX AML proliferation *in vivo*. To set gates for fast and slowly proliferating cells *ex vivo* control were established and different controls showed that cells in the slowly proliferating LRC gate truly come from CFSE positive AL cells.

5.4.3 All except one PDX AML samples contain a rare dormant subpopulation

As Sebastian Tiedt detected for the first time long-term dormant cells in ALL (Tiedt, 2014), the next aim was to investigate the proliferation pattern of AML PDX cells *in vivo*. With the CFSE labeling, PDX enrichment, and analysis methods established above, multiple AML PDX samples from different AML subgroups were studied for their growth *in vivo*. First CFSE kinetics for three different AML samples were performed to study the *in vivo* proliferation pattern of AML PDX samples over time (Figure 19).
For each AML sample 10^7 CFSE stained cells were injected into 6-7 mice and re-isolated between day 2 or 3 and day 21 or 29. At each time point one mouse was taken down, enriched for PDX cells and analyzed for CFSE content. Figure 19 shows, that all three analyzed AML samples lost CFSE content over time, indicating cell proliferation. In all three samples the PDX population did not lose the CFSE dye homogenously, instead some cells still retained the label even at late time points. Thus, all samples analyzed grow heterogeneously in mice and contain a rare subpopulation of dormant LRC.

To exclude that LRC are restricted to these three individual AML samples and to understand whether also other subgroups of AML contain long-term dormant cells, six additional AML samples were analyzed for the existence of the LRC population (Figure 20 and Figure 21). To represent the heterogeneity of AML, samples from adults and children, samples from primary disease and from first or second relapse, from different ELN classifications, and samples with and without genetic engineering were tested. As before 10^7 CFSE stained PDX cells were injected i.v. per mouse and re-isolated and analyzed for CFSE content after 14 days.

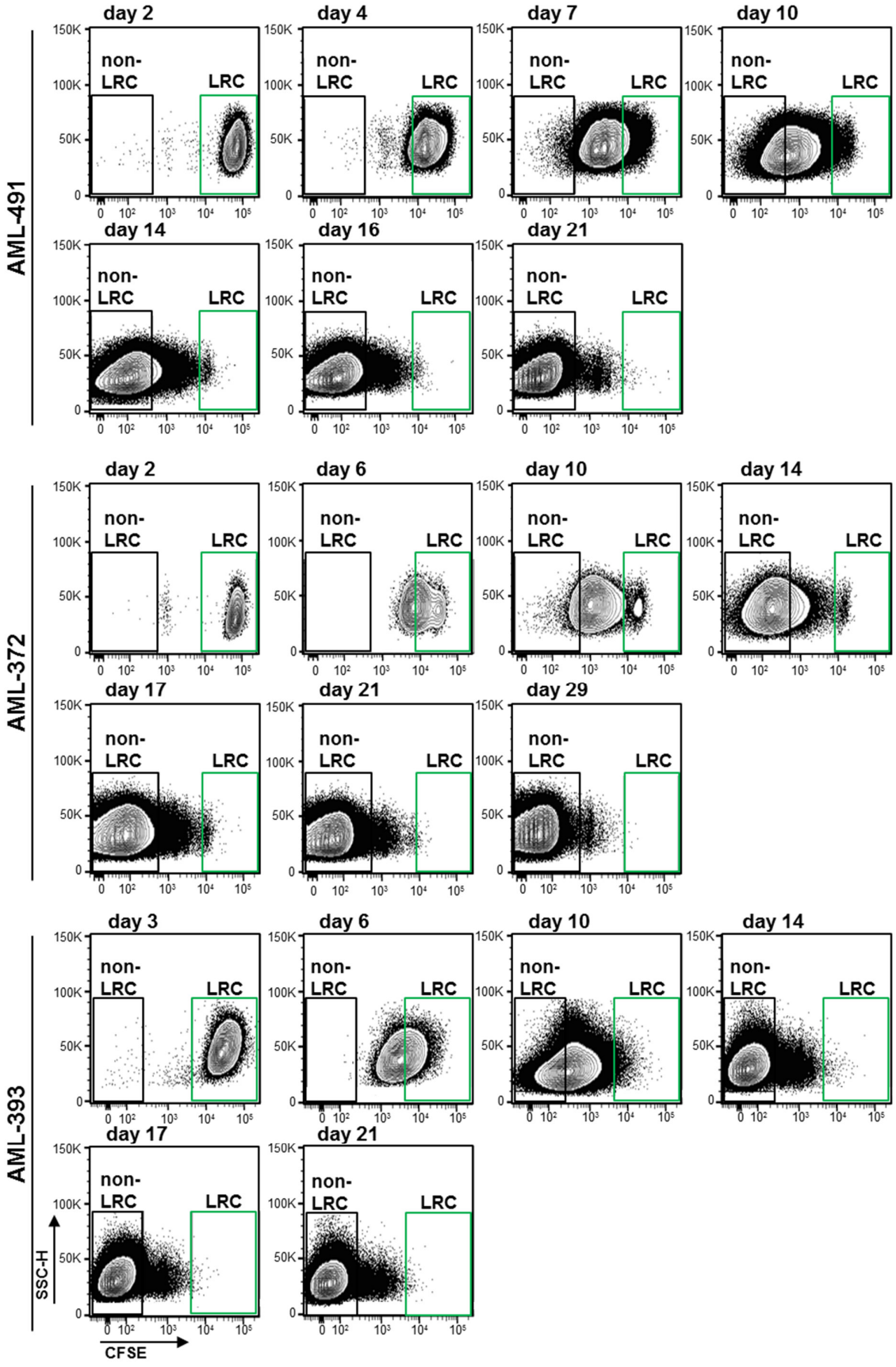
AML-491
day 2
day 4
day 7
day 10
day 14
day 16
day 21
AML-372
day 2
day 6
day 10
day 14
day 17
day 21
day 29
AML-393
day 3
day 6
day 10
day 14
day 17
day 21
non-LRC
LRC
150K
100K
50K
0
SSC-H
CFSE

Figure 19: AML PDX samples grow heterogeneously in mice over time
10^7 CFSE stained AML PDX cells were injected i.v. into 6-7 mice; PDX cells were enriched from 1 mouse at each time point and analyzed by flow cytometry for CFSE content. One representative kinetics out of two identical experiments is shown for each sample.

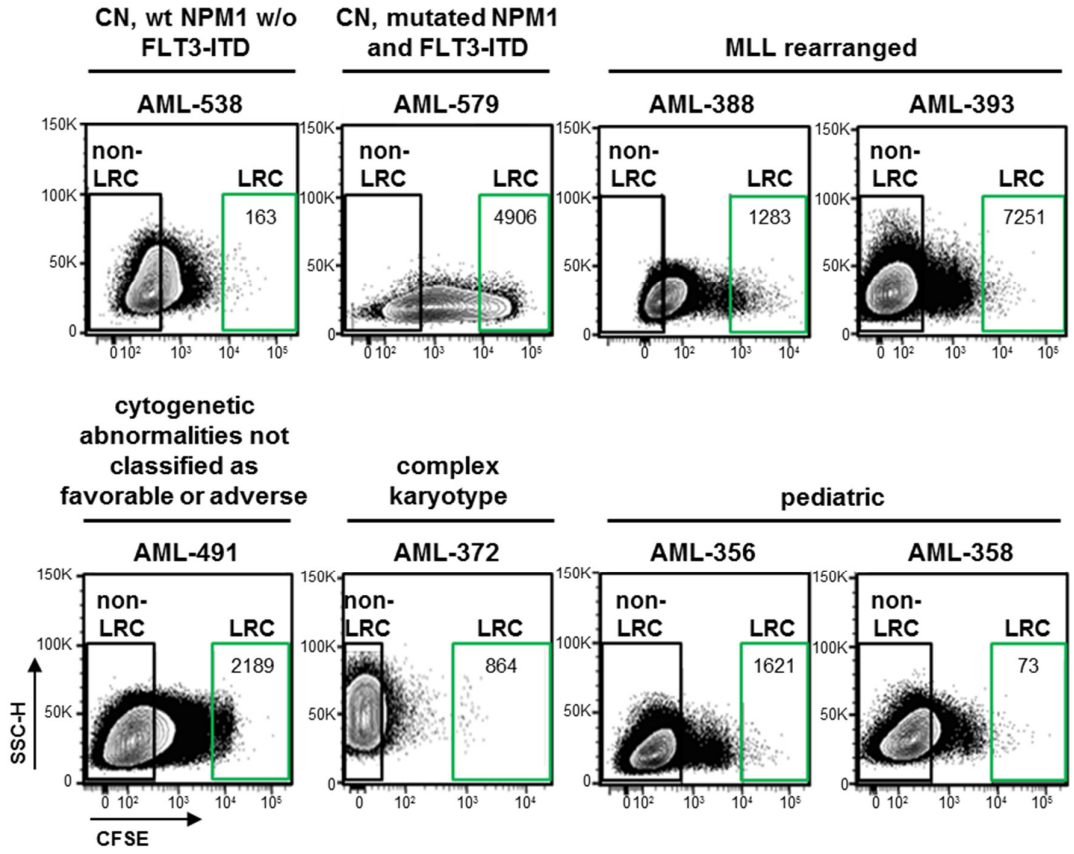

Figure 20: A rare, long-term dormant subpopulation exists in different subtypes of AML PDX cells growing in mice
PDX cells from eight AML patients were studied, including different ELN classifications, pediatric and adult samples, samples from initial diagnosis and from relapse, and samples with and without genetic engineering. 10^7 CFSE stained PDX cells were injected i.v. per mouse and were analyzed after 14 days. AML-538, AML-356 and AML-358 were not genetically engineered. Here, 10 % of the entire bone marrow isolate was analyzed without a prior MACS enrichment step. LRC numbers are indicated.

5 out of 6 of the additionally studied AML samples and 8 out of 9 of all studied PDX AML samples contained the rare subpopulation of LRC (Figure 20), suggesting that existence of long-term resting cells is a frequent phenotype in AML across different AML subtypes and characteristics. Interestingly, one PDX AML sample, AML-346 did not show long-term resting cells (Figure 21). To exclude that the absence of LRC in this sample was a measurement or staining error, this sample was analyzed several times for LRC (Figure 21).

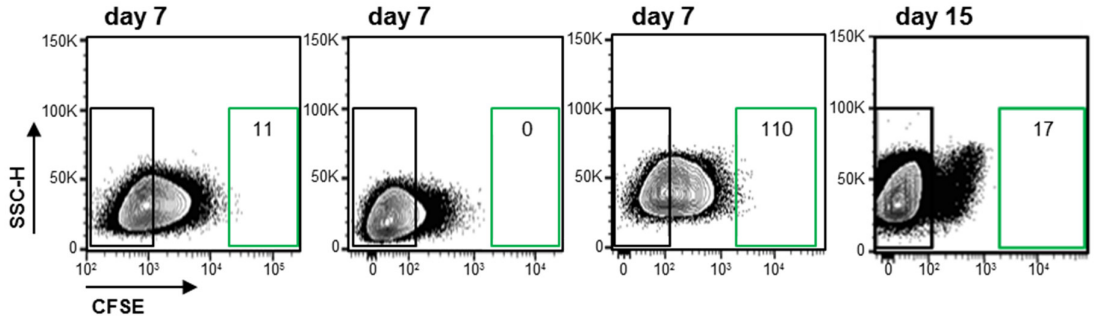

Figure 21: AML-346 has no dormant subpopulation of LRC
10^7 CFSE stained PDX cells were injected i.v. per mouse and were analyzed at indicated time points; PDX cells were enriched by MCD MACS and analyzed by flow cytometry. LRC numbers are indicated.

For AML-346 three times day 7 and once day 15 was analyzed. Mainly all cells lost the CFSE dye already after 7 days. Thus in AML-346 all cells participate to proliferation, and no dormant subpopulation was present. This sample was derived from a child with a high risk relapse. The tumor behaved highly aggressive in the patient and the patient died of the disease (Table S 1). Absence of LRC in this sample suggests that LRC are not associated with aggressiveness in patients.

In summary, it was shown that similarity to ALL most AML samples grow heterogeneously in mice and that 8 out of 9 PDX AML samples contain the rare dormant subpopulation of LRC.

5.4.4 Different subtypes of ALL contain a dormant subpopulation

In ALL, Sebastian Tiedt started to study PDX samples for their growth pattern in mice and first described the existence of LRC. But as he only studied three ALL samples (Tiedt, 2014), these experiments were verified and pursued.

Different subtypes of ALL were studied for the existence of LRC. In total, eight PDX ALL samples were studied, which included B-cell precursor-ALL and T-ALL, pediatric and adult samples, samples from primary disease and from relapse and samples with and without genetic engineering (Figure 22).

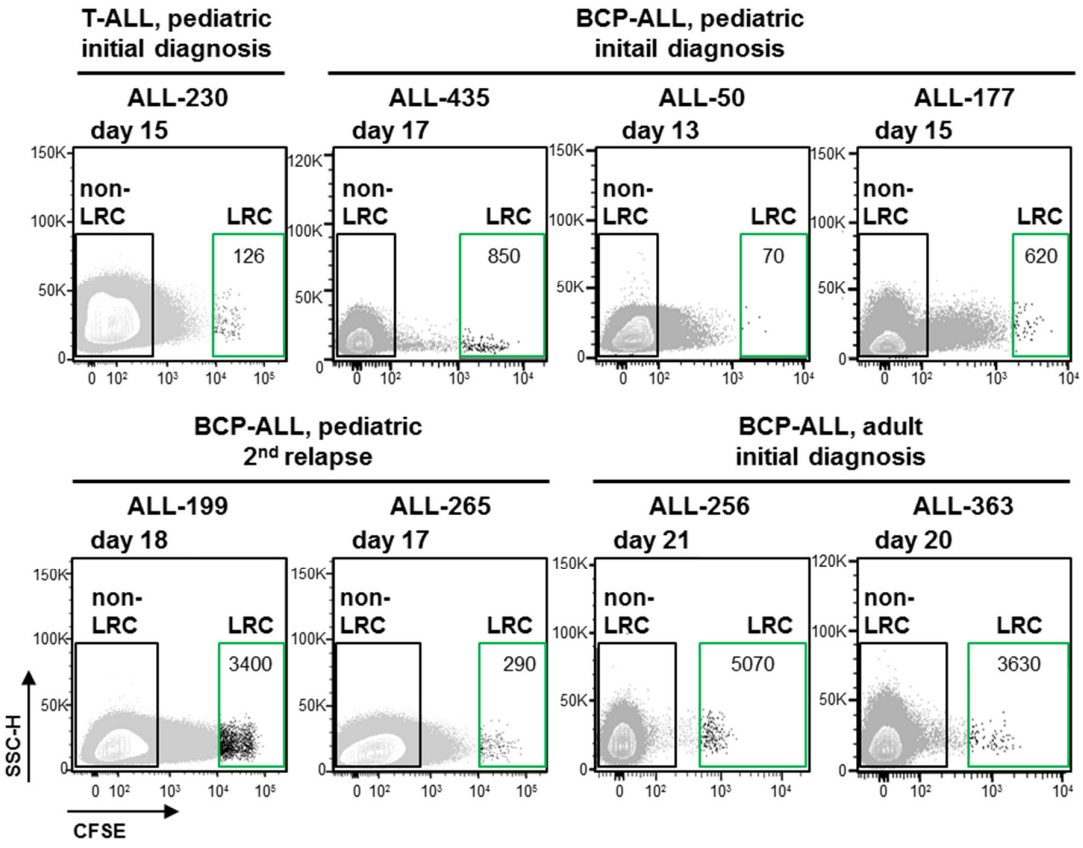

Figure 22: A rare, long-term dormant subpopulation exists in different subtypes of ALL PDX cells growing in mice
PDX cells from all eight ALL patients were studied, including B-cell precursor (BCP) ALL and T-ALL, pediatric and adult samples, samples from primary diseases and from relapse and samples with and without genetic engineering. Only ALL-199 and ALL-265 were genetically engineered. 10^7 CFSE stained PDX cells were injected i.v. per mouse and 10 % of bone marrow were analyzed at indicated time points. LRC numbers are indicated and grey indicates human non-LRC and mouse cells.

For each sample 10^7 CFSE stained PDX ALL cells were injected i.v. and analyzed for CFSE content at indicated time points. For these experiments only samples ALL-199 and ALL-265 expressed transgenes, all other samples were not genetically engineered to exclude that transgenes were responsible for the presence of LRC. Here 10 % of the entire population of bone marrow cells was directly analyzed by flow cytometry without prior MACS enrichment. To take into account the highly different proliferation rates and passaging times (Table 6) and with the aim to study late time points during passaging, most samples were analyzed when ⅓ – ½ of passaging time in mice has passed. Even at these late time points, all samples contained cells in the LRC gate, indicating that these cells did not substantially divide, while overall leukemic load had increased by three orders of magnitude.

Thus, CFSE staining disclosed that in all eight PDX ALL samples studied not all PDX ALL cells participate equally in leukemia proliferation, instead a rare subpopulation of LRC that hardly divided over prolonged periods of time exists.

In summary in AML and ALL PDX cells growing in mice a rare subpopulation of dormant cells was detected. These cells might be a surrogate for challenging leukemic cells in patients, which survive treatment and induce relapse with poor outcome.

5.5 LRC are not enriched for cancer stem cells

As long-term dormancy represents a hallmark of stem cells (Morrison and Spradling, 2008), it was analyzed, whether the dormant LRC were enriched for leukemia initiating cells (LIC) as stem cell surrogates. In ALL, Sebastian Tiedt already showed that ALL LRC are not enriched for stem cells (Tiedt, 2014). But as AML is the prototypic stem cell disease but AML stem cells remain difficult to enrich (Bonnet and Dick, 1997; Sarry et al., 2011), it was asked whether the subpopulation of LRC is enriched for cancer stem cells in AML.

Using limiting dilution transplantation assays (LDTA) as gold standard method for determining LIC frequency (Castro Alves et al., 2012; Dick and Lapidot, 2005; Eppert et al., 2011; Sarry et al., 2011), FACS sorted LRC and non-LRC were re-transplanted into groups of mice after serial dilution. To monitor positive engraftment as read-out for the presence of LIC, *in vivo* imaging (see 4.2.11 Bioluminescence *in vivo* imaging) and blood measurement (see 4.2.3 Flow cytometry of human cells in mouse peripheral blood) were performed repetitively (Figure 23, Table S 3).

Experiments were performed using AML samples AML-393 and AML-491. Limiting numbers of PDX cells were injected into groups of mice as indicated in Table S 3. Mice were counted as not engrafted when they did not show any sign of engraftment after twice the normal passaging time. LIC frequency was calculated using the online ELDA software (http://bioinf.wehi.edu.au/software/elda/) (Hu and Smyth, 2009).

For AML-393, the calculated LIC frequency of non-LRC was 1/127 and for LRC 1/172. For AML-491, the calculated LIC frequency of non-LRC was 1/1364 and for LRC 1/853. Thus and for both samples, the LIC frequencies of non-LRC and LRC were highly similar if not identical indicating that stem cell frequencies were not increased in quiescent cells.

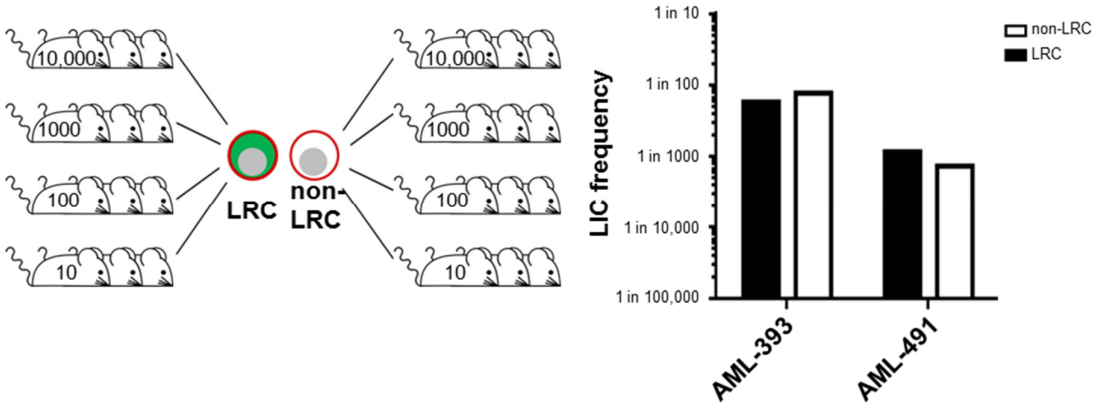

Figure 23: AML LRC are not enriched for stem cells
LRC and non-LRC isolated and sorted of donor mice 10 days after injection of CFSE labeled AML-393 or AML-491 cells were transplanted into secondary recipient mice in limiting dilutions at numbers indicated in Table S 3; bioluminescence *in vivo* imaging, blood measurement or BM FACS staining was performed to determine engraftment. LIC frequency was calculated using the ELDA software.

Thus, LRC and non-LRC exhibited similar leukemia-initiating potential in the two AML samples analyzed, as it was already shown for ALL (Ebinger et al., 2016; Tiedt, 2014). Consequently LRC are not enriched for cancer stem cells.

5.6 LRC survive systemic drug treatment *in vivo*

In patients and as major challenge, drug resistant subpopulations of cancer cells might survive chemotherapy, persist over prolonged periods in the patients, and later might induce a relapse with poor prognosis (Gokbuget et al., 2012b; Locatelli et al., 2013; Lokody, 2014; Patel et al., 2013). Especially dormant cells are known for their resistance against treatment with classical cytotoxic drugs, complicating elimination by anti-cancer therapy (Essers and Trumpp, 2010). As a rare dormant subpopulation was identified in PDX AL cells, the next question was whether this subpopulation behaves differently towards chemotherapy treatment compared to the bulk of leukemia cells. As a clinically related model, *in vivo* treatment of mice harboring PDX cells with cytotoxic drugs was performed and the different subpopulations were analyzed separately (Figure 24).

For *in vivo* drug treatment experiments, 10^7 CFSE stained PDX cells were injected. After seven days of leukemic growth, mice were treated either with buffer as control or with cytotoxic drugs in a single or multiple applications. Mice were sacrificed at day 10 and PDX cells were re-isolated and analyzed. As proof for stemness, drug resistant LRC of certain ALL samples were re-injected into next recipient mice (Figure 24).

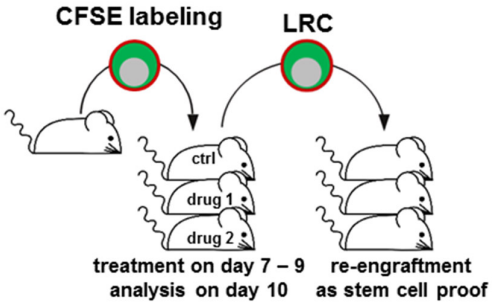

Figure 24: Experimental procedure for drug treatment *in vivo*
Mice were injected with 10^7 CFSE stained PDX cells. From day seven on mice received either buffer as control or a cytotoxic drug in a single or daily application. On day ten, mice were sacrificed and PDX cells were analyzed concerning their resting phenotype. Isolated LRC were re-transplanted as stem cell proof.

5.6.1 Most AML LRC display increased drug resistance *in vivo*

In patients, standard treatment of AML consists in cycles of an anthracycline for three days together with cytarabine for seven days. But cells might survive this treatment and later be responsible for relapse (De Kouchkovsky and Abdul-Hay, 2016; Estey and Dohner, 2006; Patel et al., 2013).

To analyze whether dormant AML LRC are more drug resistant than proliferating cells, four AML samples AML-372, AML-393, AML-388 and AML-491 were studied as indicated in Figure 24. To mimic standard chemotherapy of AML patients, a treatment combination of the anthracycline DaunoXome and cytarabine was used. Concentrations were calculated from human dose to mouse equivalent dose (see 4.2.12 *In vivo* treatment of mice).

In mice bearing AML-372, AML-393 and AML-388, the combination treatment markedly reduced leukemic load (Figure 25).

To follow up leukemia load and treatment response, mice were imaged before and after treatment. At start of treatment at day seven, all mice had identical leukemia load. When mice were sacrificed, control mice show a slight increase in leukemia load, whereas drug treated mice had a clearly reduced tumor load in imaging by around one log (Figure 25A). Isolation and quantification of PDX AML cells showed an average reduction of 90 % of the tumor for AML-372 and AML-393, and even a 99.9 % reduction for AML-388 (Figure 25B).

However, when dormant and proliferating subpopulations of AML-372, AML-393 and AML-388 were analyzed separately, marked difference became visible (Figure 26).

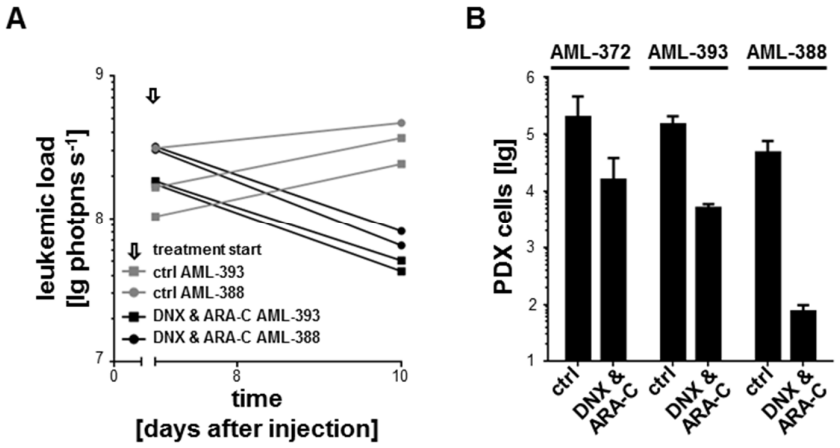

Figure 25: *In vivo* drug treatment reduced leukemic load in mice
Mice were injected with 10^7 CFSE stained AML PDX cells. On day seven mice were treated either with buffer (ctrl) or with a single application DaunoXome (DNX 20 mg/kg i.p.) and a daily application of cytarabine (ARA-C, 150 mg/kg i.p.). On day 10, mice were sacrificed and PDX cells were determined.
A Treatment response in AML-393 and AML-388 bearing mice was monitored by *in vivo* imaging.
B *In vivo* drug treatment reduced absolute numbers of living PDX cells; mean +/- standard error (AML-372 ctrl n=4, DNX & ARA-C n=6; AML-393 ctrl n=2, DNX & ARA-C n=2; AML-388 ctrl n=3, DNX & ARA-C n=4).

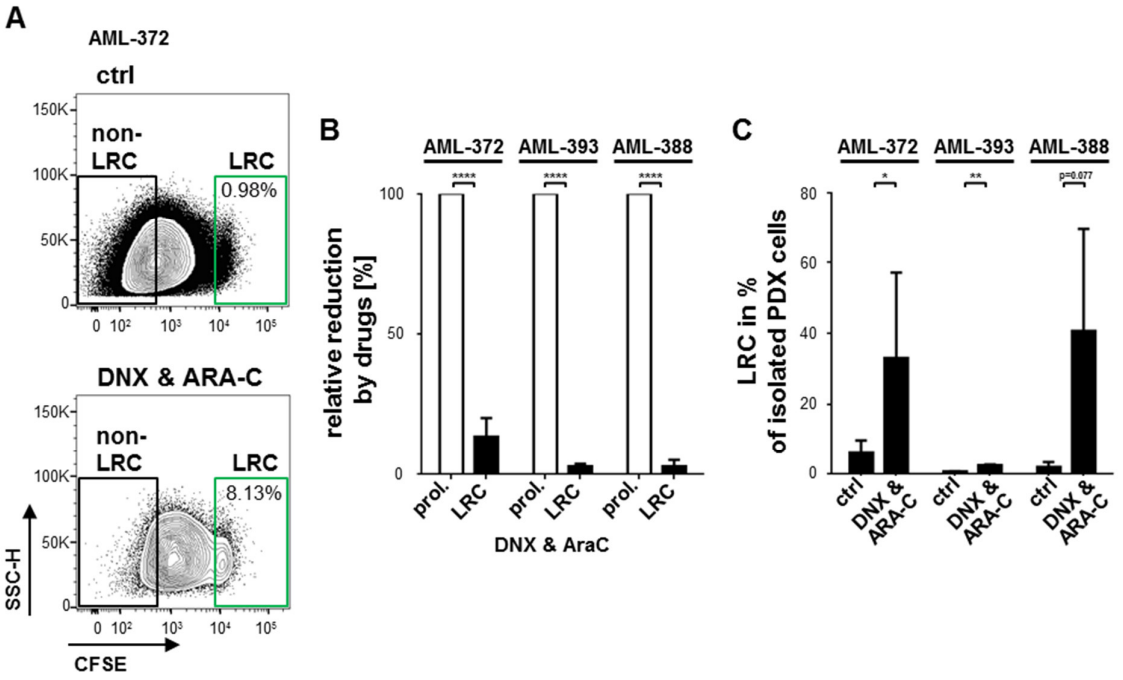

Figure 26: LRC survive systemic drug treatment *in vivo*
Analyses were performed as outlined in Figure 25.
A Shown are original FACS data of representative mice from sample AML-372.
B Quantification in all mice per group depicted as mean of relative drug effects on LRC compared to proliferating cells (100 %) +/- standard error; **** p<0.0001 by two-tailed unpaired t-test.
C Mean relative proportion of LRC of total PDX cells with and without treatment; mean +/- standard error. * p<0.05, ** p<0.01 by two-tailed unpaired t-test and for AML-372 including Welch's correction.

FACS blots for two representative mice of control and treated AML-372 sample show that in the DNX & ARA-C-treated mouse, overall leukemic burden was decreased, while the LRC population remained nearly unchanged. In relative terms, the LRC subpopulation became even more prominent and increased in percentage of total leukemic load from 0.98 % in control mice to 8.13 % in treated mice (Figure 26A). In all three AML samples analyzed, proliferating cells were 10 to 100-fold more efficiently eliminated by *in vivo* drug treatment compared to LRC (Figure 26B). As a consequence, the relative percentage of LRC within the total population of cells increased significantly after treatment. For AML-372 and AML-388, percentage of LRC in total PDX population increased from 2 % in control mice up to 40 % in treated mice. For AML-393, the increase in percentage of LRC was not that prominent, but still significant as the percentage of LRC in total population increased from 0.7 % in control mice to 2.5 % in treated mice (Figure 26C).

The forth studied sample, AML-491 behaved differently. AML-491 was shown in *in vivo* treatments trials before by Binje Vick in the hosting laboratory to be extremely sensitive towards three cycles of cytarabine application for four days. In LRC assays, AML-491 did not show major drug resistance of LRC (Figure 27).

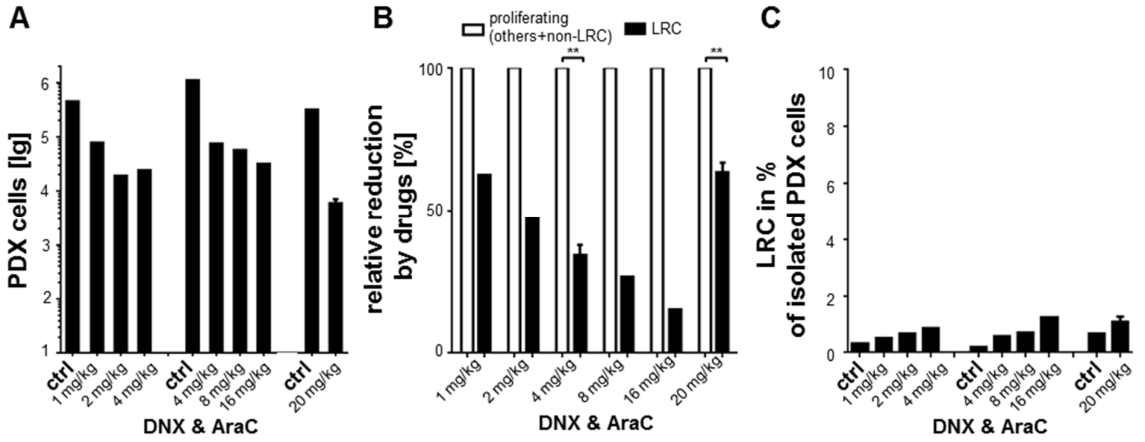

Figure 27: LRC of AML-491 do not show a clear drug resistance
Mice were injected with 10^7 CFSE stained AML-491 PDX cells. On day seven mice were treated either with buffer (ctrl) or with a single application DaunoXome (DNX 1-20 mg/kg i.p.) and for three days with a daily application of cytarabine (ARA-C, 150 mg/kg i.p.). On day 10, mice were sacrificed and PDX cells were determined.
A Absolute numbers of living PDX cells after *in vivo* drug treatment. Mean of n=2 for 20 mg/kg DNX & Ara-C +/- standard error.
B Quantification in all mice per group depicted as mean of relative drug effects on LRC compared to non-LRC (100 %); mean of n=2 for 4 mg/kg DNX & Ara-C and n=2 for 20 mg/kg DNX & Ara-C +/- standard error; ** $p<0.01$, by two-tailed unpaired t-test.
C Mean relative proportion of LRC of total PDX cells with and without treatment. For 20 mg/kg DNX & Ara-C mean +/- standard error.

In AML-491, different concentrations of DaunoXome in combination with 150 mg/kg cytarabine were tested. All concentrations, but the lowest one, reduced tumor load by at least 90 % (Figure 27A). However, if dormant LRC and proliferating cells were analyzed separately, it became obvious that also LRC were largely reduced by treatment of all concentrations. The reduction by treatment was a little less for LRC compared to proliferating cells, but AML-491 LRC did not show major drug resistance compared to LRC of the other three AML samples studied (Figure 27B). This phenomenon became also obvious, by analyzing the relative percentage of LRC within the total population of cells isolated from treated mice, here only a slight increase of LRC after treatment became visible in AML-491 (Figure 27C).

Taken together, *in vivo* treatment showed that in three of four AML samples analyzed, LRC are more drug resistant than non-LRC, indicating that dormancy might be a reason for the survival of malignant cells after chemotherapy treatment.

5.6.2 ALL LRC are drug resistant *in vivo*

In ALL, Sebastian Tiedt used two samples without technical or biological replicates to first describe that PDX ALL LRC were drug resistant (Tiedt, 2014). Here the task was to verify and pursue these experiments.

First, the *in vivo* cytotoxic drug response in ALL-50 and ALL-435, two samples obtained from patients at initial diagnosis, was studied (Figure 28).
The experiments were performed as described before (Figure 24). Routine ALL treatment in patients involves more different drugs compared to AML. In ALL and beyond the anthracyclines and purin-analogs used in AML patients, drugs like antimicrotubule agents and topoisomerase II inhibitors are used (Inaba et al., 2013; Pui et al., 2008).
For ALL-50, mice were treated with either cytarabine, etoposide, amsacrine or epirubicine. For ALL-435, mice were treated with either etoposide, amsacrine or epirubicine. The i*n vivo* imaging before and after treatment in ALL-50 showed increase of leukemic load in control mice and reduction of leukemic load after treatment by 1 log or more (Figure 28A). All PDX cells were re-isolated by MCD MACS and quantified in flow cytometry. Drug treatment with all drugs resulted in clear reduction of leukemic burden by over 90 % in both samples (Figure 28B). The same experiment was performed with the two relapse samples ALL-199 and ALL-265, to indicate that the results were not restricted to a certain disease stage (Figure 29).

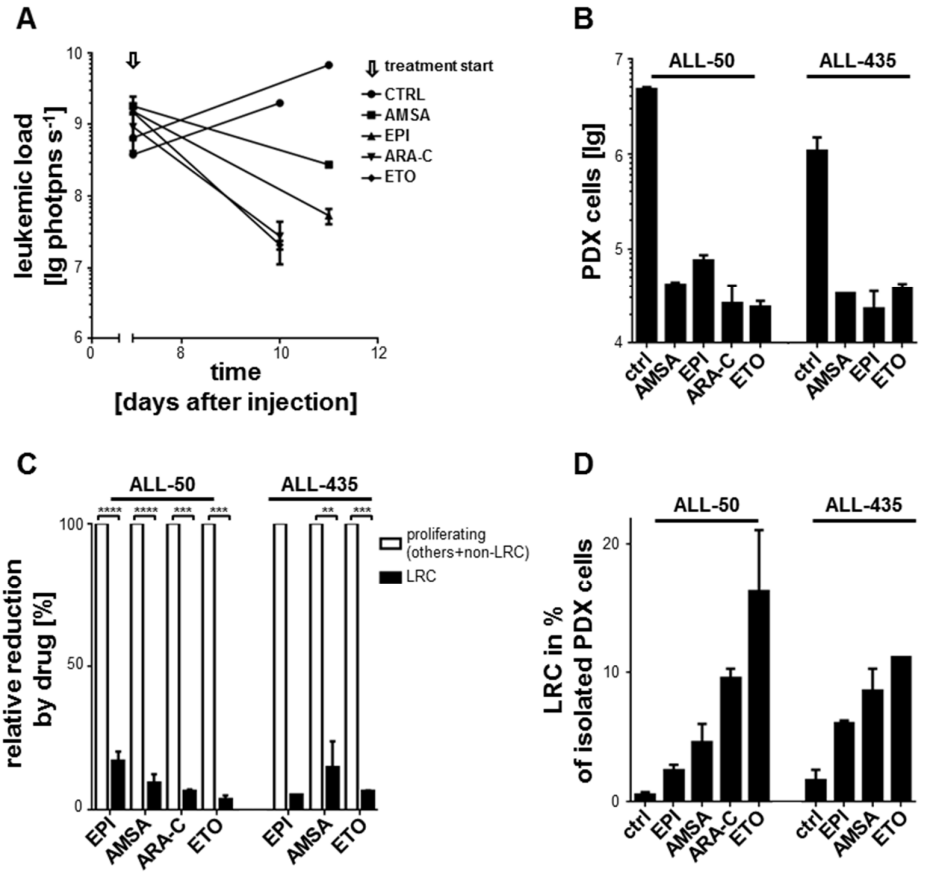

Figure 28: LRC survive systemic drug treatment *in vivo* in ALL initial diagnosis samples
Mice were injected with 10^7 CFSE stained ALL-50 or ALL-435 PDX cells. From day 7 on mice injected with ALL-50 received either buffer (ctrl), a daily application of cytarabine (ARA-C, 150 mg/kg i.p.; n=2), a daily application of etoposide (ETO, 33 mg/kg i.p.; n=2), a daily application of amsacrine (AMSA, 25 mg/kg i.p.; n=2) or a single application of epirubicine (EPI, 25 mg/kg i.p.; n=2). From day 7 on mice injected with ALL-435 received either buffer (ctrl), ETO (33 mg/kg, i.p.; n=2), AMSA (25 mg/kg i.p.; n=2) or EPI (25 mg/kg i.p.; n=1). On day 10, mice were sacrificed and LRC were analyzed.
A Treatment response in ALL-50 bearing mice was monitored by *in vivo* imaging.
B *In vivo* drug treatment reduced absolute numbers of living PDX cells.
C Quantification in all mice per group depicted as mean of relative drug effects on LRC compared to non-LRC (100 %) +/- standard error; ** p< 0.01, *** p<0.001, **** p<0.0001 by two-tailed unpaired t-test.
D Mean relative proportion of LRC of total PDX cells with and without treatment +/- standard error.

For ALL-199, single applications of etoposide or vincristine were used in 8-9 mice each; for ALL-265, single applications of etoposide or cyclophosphamide were used in 3-4 mice each. Similar to the experiments performed in AML, all cytotoxic drugs reduced overall leukemic burden by more than 90 % (Figure 29A). When drug response was evaluated separately for LRC and proliferating cells, a marked difference became visible. Proliferating cells were eliminated 10 to 100-fold more efficiently *in vivo* compared to LRC (Figure 28C and Figure 29B). As a consequence, the relative percentage of LRC within the total population of cells increased after treatment (Figure 28D and Figure 29C).

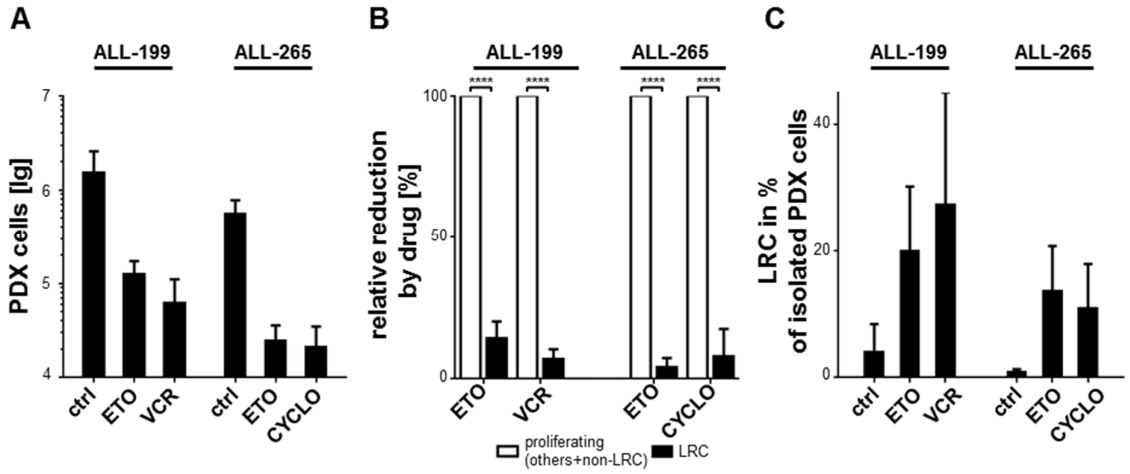

Figure 29: LRC survive systemic drug treatment *in vivo* in ALL relapse samples.
Mice were injected with 10^7 CFSE stained ALL-199 or ALL-265 PDX cells/mouse and received either buffer (ctrl, n=7 for ALL-199; n=3 for ALL-265), etoposide (ETO, 50 mg/kg, i.p.; n=8 for ALL-199; n=3 for ALL-265), vincristine (VCR, 1.5 mg/kg, i.v.; n=9 for ALL-199) or cyclophosphamide (CYCLO, 150 mg/kg, i.p.; n=4 for ALL-265) on day 7; on day 10, mice were sacrificed, LRC analyzed and re-transplanted into secondary recipients.
A *In vivo* drug treatment reduced absolute numbers of living PDX cells.
B Mean of all 3-9 mice per treatment, depicted as relative drug effect on LRC compared to non-LRC (100 %) +/- standard error; **** $p<0.0001$ by two-tailed unpaired t-test.
C Mean relative proportion of LRC of total PDX cells with and without treatment +/- standard error.

Thus, while ALL proliferating cells of four different samples were decreased by *in vivo* treatment by more than 1 order of magnitude, most ALL LRC survived chemotherapy, suggesting increased *in vivo* treatment resistance of LRC. Compared to AML, ALL LRC behaved more homogeneous, as all tested LRC were drug resistant. But it has to be considered that for both leukemia subtypes the sample size was low.

5.6.3 ALL LRC have leukemia-initiating potential

In patients, cells which survived chemotherapy treatment might be responsible for tumor relapse. Due to the cancer stem cell theory, tumors are hierarchically organized with cancer stem cells on top of the hierarchy. Only cancer stem cells are able to propagate and induce new tumors (Wang and Dick, 2005). Therefore it was studied whether drug resistant LRC have stem cell potential and were able to induce a new tumor by transplanting drug resistant LRC into next generation mice (Figure 30).

Drug resistant LRC of ALL-199 and ALL-265 were isolated from bone marrow of treated mice and re-injected into next generation mice. Re-engraftment was followed by *in vivo* imaging (see 4.2.11 Bioluminescence *in vivo* imaging).

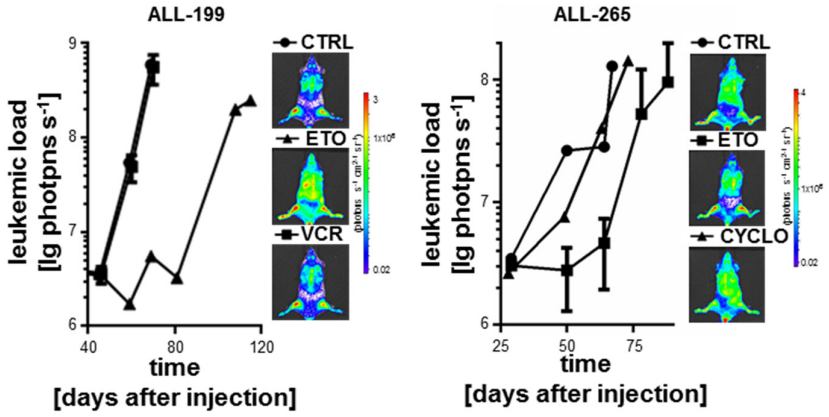

Figure 30: LRC reveal stem cell potential.
LRC from drug treated mice were isolated, re-transplanted, tumor growth was monitored by *in vivo* imaging, and bioluminescence signals were quantified. Imaging pictures from dpi 60 (ALL-199; ctrl; VCR), dpi 108 (ALL-199; ETO), dpi 67 (ALL-265; ctrl), dpi 78 (ALL-265; ETO) and dpi 73 (ALL-265; CYCLO) are shown.

Upon re-transplantation, all drug resistant LRC harbored leukemia-initiating potential as they gave rise to new leukemia. Regarding proliferations kinetics, LRC after drug treatment induced leukemia at similar kinetics than untreated control LRC indicating that short term drug treatment did not induce changes in LRC (Figure 30).

Thus ALL LRC have stem cell potential. They might represent surrogates for relapse-inducing cells in patients, as they can induce a new tumor after surviving treatment.

Taken together, LRC share the most important functional features that impede to cure cancer in patients: (i) dormancy; (ii) *in vivo* drug resistance and; (iii) leukemia-initiating potential. LRC might thus serve as preclinical surrogate for relapse-inducing cells in ALL and AML.

5.7 Release from environment induces proliferation in LRC

A treatment option to target relapse-inducing, drug resistant and dormant cells might be the conversion of these dormant cells into cycling cells to target them afterwards with cytotoxic drug (Essers and Trumpp, 2010; Zeng et al., 2009).
Therefore, it was studied whether LRC inherit permanent biological characteristics or whether they might represent a reversible functional phenotype. As dormancy was the main feature defining LRC, experiments were performed to study whether dormancy of LRC was a cell inherent, cell autonomous characteristic.

To address these questions, LRC and non-LRC of AML-491, AML-393 and ALL-199 were isolated from mouse bone marrow and sorted into LRC and non-LRC as described above and thereby dissociated from their environment; LRC and non-LRC were separately re-transplanted into secondary recipient mice (Figure 31).

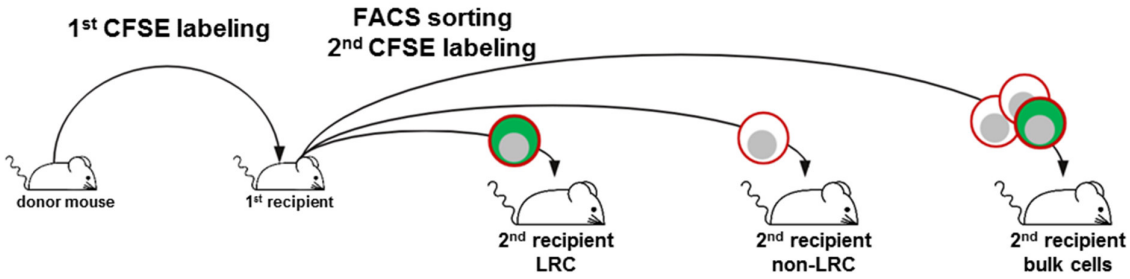

Figure 31 Experimental procedure for isolation and re-transplantation of LRC and non-LRC
From a 1st recipient mouse carrying CFSE stained ALL-199 cells, LRC, non-LRC and bulk cells were obtained at day 10; bulk cells and non-LRC were re-labeled with CFSE, re-transplanted into secondary recipient mice at high numbers and re-analyzed at day 10 using flow cytometry; bulk cells, LRC and non-LRC were re-transplanted at low numbers into groups of mice and leukemia growth was monitored over time.

A first readout was determining the distribution between LRC and non-LRC in second recipient mice. For this readout, second recipient mice were transplanted with 10 million cells of either the bulk mixture of all cells or non-LRC and analysis performed at day 10 by flow cytometry. As this approach required transplantation of high cell numbers, it was unfeasible performing it with LRC, as only low numbers of LRC can be recovered from each mouse. The distribution between LRC and non-LRC was highly similar, if not identical for the bulk mixture of all cells or non-LRC and both populations displayed a clear subpopulation of LRC (Figure 32A). Thus, upon re-transplantation of a populations exclusively containing non-LRC, LRC were derived in next recipient mice. These data suggest that fast proliferating non-LRC retain the capacity to convert into dormant LRC.

To test the opposite question whether slowly proliferating LRC might be able to convert into fast proliferating non-LRC, a second readout was used which used low cell numbers and could be applied to all three populations, namely the bulk mixture of all cells, LRC and non-LRC. When low cell numbers of either LRC, non-LRC or bulk cells were re-transplanted into next recipient mice, all populations initiated leukemic growth at identical speed in mice as monitored by *in vivo* imaging. For AML-491 after 13 weeks all three populations showed leukemic loads of around $1x10^{10}$ lg photons/s. The leukemic load of one mouse, transplanted with LRC had a delayed tumor growth, but also reached the same leukemic load. Probably, due to cell losses

during the complex isolation and injection procedure, fewer LRC cells were injected and engrafted and needed more time to induce the full leukemia.

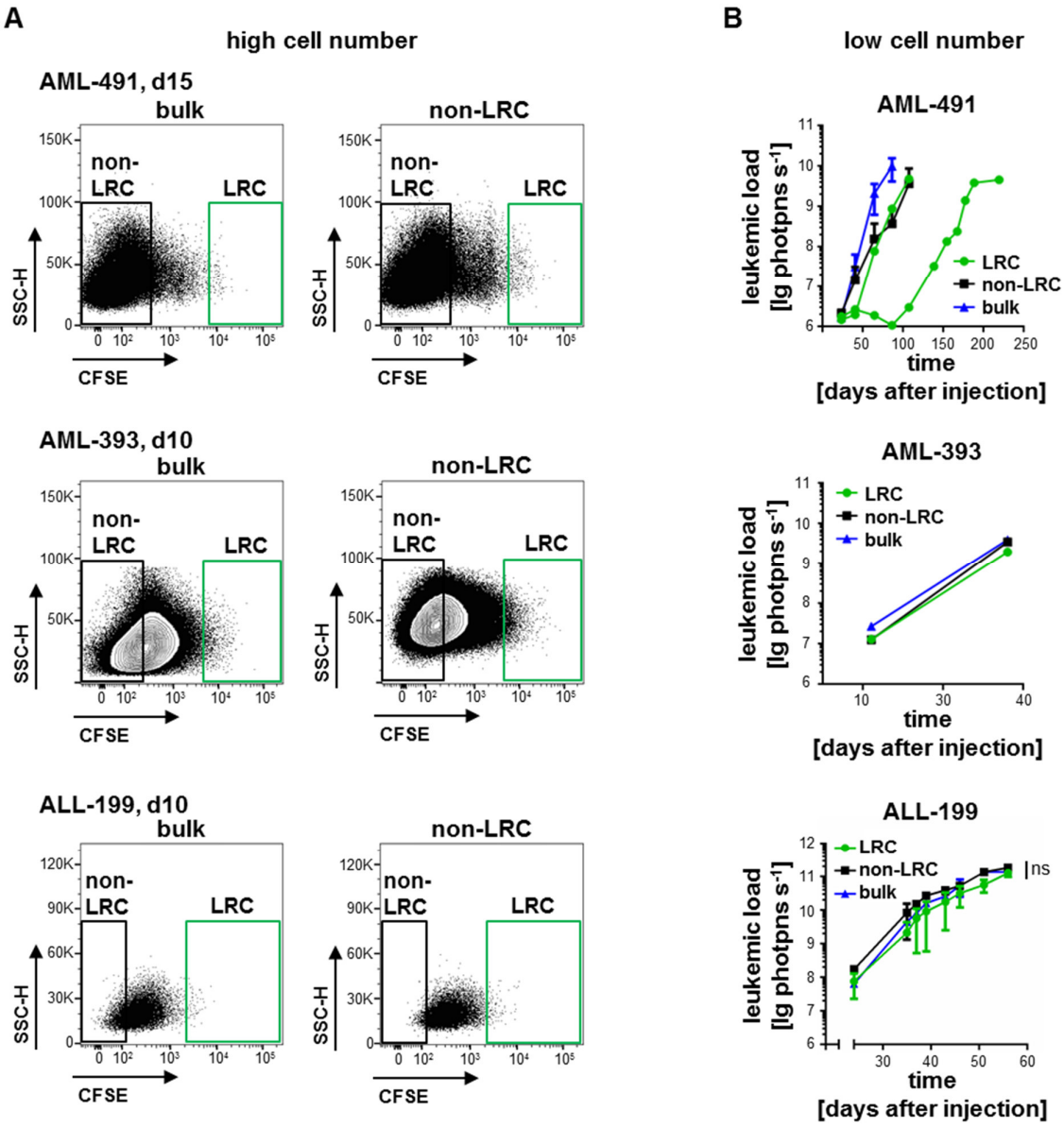

Figure 32: Release from the environment induces proliferation in AML LRC
From a 1st recipient mouse carrying CFSE stained AML-491 or AML-393 cells, LRC, non-LRC and bulk cells were obtained at day 10 (AML-393) or at day 15 (AML-491).
A Bulk cells and non-LRC were re-labeled with CFSE, re-transplanted in secondary recipient mice at high numbers and CFSE staining was re-analyzed at day 10 or day 15 using flow cytometry.
B Growth curve in secondary recipients; bulk cells, LRC and non-LRC were re-transplanted at low numbers into groups of mice and leukemia growth was monitored over time by *in vivo* imaging. For ALL-199 no statistical significance was found between the linear regression slopes by Kruskal-Wallis test and Dunn's multiple comparison tests.

For AML-393 and ALL-199 all three population needed 6 or 8 weeks to show leukemic loads of $5x10^9$ or $1x10^{11}$ lg photons/s, respectively (Figure 32B). The data show that re-

transplantation into secondary recipient mice converted dormant LRC into fast proliferating cells.

Thus, slowly proliferating LRC can give rise to fast proliferating cells upon re-transplantation and convert into non-LRC and vice versa; fast proliferating non-LRC can give rise to dormant LRC in the next generation of mice. These results suggest that LRC and non-LRC represent a reversible functional phenotype. AL cells exhibit a major functional plasticity and respond on the environmental context they are in. Therefore LRC might be targetable, by dissociating them from their environmental context and thereby converting them into treatable proliferating cells.

The data showed in a PDX AL model the isolation and functional characterization of dormant cells which might be a surrogate for relapse-inducing cells in patients. This dormant and drug resistant stem cell subpopulation can be converted to proliferating cells by releasing them from their microenvironment. The developed model and the consequent findings will be of translational importance as they establish a basis to develop new treatment strategies to eradicate relapse-inducing cells in AL patients.

6 Discussion

Acute leukemias (AL) consist of heterogeneous cell populations and the subgroup which displays treatment resistance determines the patients' prognosis. Most AL patients initially respond to anti-leukemia therapy, but the majority of acute myeloid leukemia (AML) and 40-50 % of acute lymphoblastic leukemia (ALL) patients develop disease relapse which is associated with poor outcome. Minimal residual disease (MRD) cells are a reason for relapse, as these cells survived chemotherapy and might persist even after prolonged time of therapy (Gokbuget et al., 2012b; Locatelli et al., 2013; Lokody, 2014; Patel et al., 2013).

Novel treatment options are urgently needed to eradicate residual, treatment resistant cells, which have stem cell potential and therefore are able to induce relapse, to finally improve the cure rate and prognosis of patients with acute leukemia. For this a deep understanding is required on mechanisms determining treatment-resistance *in vivo* and the ability to induce relapse. Before this study, no functional studies on isolated MRD cells were performed as technical limitations like the reliable differentiation of malignant and healthy cells and the enrichment and isolation of very minute numbers of malignant cells hampered these studies so far. As treatment resistant cells are challenging to isolate, but considered to be dormant (Aguirre-Ghiso, 2007; Essers and Trumpp, 2010; Schillert et al., 2013), in this study dormancy was used as benchmark in searching for a therapeutically relevant subpopulation of AL cells. In this work, a preclinical mouse model was further optimized, which allowed the identification, isolation and enrichment of a rare subpopulation of *in vivo* long-term dormant cells in the PDX model of ALL and AML. Dormant cells were identified by label retaining cells (LRC) of the fluorescence dye 5-(6)-Carboxyfluorescein-Succinimidyl Ester (CFSE). The characterization of these LRC showed that they combine the three major adverse characteristics that challenge to cure cancer, namely (i) dormancy, (ii) *in vivo* drug resistance, and (iii) leukemia-initiating potential. In conclusion, LRC represent a preclinical surrogate for treatment resistant, dormant, and relapse-inducing cells in acute leukemias. Therefore, PDX LRC cells represent a valuable tool to investigate mechanisms of resistance, dormancy, and relapse in patients. The new insights, which could be gained with help of this model, might finally lead to the development of novel therapies to eliminate treatment resistant cells, prevent disease relapse and increase the prognosis of patients with ALL.

6.1 Isolation of minute numbers of PDX cells enables studies on non-dividing AL cells

The basis for this study was the NSG PDX model of acute leukemias. This model is an attractive possibility to experimentally study patients' tumor cells *in vivo*, which uses immuno-compromised mice to expand and study tumor cells from patients (Shultz et al., 2005; Terziyska et al., 2012; Vick et al., 2015). It circumvents the limitations of *in vitro* approaches as cell lines display altered proliferation behavior and gained additional mutations by their immortalization, departing them from the original patients' leukemia (Pan et al., 2009). As cell lines do not have genetic or dormant subclones and all cells participate in proliferation, cell lines could not be used within this study to search for challenging subpopulations. In addition the number of available cancer cell lines is inadequate regarding the diversity of cancer subtypes (Gillet et al., 2011; Hausser and Brenner, 2005). Also *in vitro* approaches with primary tumor cells have significant limitations as they are reluctant to proliferate *in vitro* and material is limited (Mitra et al., 2013). Nowadays, a large amount of different leukemia PDX models have been established (Lee et al., 2007; Liem et al., 2004; Townsend et al., 2016). The broad number of available xenografts can reflect the complexity of the disease regarding different subtypes of the disease, namely different precursor cells, different genetic alterations, diagnosis and relapse samples, pediatric and adult patients, with and without cytogenetic changes. Furthermore, studies within the bone marrow microenvironment are possible (Townsend et al., 2016). As shown previously, PDX AL cells retain important characteristics of primary AL cells and remain mainly stable after successive passaging in mice regarding important characteristics such as time to overt leukemia, cell surface markers, response to drugs *in vitro*, and mutation pattern (Castro Alves et al., 2012; Lock et al., 2002; Rosfjord et al., 2014; Schmitz et al., 2011; Terziyska et al., 2012; Townsend et al., 2016; Vick et al., 2015). PDX models are mostly used for preclinical treatment trials (Gao et al., 2015; Suryani et al., 2014; Townsend et al., 2016). Here the model was developed further to isolate, enrich and characterize minimal numbers of AL cells from mice, based on transgenic expression of artificial molecular markers. Genomically integrated molecular tags were used to reliably and stably mark the PDX cells. Lentiviral integration into the genome of xenograft cells could possibly alter their properties, as the vectors might lead to clonal imbalance, and malignant cell transformation due to integration and upregulation of proto-oncogenes (Modlich et al., 2009). However, until now, no alterations in functional behavior of PDX cells before and after genetic engineering, that could have been caused by lentiviral transduction and the EF-1α as non-viral promoter, have

been detected (Barrett et al., 2011; Bomken et al., 2013; Iacobucci et al., 2016; Terziyska et al., 2012; Vick et al., 2015). The advantage of the molecular approach with artificial molecular markers lies in the unbiased isolation of PDX cells independently from endogenous surface antigens, which might be restricted to leukemia subpopulations. For example, in BCP-ALL it has been shown that previous CD19 expressing ALL cells can develop a CD19 negative relapse (Maude et al., 2015). Meaning that here the use of the endogenous marker CD19 for the identification of ALL cells would fail to identify the cells responsible for the relapse.

The optimized and developed methods enabled the enrichment and isolation of transgenic PDX cells at early time points and low cell numbers. In patients, AL is frequently detected at advanced stages of the disease, when disease symptoms, like bleeding and infections, appear and bone marrow already contains in average between 30 % and 80 %, sometimes even more, malignant cells (De Kouchkovsky and Abdul-Hay, 2016). Most patients receive anti-leukemia treatment directly after diagnosis. Without treatment, patients die within few months due to bone marrow failure (De Kouchkovsky and Abdul-Hay, 2016; Estey and Dohner, 2006; Pui and Evans, 2013). But as a consequence, little is known about the growth of leukemia in patients. Investigations on leukemia biology were performed at diagnosis, meaning at late time points of the disease, during treatment process or at relapse (De Kouchkovsky and Abdul-Hay, 2016; Pui et al., 2015). Investigations on early leukemia development are missing. Due to technical limitations even *in vivo* models concentrate on late time points, when a large amount of leukemic cells can easily be isolated and studied. Suitable models and techniques are urgently needed to study engraftment and investigations on early leukemic development (Barrett et al., 2011). So far, the same technical obstacles hampered characterizing phenotypic and functional features of relapse-inducing cells in leukemia patients in detail. These cells are difficult to clearly identify, and only exist at low numbers, hampering their isolation and availability for further experiments or characterization. Whereas the present study enables for the first time isolation of low numbers of pure leukemic cells and therefore investigations on early leukemia growth.

Sebastian Tiedt started the study with the two high risk relapse samples ALL-199 and ALL-265. By CFSE labeling he identified *in vivo* long-term resting cells in these two samples. Without technical or biological replicates he showed that the long-term resting cells are treatment resistant (Tiedt, 2014). To exclude that only relapse samples show the identified dormant and drug resistant phenotype, a broader representative pool was chosen for this study. Relapse samples have already been exposed to chemotherapy, and might therefore represent a selected subset of particularly restive cells from the primary tumor. This might be a reason why they are

highly aggressive and grow best with short passaging times in mice compared to initial diagnosis samples (Meyer et al., 2011). In total, eight different AML and eight different ALL PDX samples were analyzed for the presence of a dormant subpopulation. To cover a high heterogeneity, the selected samples include different mutations, differences in cytogenetics and age, and samples were obtained from patients at initial diagnosis or from patients suffering from 1st or 2nd relapse. Furthermore, these PDX samples have different passaging times between 30 and 130 days. As all but one sample analyzed contained a long-term dormant subpopulation *in vivo*, it is concluded that the findings obtained in this study reflects a phenotype that is not restricted to single AL samples, but is rather a prerequisite of almost all AL samples.

For the study two enrichment methods were used. The one based on NGFR MACS was optimized and the one based on mouse cell depletion (MCD) MACS was established.

For the total study the optimization of the NGFR MACS lead to material savings and thereby to an enormous amount of cost reduction, while the experiments could still be reliably performed.

The advantage of this new enrichment method based on MCD MACS is the independence of the second lentiviral construct containing the NGFR. Validation of this method showed the reliable isolation of few PDX cells from mouse bone marrow with only minor false positive events. Comparing both enrichment methods showed that both reliably identify and isolate identical small numbers of PDX cells from mouse bone marrow. Thus, both methods are adequate for the present study.

In this study, two protocols were established, compared, and quality controlled to isolate, identify, and enrich minute numbers of PDX cells from mouse bone marrow with high reliability, sensitivity, and purity.

6.2 Interaction between different AL samples and mouse bone marrow depends on sample specific characteristics

The here developed enrichment methods enable the direct quantification of homed AL PDX cells to mouse bone marrow. The established models circumvent the former technical limitations of the identification, isolation, and enrichment of minute numbers of cells and enables thereby for the first time especially new insights into leukemia biology at early time points with direct cell number quantifications. Already Barrett and colleagues claimed that suitable models and techniques are urgently needed to study engraftment and investigations on early leukemic development. As different ALL samples show different kinetics in xenograft

models, detection and quantification of treatment effects in these models at early disease time points are interesting for new treatment options or the determination of patients' outcome (Barrett et al., 2011). To investigate engraftment capacities of AL samples to mouse bone marrow, the gold standard method are limiting dilution transplantations assays (LDTA). They are used to compare differences of leukemia initiating cell (LIC) frequencies between different AML samples, between subpopulations regarding surface markers (Eppert et al., 2011; Sarry et al., 2011) and between treated and untreated samples (Castro Alves et al., 2012). The read-out is a qualitative one; the engraftment or the non-engraftment of cells in immunodeficient mice. The rates of positive and negative response at different doses allow the quantitative calculation of the LIC frequency with help of the ELDA software (Hu and Smyth, 2009). In addition the current standard method to detect engraftment of leukemia is the measurement of leukemia cells in the blood and most mice were only evaluated during endpoint analyzes. But these current methods do not give full insights into early leukemia growth, leukemia development or treatment response (Barrett et al., 2011), whereas the developed enrichment methods in this study now give the opportunity to study and quantify the early engraftment of AL.

For engraftment studies, 10^7 PDX cells of eight ALL samples and of eleven AML samples were injected into mice and quantified from mouse bone marrow two or three days later. The homing capacity of the different PDX samples differed by more than two orders of magnitude. The maximum efficiency was around 4 % of injected cells that could be redetected after isolation, whereas the minimum efficiency was 0.01 % of the injected PDX cells.

In addition, for the sample ALL-199, different cell numbers between 10^7 and 10^5 PDX cells were injected into mice and quantified from mouse bone marrow three days later. When higher cell numbers were injected, homing efficiency increased to a maximum of 1.2 %, whereas the injection of the lowest cell number only lead to a homing efficiency of 0.03 %. This shows that different PDX AL samples seem to have different engraftment rates to mouse bone marrow and the homing capacity depends on the cell number injected. The heterogeneity of homing capacity of different samples and different cell numbers are in line with previously published data, which show that AML or ALL PDX engraftment is a selective event, and that engraftment efficiency and time to full blown leukemia varies between different samples (Liem et al., 2004; Lock et al., 2002; Notta et al., 2011; Samuels et al., 2010; Sanchez et al., 2009). The current literature mainly concludes that different samples or different subpopulations might contain different frequencies of LIC.

Later on in the study, qualitative LDTAs were performed for AML-393 and AML-491. Here LIC frequencies between 1/130 and 1/1400 were calculated. The data is in line with the direct

quantitative analysis of homed cells after three days for ALL-393 and AML-491, as here 0.3 and 1 % of 10^7 injected cells homed to the mouse bone marrow.

In contrast for ALL-199, qualitative analysis by LDTA showed 50 % engraftment for the group of 10 cells in the mouse bone marrow. Considering cell loss during the complex procedure of cell preparation and injection, these data suggest that each and every cell in this sample contains stem cell properties (Ebinger et al., 2016; Tiedt, 2014). In addition, other studies showed that in ALL almost every cell is a LIC, as LIC frequencies are very high (Morisot et al., 2010; Rehe et al., 2013). But in the present study, it seems that the engraftment rate drops if lower cell numbers are injected. A possible reason is the competition of transplanted cells with host bone marrow cells. Colvin and colleagues showed that transplanted cells and cells of the host bone marrow are in direct competition and the engraftment is directly related to the ratio of injected cells and bone marrow cells (Colvin et al., 2004). A reason for the high LIC frequency determined by LDTA might be the long-term evaluation. Here even very small cell numbers have time to increase to visible population. At early time points the present model might fail to quantify these few cells and might underestimated very small numbers. Further studies are necessary to explain on the one hand the decrease of homing efficiency for smaller cell numbers, but on the other hand the engraftment of very small cell numbers in ALL and AML at late time points as shown by LDTA.

To calculate doubling times of eight different AML PDX samples, 10^7 PDX cells were injected into at least three different mice, and absolute numbers of PDX cells in the mouse bone marrow were quantified at different time points. From these numbers doubling times were calculated. The doubling times between the different AML PDX growing in mice differ broadly. The fastest sample has a doubling time of 1 day whereas the slowest sample has a doubling time of nearly 4 days. These different doubling times can explain the differences in passaging time of PDX AML and ALL samples in our group and in published data (Lock et al., 2002; Notta et al., 2011; Sanchez et al., 2009; Vick et al., 2015), as low doubling times lead to a faster increase of PDX cells and therefore to an earlier advanced leukemia burden in the mouse.

Interestingly, the majority of cells that were injected in the present study are not able to home to the mouse bone marrow, as only minor fractions of injected cells were detected. A possible reason might be the homing of these cells to other organs than the bone marrow, which were not analyzed within this study. Other studies showed an early engraftment of leukemic cells to the liver (Barrett et al., 2011) and cells that home to the liver very early but left the liver again (Vick et al., 2015). But the early engraftment of the liver seems to be sample dependent as other studies showed a later engraftment of PDX within the liver (Bomken et al., 2013), whereas all

studies showed an obvious first engraftment to the bone marrow of the lower extremities. Thus, the bone marrow is the most important organ to investigate for engraftment rates. Furthermore, in this study around 75 % of the mouse bone marrow was analyzed (Colvin et al., 2004). It might be that the remaining bone marrow of thoracic limbs, skull or rib cage harbor more PDX cells. But it has been show that mainly the bone marrow of the lower extremities harbors leukemia cells at early time points (Barrett et al., 2011; Bomken et al., 2013) and therefore it seems to be very unlikely that the remaining bone marrow contains all the missing PDX cells. In theory cells might still circulate in the bloodstream and will engraft later. But for normal hematopoiesis it has been shown that the engraftment of injected hematopoietic stem cells (HSC) is finished after 4 hours and afterward no additional cells are engrafting (Ellis et al., 2011). It seems likely that the same is true for AL cells. As a consequence, most injected cells, including the LIC, might have died and were degraded.

These data indicate that the engraftment of specific leukemic sample into mouse bone marrow depends on the cell number injected and on specific characteristics of the individual samples, like different cell distribution in the mouse, different cell dying, or additional homing to other niches than the bone marrow, which might not been seen with the present model. Until now, no data exists about the number of niches in the bone marrow (Nombela-Arrieta and Manz, 2017). The data argue against the presence of a preformed and fixed number of niche places present in the bone marrow of each NSG mouse, which are able to house PDX cells (Ugarte and Forsberg, 2013). In contrast, depending on the characteristics of the sample and the cell number injected, the bone marrow of each mouse seems to be able to home a different number of human leukemic cells.

In summary, it was shown that the established model enables insight into early leukemia bone marrow engraftment and that the engraftment depends on sample specific characteristics.

6.3 AL PDX samples show a logistic growth in mice

Besides insights into early engraftment of AL PDX, also investigations on AL PDX growth would help to understand the biology of the disease in more detail to finally improve or develop new treatment strategies.

In the present study lentiviral transduction of AL PDX samples enables enrichment and quantification of minute numbers of PDX cells from mouse bone marrow for detailed kinetics. Quantitative and relative analysis of PDX cells in mouse bone marrow over time showed an exponential increase of leukemic load for all analyzed samples over around two third of the

time from injection to leukemia induced death of the mouse, and growth slowed down thereafter. Mathematically, the early growth of PDX cells in mice is logarithmic, but slows down if about 10 % of cells within the mouse bone marrow are of human origin. This results mathematically in an overall logistic growth, which is an indicator for non-optimal nutrient supply (Schacht, 1980). A reason for logistic growth is space restriction, which seems on the one hand unlikely because the slowdown already happens when only 10 % of cells where of human origin but on the other hand it is likely because the bone marrow is surrounded by solid bone marrow, which cannot expand. Insufficient supply of critical resources like nutrients and oxygen by the bone marrow environment might diminish the proliferation rate of the leukemia cells, and is known to be another reason for the logistic growth of solid tumors (Araujo and McElwain, 2004; Bru et al., 2003; Casciari et al., 1992; Vaidya and Alexandro, 1982). Another reason for logistic growth could be an increase of cell death at high densities (Schacht, 1980). As it is known that PDX cells are spreading to other organs at later time points and that even the mouse bone marrow has up to more than 90 % leukemic cells at advanced leukemic stages (Bomken et al., 2013; Castro Alves et al., 2012; Jones et al., 2017; Wang et al., 2017), the possible increased cell death rate has to be compensated by a very high proliferations rate (Labi and Erlacher, 2015). Further studies are required to decipher the mechanisms which slow down leukemia growth at these low phases of leukemic infiltration in bone marrow.

6.4 Subpopulation of dormant cells as model for relapse-inducing cells in patients

In the present study CFSE staining was established to follow up proliferation. CFSE has already been used as proliferation marker in lymphocytes (Lyons and Parish, 1994; Parish, 1999), mouse HSC (Takizawa et al., 2011), and xenografts of solid tumors (Moore et al., 2012). Within this study, CFSE staining was established for ALL and AML PDX cells. By double staining with the widely used proliferation marker BrdU (Kee et al., 2002; Nakamura et al., 1991; Ninomiya et al., 2007), and the correlation of CFSE loss versus increase in absolute cell numbers in the mouse bone marrow, the present study shows that CFSE can reliably be used as proliferation marker of PDX cells. To analyze BrdU incorporation into DNA, permeabilization of these cells is necessary, meaning that cells die during this method. An advantage of CFSE is the detection of the signal in living cells without permeabilization, meaning that living cells can be further functionally characterized, and be re-injected for further studies.

Using the established enrichment methods combined with CFSE labeling, the present study discovered that PDX AML and ALL cells growing in mice reveal heterogeneity regarding proliferation. 10^7 PDX cells of several AML and ALL samples were labeled with CFSE, injected into mice, and PDX cells were enriched from mouse bone marrow and analyzed for CFSE content at different time points. AML and ALL contain a rare subpopulation of label retaining cells (LRC) which barely divide, even if tumor mass proliferated substantially. LRC existed in all but one different tested types of AL samples, in pediatric and in adult AL samples, in different risk groups as they exist in relapse and initial diagnosis samples. However, one AML sample did not contain LRC, indicating that the presence of LRC is not a mere stochastical event. Furthermore, LRC are not an artefact induced by the genetic engineering of the samples, because they also exist in samples without any lentiviral transduction or transgene expression.

Thus, for the majority of samples, a few cells did not participate in proliferation. Like in normal hematopoiesis (Trumpp et al., 2010), PDX AML and ALL harbor rare, long-term dormant cells. In addition dormant cells were identified in primary ALL samples by Ki-67 staining (Lutz et al., 2013). However, the present study provides for the first time a preclinical tool to study dormant human AML and ALL cells *in vivo* and describes that long-term resting cells exist in AML and ALL. This fact was unknown so far, as immunohistochemistry and flow cytometry of primary patients' samples only allow quantifying dormant cells as a snapshot at a given moment when cells e.g., lacking Ki-67 expression. But these methods fail to distinguish between short-term and long-term resting cells (Lutz et al., 2013). In contrast, LRC represent long-term resting cells which did not divide for up to 29 days explaining their minor abundance compared to primary samples. In the present model system, the LRC fraction constantly diminished over time; one reason for this might lay in the technical limitation that cells which proliferate first and become dormant later lost their CFSE label, and thereby the present method might underestimate the frequency of resting cells.

Development of relapse is a complex process involving genetic and non-genetic factors (Inaba et al., 2013). In adult ALL patients pre-existing minor clones with mutations responsible for drug resistance might lead to early relapse. Relapse originates often from treatment resistant cells that persist at MRD in the patients (Pui et al., 2008). Genome sequencing of matched diagnosis and relapse samples reveal that relapse samples often harbor specific genetic alterations. These genetic alterations were either acquired at relapse or already exist as minor clone at diagnosis and are responsible for the growth advantage and/or the treatment resistance of the subclone (Ding et al., 2012; Inaba et al., 2013; Pui et al., 2012). But some ALL cases are

genetically very stable, suggesting that here relapses are not mediated by mutational mechanisms (Staal et al., 2010). As cells at late relapse, meaning later than 30 month of diagnosis, often respond to the same treatment regimens as the cells at initial diagnosis, long-term dormant leukemic cells without any additional mutation might be responsible for the relapse. Therefore ALL LRC might represent surrogates for cells responsible for late relapse and for relapse cells without any additional mutations, as often seen in children (Staal et al., 2010).

The fact that LRC exist might explain why patients suffering from leukemia profit from maintenance therapy. ALL patients are routinely treated with oral low dose chemotherapy from end of intensive chemotherapy until, e.g., 2 years after diagnosis, and maintenance therapy improves patients' prognosis (Schrappe et al., 2000). Low dose maintenance therapy might act by removing long-term resting leukemia cells with relapse-inducing potential when they start to proliferate.

In conclusion the developed PDX model represents a unique tool to study long-term resting human leukemia cells *in vivo* and provides inside into leukemia biology. With the model, a rare dormant subpopulation within PDX AL cells was identified which might be a surrogate for relapse-inducing cells in patients. Therefore the developed model might be used as convenient tool to investigate new treatment strategies against dormant and relapse-inducing cells in patients. This tool enables for the first time improved research very close to the patients.

6.5 Stemness and dormancy are not directly connected in AML

A cancer stem cell (CSC) hierarchy has been described in numerous tumor entities including solid tumors (Visvader and Lindeman, 2008) and AML (Bonnet and Dick, 1997). Leukemia stem cells (LSC) are recognized as a clinically highly relevant subgroup of cells and are characterized by specific features such as self-renewal and dormancy (Essers and Trumpp, 2010; Ishikawa et al., 2007; Viale et al., 2009). The identified LRC within this study are defined by their reduced proliferation rate. Additionally, Erbey Özdemir, a colleague in the hosting laboratory, showed that LRC are localized mainly within the endosteal bone marrow niche, which was defined as the region around the bone matrix with a distance of less than 100 µm to the closest bone matrix (Ebinger et al., 2016; Özdemir, 2017). The endosteal bone marrow niche was originally identified as the location of hematopoietic stem cells (HSC) and it has been shown that HSC rarely proliferate (Malhotra and Kincade, 2009; Trumpp et al., 2010). The same has been shown for CSC (Ishikawa et al., 2007). Therefore, it was studied whether AML

LRC are surrogates for LSC and whether AML stem cells can be enriched by the dormant phenotype.

As surrogates for the LSC frequency, the leukemia initiating cell (LIC) frequency was determined by using the gold standard method LDTA (Castro Alves et al., 2012; Dick and Lapidot, 2005; Eppert et al., 2011; Sarry et al., 2011). In this study, the LIC frequency of sorted LRC and non-LRC in two different samples was compared. Sorted LRC and non-LRC were injected at different cell numbers into groups of mice and the engraftment of these cells was followed by blood measurement and *in vivo* imaging. From engraftment rates LIC frequencies was calculated using the ELDA software. Unexpectedly, CSC frequency was not higher in the LRC population; as LRC and non-LRC populations showed highly similar calculated LIC frequencies. These results are consistent with data of ALL LRC, as in ALL also LRC and non-LRC have similar LIC frequencies (Ebinger et al., 2016; Tiedt, 2014). But the literature showed that LSC are mainly dormant (Ishikawa et al., 2007; Viale et al., 2009) and that only LSC can induce new tumors and propagate the disease (Bonnet and Dick, 1997; Huntly and Gilliland, 2005; Lapidot et al., 1994; Reya et al., 2001). The current study showed that even fast proliferating leukemia cells have stem cell properties and can induce new tumors and that dormancy might not be an intrinsic characteristic of the here detected LRC, as pure LRC populations start to proliferate and induce new tumors. But the sample size within this study is very low and LRC and non-LRC were taken from their environment and re-injected into new mice for the LDTA. There might be putative extrinsic factors, that are responsible for the differences between LRC and non-LRC, but which are lost if they are taken from their former environment and placed into a new environment.

The presented results that LSC exist in different phenotypic cell types are in line with current data about the heterogeneity of LSC. In contrast to the former theory that AML stem cells always express the markers $lin^-CD34^+CD38^-$, and only these cells are able to induce a leukemia (Bonnet and Dick, 1997; Lapidot et al., 1994), present data shows that LSC are phenotypically heterogeneous (Eppert et al., 2011; Goardon et al., 2011; Jamieson et al., 2004; Sarry et al., 2011; Taussig et al., 2010).

Thus, as LRC and non-LRC have the same leukemia initiating potential, but different proliferation behavior *in vivo*, stemness and dormancy seems not to be directly connected in AML.

6.6 Drug resistance of LRC might be a consequence of their dormancy and bone marrow localization

Tumor cells often display two challenging features, namely dormancy and drug resistance. Dormant cells are known for their resistance against cytotoxic drugs, complicating elimination by anti-cancer therapy (Essers and Trumpp, 2010). However, it is unclear whether either dormancy or drug resistance is pivotal in respect to the other, so that dormancy is a consequence of resistance or *vice versa* (Blatter and Rottenberg, 2015).

As the identified LRC are defined by their dormant nature, the drug response of the dormant LRC and the fast proliferating non-LRC was compared. For this purpose as clinically related model, systemic *in vivo* drug treatment trials were performed. 10^7 CFSE labeled PDX cells were injected into mice. After seven days mice were treated with chemotherapy, followed by PDX cell enrichment and analysis for CFSE content 3 days later. LRC show marked resistance against *in vivo* chemotherapy. While systemic chemotherapy in mice reduced overall tumor mass by 90 %, most LRC survived chemotherapy. The relative drug reduction showed that proliferating cells were 10 to 100 fold more efficiently eliminated by *in vivo* chemotherapy than LRC. As a consequence, the relative percentage of LRC within the total population of cells isolated from treated mice increased significantly during treatment. LRC displayed *in vivo* resistance against a variety of different drugs of current ALL chemotherapy protocols used either in front line or in relapse. The study shows that acute leukemias consists of functionally heterogeneous cells regarding proliferation rate and drug resistance similar to functional heterogeneity shown in other tumor entities (Kreso et al., 2013). As LRC did not substantially participate in proliferation during growth of leukemia over weeks, and in treatment experiments over 10 days, LRC existed before onset of therapy and were not developed as a consequence of treatment. Drug resistance is associated with stem cell features of cancer cells (Wang, 2007). But as both LRC and non-LRC contain similar amounts of leukemia stem cells (LSC), but show different sensitivity towards drug treatment *in vivo*, the data implicate that stemness and drug resistance are not directly connected in acute leukemias. This assumption is supported by another current study, where it has been shown that cytarabine treatment resistant AML cells are not enriched for leukemia stem cells in an AML PDX model (Farge et al., 2017).

In one AML sample, AML-491, also the LRC were largely reduced by the treatment. The reduction by the treatment was little less for LRC compared to proliferating cells, but the AML-491 LRC did not show major drug resistance compared to the LRC of the other samples. In *in vivo* treatment trials with six different AML samples of a colleague in the hosting laboratory,

Binje Vick, only AML-491 was highly sensitive towards cytarabine treatment. Even one mouse was cured completely after treatment. The reason for this sensitivity might be that in this sample also the LRC are sensitive towards treatment. It shows that treating LRC might have a direct effect on the survival of mice. The data suggests that patients might benefit from treatment which targets dormant and drug resistant subpopulation. But the sample size with only one sample is very low and further samples which show LRC sensitivity would be needed to prove the correlation and to investigate the reasons for the drug sensitivity of these samples.

Leukemia initiating cells are thought to be located in the hematopoietic niche where they interact with the environment, which might protect them from chemotherapy (Lane et al., 2009; Tabe and Konopleva, 2014). These cells might survive chemotherapy and could induce a new tumor. The results in this study are in line with this hypothesis, because the re-injection of drug resistant LRC into new recipient mice induced a new leukemia in those mice. Thus drug resistant LRC have stem cell properties.

Furthermore, an interaction of LRC with the hematopoietic niche would explain their dormant phenotype, as a direct correlation between dormancy of HSC and their localization within the hematopoietic niche has been observed (Arai et al., 2004; Fleming et al., 2008; Wilson et al., 2008). Moreover, even a drug resistance of HSC localized in the niche has been shown (Cheng et al., 2000). Indeed further studies of the hosting laboratory by Erbey Özdemir on the localization of LRC in the mouse bone marrow showed that LRC are significantly more located within the endosteal niche than non-LRC (Ebinger et al., 2016; Özdemir, 2017).

As the identified LRC are drug resistant and are able to induce a new leukemia they might be surrogates for minimal residual disease (MRD) cells in patients; these cells survived drug treatment in patients and are often responsible for relapse. MRD levels are even a prognostic factor, as the level of MRD correlates with the risk for relapse (Gokbuget et al., 2012b; Locatelli et al., 2013; Paietta, 2015; Pettit et al., 2016).

Taken together, LRC are characterized by a combination of three features that challenge anti-leukemia treatment: dormancy, leukemia initiating potential and drug resistance, which might be a consequence of their bone marrow localization. As the established PDX model presented here covers all three features, this model might help to further characterize these cells and ultimately used to test new treatment regimens to increase outcome in patients and to prevent relapse.

6.7 The reversible phenotype of LRC might be a clinical treatment option

One new treatment strategy against drug resistant cells might be to break their dormancy. For dormant HSC it has been shown that they can be modified by different factors to start proliferation. As a result the former drug resistant HSC were sensitized towards chemotherapy (Trumpp et al., 2010).

Therefore, the question rises whether the detected subpopulation of LRC can be transformed to proliferating and thereby treatment sensitive cells. Regarding dormancy and proliferation the study investigated whether AL cells have a reversible or fixed phenotype. If LRC and non-LRC have a genuinely different biology harboring distinct and constant intrinsic characteristics, they might be organized in a hierarchical way similar to the known stem cell hierarchy existing in many tumors including AML (Kreso and Dick, 2014). If LRC and non-LRC have a temporary and reversible phenotype, they might behave like long-term dormant HSC. These cells can start cycling in response to stress for a defined period of time and turn back into dormancy later (Trumpp et al., 2010).

In this study, re-transplantation experiments of dormant LRC showed that they started to proliferate when they were dissociated from their environment and injected into next recipient mice. When fast proliferating non-LRC were dissociated from their environment, re-labeled with CFSE and injected into next recipient mice, they gave rise to the same heterogeneous pattern as before, including dormant LRC. Thus, the study detected that dormant cells can convert into fast proliferating cells and *vice versa*. Therefore, this data favors the second scenario, as LRC and non-LRC exhibit their proliferation phenotypes as reversible, temporary, transient functional phenotypes.

These new insights harbor direct translational consequences. As LRC lose their clinical relevant phenotype after release from the bone marrow environment, rapid sample processing might be critical for reliable profiling for diagnostics. But this is still a challenge in clinical routine (Bacher et al., 2010).

The phenotypic reversibility detected in acute leukemias parallels to normal hematopoiesis, in which long-term dormant HSC start cycling in response to stress for a defined period of time and turn back into dormancy later (Essers et al., 2009; Wilson et al., 2008). For HSC it has even been shown that breaking their dormancy with different factors sensitized them towards chemotherapy (Essers et al., 2009; Trumpp et al., 2010). The data indicates that it also might be possible to convert dormant AL cells into proliferating cells by treating them with certain factors, and thereby converting the former drug resistant dormant cells into drug sensitive cells.

And indeed for leukemia stem cells (LSC) it has been already shown that converting LSC from a dormant state into proliferation can efficiently sensitize them towards chemotherapy (Essers and Trumpp, 2010). In AML, treatment efficacy was enhanced *in vitro* and *in vivo* by converting dormant AML cells into proliferation (Kuhne et al., 2013; Nervi et al., 2009; Saito et al., 2010b; Zeng et al., 2009). In ALL, similar therapeutic strategies were efficient (Parameswaran et al., 2011; Sison et al., 2013; Welschinger et al., 2013).

In addition this study showed that AL cells sustain major biological plasticity for adapting to the current situation and on external stimuli. Putative extrinsic factors influencing AL proliferation rates might result from the direct *in vivo* environment. As this study was restricted to bone marrow and the identified LRC are localized within a certain bone marrow microenvironment, the endosteal bone marrow niche (Ebinger et al., 2016; Özdemir, 2017), the bone marrow niche might play an important role in determining proliferation rate in this study. Already in healthy hematopoiesis, it has been shown that dormant HSC are located in the endosteal bone marrow niche (Wilson et al., 2007). Within this bone marrow niche, different cellular compartments and the molecular crosstalk by secreted factors regulate the maintenance of HSC in the niche (Kiel and Morrison, 2008; Wilson and Trumpp, 2006). In addition in leukemia increasing evidence exists regarding the close interplay between the bone marrow niche and leukemia cells residing therein, and mechanisms by which the niche supports the leukemic disease start to become unraveled (Raaijmakers, 2011). For ALL, it has been shown, that these cells are located in special bone marrow niches (Pitt et al., 2015) and that leukemic cells within the niche are quiescent (Saito et al., 2010b). Therefore, LRC might be dormant because of their localization close to the endosteal bone marrow niche. This is supported by the fact that LRC start to proliferate when they were dissociated from their environment.

Disrupting this leukemia-niche interaction might represent an interesting concept for future therapies (Tabe and Konopleva, 2014). If treatment can release LRC from their *in vivo* environment, LRC might start to proliferate and thereby become sensitive towards chemotherapy. In normal hematopoiesis the interaction between HSC and their microenvironment can be disturbed to mobilize HSC (Morrison et al., 1997; Rettig et al., 2012). But also in AML, a treatment option is to induce mobilization of AML cells, to get them into circulation, which then enhances treatment effects of chemotherapy (Kuhne et al., 2013; Nervi et al., 2009; Zeng et al., 2009). In addition, targeting the niche in ALL, by disturbing the signaling between CXCL12 and its receptor CXCR4, leads to decreased development of leukemia (Pitt et al., 2015). The cytokine CXCL12 is produced by stromal cells and known to be important for the localization and maintenance of HSC (Lane et al., 2009).

As the current study showed that the dormant state of LRC is not an intrinsic but rather a convertible, temporary characteristic, also drug resistance might be a transient characteristic of LRC. In addition localization of LRC to the bone marrow niche seems to influence both, their dormancy and their drug resistance. These findings enable a first step towards new therapies. If dormant cells can be converted into proliferating cells, probably by targeting the bone marrow microenvironment, it should be able to target them afterwards with chemotherapy, reduce minimal residual disease and finally prevent relapse in patients.

6.8 Outlook

In this study, a dormant, drug resistant and stem cell like subpopulation within patient derived xenograft (PDX) acute leukemia (AL) cells was identified and characterized. It could be shown that this subpopulation is long-term resting, does not respond to chemotherapy-treatment *in vivo*, and is capable of inducing a new tumor (Figure 33). Therefore, these cells combine all adverse characteristics that challenge clinical success in AL patients (Lutz et al., 2013). As these cells might survive standard therapy and eventually lead to a relapse, they jeopardize patients' prognosis.

However, and as demonstrated in Figure 33, the rare population identified in this study has a reversible phenotype. When located on the endosteal bone marrow niche, which seems to have a protective influence, this subpopulation is dormant, drug resistant, and has leukemia stem cell properties. By release from the microenvironment, this population can be converted to a proliferating phenotype and might therefore be responsive towards therapy. This feature might therefore be a promising approach to target this adverse population.

As demonstrated in further studies by Erbey Özdemir (Ebinger et al., 2016; Özdemir, 2017), the LRC population characterized here, resembles minimal residual disease (MRD) cells of AL patients. During the treatment of AL, treatment resistant cells represent a major challenge, as they eventually induce relapse which is associated with poor prognosis (Gokbuget et al., 2012b; Locatelli et al., 2013; Paietta, 2015; Pettit et al., 2016). To prevent relapse in patients it is important to eradicate treatment resistant, dormant tumor cells.

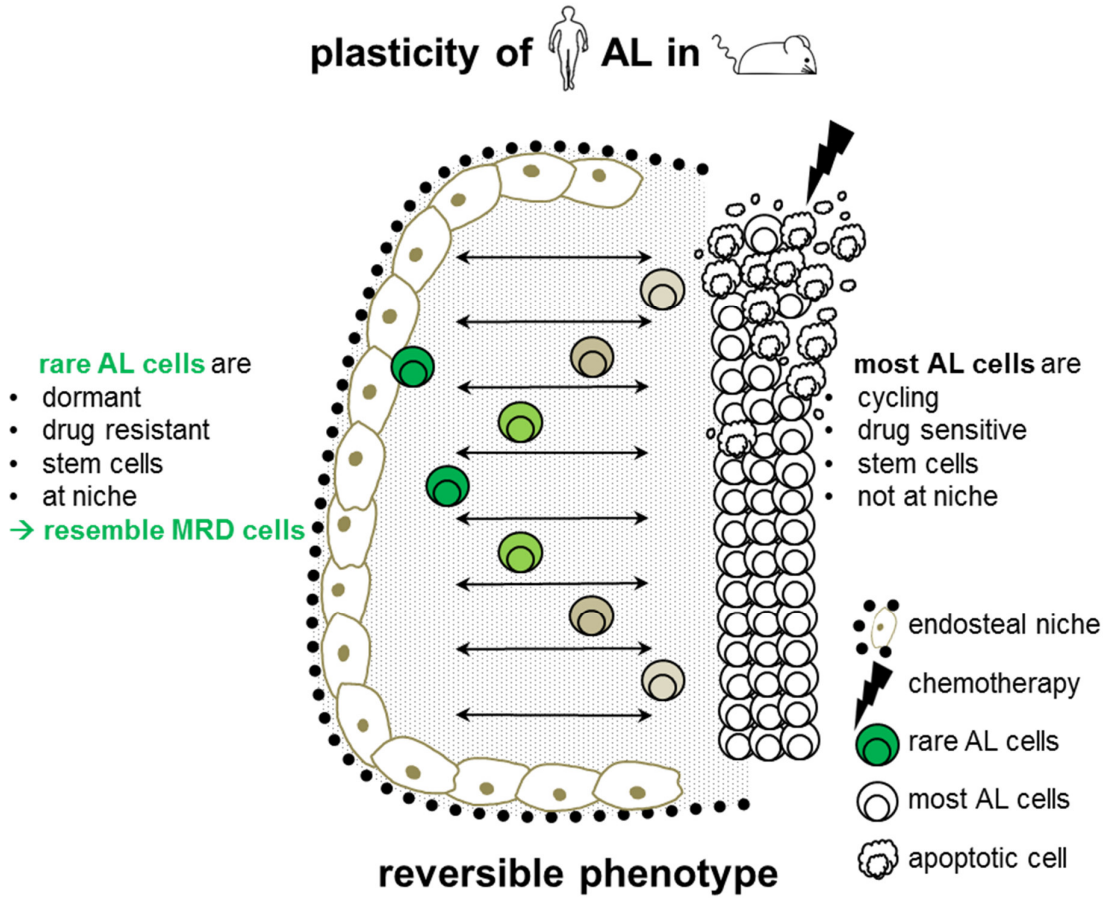

Figure 33: Plasticity hypotheses of human acute leukemic cells growing in mice.
Newly identified rare acute leukemic cells are dormant, drug resistant, have stem cells properties and are localized in the endosteal niche whereas most acute leukemic cells are proliferating, are drug sensitive, have stem cell properties and are not localized in the endosteal niche. But cells do not have a fixed phenotype: depending on the microenvironment they can convert into one or the other phenotype.

This plasticity of AL cells has a putative clinical relevance. For potential novel treatment strategies, the transient nature of the adverse characteristics of LRC suggests aiming at removing MRD cells from their protective environment in order to sensitize them towards chemotherapy treatment (Essers et al., 2009; Essers and Trumpp, 2010). The interaction between MRD cells and their bone marrow niche represents a promising target for novel therapeutic approaches to prevent relapse.

More research is required to define the vulnerable targets of the LRC subpopulation or of the niche cells providing protection.

Possible candidates for therapeutic targets are surface antigens that are differently expressed on LRC and non-LRC. Their inhibition on LRC might release these cells from their protective microenvironment. Beyond targeting the tumor cells, also the bone marrow microenvironment might be an effective target. Here signaling or surface molecules might be inhibited to shut

down environmental support. But as each non-LRC can convert into a drug resistant LRC, when it gets access to the protective niche, a persistent therapeutic inhibition might be required over prolonged periods of time.

As the study showed that the microenvironment influences the functional phenotype of AL cells like dormancy and drug resistance, this data might explain the limited explanatory power of *in vitro* assays: Both constantly proliferating cell line cells and non-cycling, primary leukemia or PDX cells are highly sensitive towards chemotherapy *in vitro*, and can therefore not mimic drug-resistant MRD cells in the patient. Drugs that are effective in these *in vitro* assays often fail in patients (Kamb, 2005; Sun et al., 2006). One reason might be the missing influence of the microenvironment (Dhami et al., 2016; Pemovska et al., 2013; Wu et al., 2010). Recently, to improve drug testing *in vitro*, the bone marrow microenvironment is often included by using co-culture systems with human or mouse bone marrow stromal cells (Dhami et al., 2016; Frismantas et al., 2015; Pemovska et al., 2013; Suryani et al., 2014). However, as the critical factors responsible for the protective niche are not yet characterize, it is unclear if these methods are suitable model systems with predictive value. Furthermore, direct research on patients MRD cells is difficult due to their cryptic nature and minute number. This limits their isolation for further research (Hedley and Keeney, 2013; Ommen, 2016). PDX models circumvent these limitations. PDX models of different tumor entities have been already successfully used for the prediction of clinical outcome, for preclinical drug development, for the identification of biomarkers and for personalized medicine strategies (Bertotti et al., 2011; Dong et al., 2010; Gao et al., 2015; Garrido-Laguna et al., 2010; Hidalgo et al., 2011; Keysar et al., 2013; Liem et al., 2004; Rajeshkumar et al., 2009). In addition, in personalized treatment PDX have been already successfully used for new treatment strategies (Trahair et al., 2016).

LRC in the here presented PDX model can repetitively be studied as highly enriched, pure fraction following the established isolation and enrichment protocol. The model allows the repetitive work on pure vivid LRC and thereby allowed the functional and phenotypical characterization of the population, which would not have been possible with primary patients' MRD cells. LRC might represent a preclinical surrogate for a clinically relevant subpopulation threatening AL patients. Furthermore, LRC in the acute leukemia PDX model will serve as informative tool for the development of novel treatment strategies aiming at preventing AL relapse. Therefore LRC in the here developed preclinical model can now be used as surrogates for relapse-inducing cell, for developing novel therapies in order to prevent relapse and increase the prognosis of AL patients.

7 References

Agorku, D., Bosio, A., and Hardt, O. (2014). Abstract 95: Depletion of mouse cells from human tumor xenografts significantly reduces bias in molecular analysis and improves culture of target cells. Cancer Research *74*, 95-95.

Aguirre-Ghiso, J. A. (2007). Models, mechanisms and clinical evidence for cancer dormancy. Nature reviews Cancer *7*, 834-846.

Al-Hajj, M., Wicha, M. S., Benito-Hernandez, A., Morrison, S. J., and Clarke, M. F. (2003). Prospective identification of tumorigenic breast cancer cells. Proceedings of the National Academy of Sciences of the United States of America *100*, 3983-3988.

Alruwetei, A. M., Carol, H., Sutton, R., Marshall, G. M., and Lock, R. B. (2015). Evaluation of Patient-Derived Xenografts for Modeling Outcome of Pediatric B-Cell Precursor Acute Lymphoblastic Leukemia. Blood *126*, 3759-3759.

Anderson, K., Lutz, C., van Delft, F. W., Bateman, C. M., Guo, Y., Colman, S. M., Kempski, H., Moorman, A. V., Titley, I., Swansbury, J.*, et al.* (2011). Genetic variegation of clonal architecture and propagating cells in leukaemia. Nature *469*, 356-361.

Arai, F., Hirao, A., Ohmura, M., Sato, H., Matsuoka, S., Takubo, K., Ito, K., Koh, G. Y., and Suda, T. (2004). Tie2/angiopoietin-1 signaling regulates hematopoietic stem cell quiescence in the bone marrow niche. Cell *118*, 149-161.

Araujo, R. P., and McElwain, D. L. (2004). A history of the study of solid tumour growth: the contribution of mathematical modelling. Bulletin of mathematical biology *66*, 1039-1091.

Bacher, U., Kohlmann, A., and Haferlach, T. (2010). Gene expression profiling for diagnosis and therapy in acute leukaemia and other haematologic malignancies. Cancer Treat Rev *36*, 637-646.

Baersch, G., Mollers, T., Hotte, A., Dockhorn-Dworniczak, B., Rube, C., Ritter, J., Jurgens, H., and Vormoor, J. (1997). Good engraftment of B-cell precursor ALL in NOD-SCID mice. Klinische Padiatrie *209*, 178-185.

Bansal, N., and Banerjee, D. (2009). Tumor initiating cells. Current pharmaceutical biotechnology *10*, 192-196.

Barrett, D. M., Seif, A. E., Carpenito, C., Teachey, D. T., Fish, J. D., June, C. H., Grupp, S. A., and Reid, G. S. (2011). Noninvasive bioluminescent imaging of primary patient acute lymphoblastic leukemia: a strategy for preclinical modeling. Blood *118*, e112-117.

Bertotti, A., Migliardi, G., Galimi, F., Sassi, F., Torti, D., Isella, C., Cora, D., Di Nicolantonio, F., Buscarino, M., Petti, C.*, et al.* (2011). A molecularly annotated platform of patient-derived xenografts ("xenopatients") identifies HER2 as an effective therapeutic target in cetuximab-resistant colorectal cancer. Cancer discovery *1*, 508-523.

Bhatia, M., Wang, J. C., Kapp, U., Bonnet, D., and Dick, J. E. (1997). Purification of primitive human hematopoietic cells capable of repopulating immune-deficient mice. Proceedings of the National Academy of Sciences of the United States of America *94*, 5320-5325.

Blatter, S., and Rottenberg, S. (2015). Minimal residual disease in cancer therapy--Small things make all the difference. Drug Resist Updat *21-22*, 1-10.

Bomken, S., Buechler, L., Rehe, K., Ponthan, F., Elder, A., Blair, H., Bacon, C. M., Vormoor, J., and Heidenreich, O. (2013). Lentiviral marking of patient-derived acute lymphoblastic leukaemic cells allows in vivo tracking of disease progression. Leukemia *27*, 718-721.

Bonnet, D. (2008). In vivo evaluation of leukemic stem cells through the xenotransplantation model. Current protocols in stem cell biology *Chapter 3*, Unit 3.2.

Bonnet, D., and Dick, J. E. (1997). Human acute myeloid leukemia is organized as a hierarchy that originates from a primitive hematopeitic cell. Nature Medicine *3*, 730-737.

Bosma, G. C., Custer, R. P., and Bosma, M. J. (1983). A severe combined immunodeficiency mutation in the mouse. Nature *301*, 527-530.

Bru, A., Albertos, S., Luis Subiza, J., Garcia-Asenjo, J. L., and Bru, I. (2003). The universal dynamics of tumor growth. Biophysical journal *85*, 2948-2961.

Burrell, R. A., McGranahan, N., Bartek, J., and Swanton, C. (2013). The causes and consequences of genetic heterogeneity in cancer evolution. Nature *501*, 338-345.

Casciari, J. J., Sotirchos, S. V., and Sutherland, R. M. (1992). Variations in tumor cell growth rates and metabolism with oxygen concentration, glucose concentration, and extracellular pH. Journal of cellular physiology *151*, 386-394.

Castro Alves, C., Terziyska, N., Grunert, M., Gündisch, S., Graubner, U., Quintanilla-Martinez, L., and Jeremias, I. (2012). Leukemia-initiating cells of patient-derived acute lymphoblastic leukemia xenografts are sensitive toward TRAIL. Blood *119*, 4224-4227.

Cheng, T., Rodrigues, N., Shen, H., Yang, Y., Dombkowski, D., Sykes, M., and Scadden, D. T. (2000). Hematopoietic stem cell quiescence maintained by p21cip1/waf1. Science (New York, NY) *287*, 1804-1808.

Cheshier, S. H., Morrison, S. J., Liao, X., and Weissman, I. L. (1999). In vivo proliferation and cell cycle kinetics of long-term self-renewing hematopoietic stem cells. Proceedings of the National Academy of Sciences of the United States of America *96*, 3120-3125.

Clevers, H. (2011). The cancer stem cell: premises, promises and challenges. Nat Med *17*, 313-319.

Colvin, G. A., Lambert, J. F., Abedi, M., Hsieh, C. C., Carlson, J. E., Stewart, F. M., and Quesenberry, P. J. (2004). Murine marrow cellularity and the concept of stem cell competition: geographic and quantitative determinants in stem cell biology. Leukemia *18*, 575-583.

De Kouchkovsky, I., and Abdul-Hay, M. (2016). 'Acute myeloid leukemia: a comprehensive review and 2016 update'. Blood cancer journal *6*, e441.

Dhami, S. P., Kappala, S. S., Thompson, A., and Szegezdi, E. (2016). Three-dimensional ex vivo co-culture models of the leukaemic bone marrow niche for functional drug testing. Drug discovery today *21*, 1464-1471.

Dick, J. E. (2008). Stem cell concepts renew cancer research. Blood *112*, 4793-4807.

Dick, J. E., and Lapidot, T. (2005). Biology of normal and acute myeloid leukemia stem cells. International journal of hematology *82*, 389-396.

Ding, L., Ley, T. J., Larson, D. E., Miller, C. A., Koboldt, D. C., Welch, J. S., Ritchey, J. K., Young, M. A., Lamprecht, T., McLellan, M. D.*, et al.* (2012). Clonal evolution in relapsed acute myeloid leukaemia revealed by whole-genome sequencing. Nature *481*, 506-510.

Dong, X., Guan, J., English, J. C., Flint, J., Yee, J., Evans, K., Murray, N., Macaulay, C., Ng, R. T., Gout, P. W.*, et al.* (2010). Patient-derived first generation xenografts of non-small cell lung cancers: promising tools for predicting drug responses for personalized chemotherapy. Clinical cancer research : an official journal of the American Association for Cancer Research *16*, 1442-1451.

Dördelmann, M., Reiter, A., Borkhardt, A., Ludwig, W.-D., Götz, N., Viehmann, S., Gadner, H., Riehm, H., and Schrappe, M. (1999). Prednisone Response Is the Strongest Predictor of Treatment Outcome in Infant Acute Lymphoblastic Leukemia. Blood *94*, 1209-1217.

Dores, G. M., Devesa, S. S., Curtis, R. E., Linet, M. S., and Morton, L. M. (2012). Acute leukemia incidence and patient survival among children and adults in the United States, 2001-2007. Blood *119*, 34-43.

Dull, T., Zufferey, R., Kelly, M., Mandel, R. J., Nguyen, M., Trono, D., and Naldini, L. (1998). A third-generation lentivirus vector with a conditional packaging system. Journal of virology *72*, 8463-8471.

Ebinger, S., Ozdemir, E. Z., Ziegenhain, C., Tiedt, S., Castro Alves, C., Grunert, M., Dworzak, M., Lutz, C., Turati, V. A., Enver, T.*, et al.* (2016). Characterization of Rare, Dormant, and Therapy-Resistant Cells in Acute Lymphoblastic Leukemia. Cancer cell *30*, 849-862.

Ellis, S. L., Grassinger, J., Jones, A., Borg, J., Camenisch, T., Haylock, D., Bertoncello, I., and Nilsson, S. K. (2011). The relationship between bone, hemopoietic stem cells, and vasculature. Blood *118*, 1516-1524.

Eppert, K., Takenaka, K., Lechman, E. R., Waldron, L., Nilsson, B., van Galen, P., Metzeler, K. H., Poeppl, A., Ling, V., Beyene, J.*, et al.* (2011). Stem cell gene expression programs influence clinical outcome in human leukemia. Nat Med *17*, 1086-1093.

Esparza, S. D., and Sakamoto, K. M. (2005). Topics in pediatric leukemia--acute lymphoblastic leukemia. MedGenMed : Medscape general medicine *7*, 23.

Essers, M. A., Offner, S., Blanco-Bose, W. E., Waibler, Z., Kalinke, U., Duchosal, M. A., and Trumpp, A. (2009). IFNalpha activates dormant haematopoietic stem cells in vivo. Nature *458*, 904-908.

Essers, M. A. G., and Trumpp, A. (2010). Targeting leukemic stem cells by breaking their dormancy. Molecular oncology *4*, 443-450.

Estey, E., and Dohner, H. (2006). Acute myeloid leukaemia. Lancet (London, England) *368*, 1894-1907.

Estey, E. H. (2014). Acute myeloid leukemia: 2014 update on risk-stratification and management. American journal of hematology *89*, 1063-1081.

Farge, T., Saland, E., de Toni, F., Aroua, N., Hosseini, M., Perry, R., Bosc, C., Sugita, M., Stuani, L., Fraisse, M.*, et al.* (2017). Chemotherapy Resistant Human Acute Myeloid Leukemia Cells are Not Enriched for Leukemic Stem Cells but Require Oxidative Metabolism. Cancer discovery.

Fehse, B., Uhde, A., Fehse, N., Eckert, H. G., Clausen, J., Ruger, R., Koch, S., Ostertag, W., Zander, A. R., and Stockschlader, M. (1997). Selective immunoaffinity-based enrichment of CD34+ cells transduced with retroviral vectors containing an intracytoplasmatically truncated version of the human low-affinity nerve growth factor receptor (deltaLNGFR) gene. Hum Gene Ther *8*, 1815-1824.

Ferlay, J., Steliarova-Foucher, E., Lortet-Tieulent, J., Rosso, S., Coebergh, J. W., Comber, H., Forman, D., and Bray, F. (2013). Cancer incidence and mortality patterns in Europe: estimates for 40 countries in 2012. European journal of cancer (Oxford, England : 1990) *49*, 1374-1403.

Fleming, H. E., Janzen, V., Lo Celso, C., Guo, J., Leahy, K. M., Kronenberg, H. M., and Scadden, D. T. (2008). Wnt signaling in the niche enforces hematopoietic stem cell quiescence and is necessary to preserve self-renewal in vivo. Cell stem cell *2*, 274-283.

Frismantas, V., Dobay, M. P., Rinaldi, A., Joachim, K., Marovca, B., Horvath, P., Delorenzi, M., Cario, G., Schrappe, M., Stanulla, M.*, et al.* (2015). Drug Response Profiling to Identify Selective Pharmacological Activity in Drug Resistant ALL. Blood *126*, 2532-2532.

Gao, H., Korn, J. M., Ferretti, S., Monahan, J. E., Wang, Y., Singh, M., Zhang, C., Schnell, C., Yang, G., Zhang, Y.*, et al.* (2015). High-throughput screening using patient-derived tumor xenografts to predict clinical trial drug response. Nat Med *21*, 1318-1325.

Gao, M. Q., Choi, Y. P., Kang, S., Youn, J. H., and Cho, N. H. (2010). CD24+ cells from hierarchically organized ovarian cancer are enriched in cancer stem cells. Oncogene *29*, 2672-2680.

Garrido-Laguna, I., Tan, A. C., Uson, M., Angenendt, M., Ma, W. W., Villaroel, M. C., Zhao, M., Rajeshkumar, N. V., Jimeno, A., Donehower, R.*, et al.* (2010). Integrated preclinical and clinical development of mTOR inhibitors in pancreatic cancer. British journal of cancer *103*, 649-655.

Gillet, J. P., Calcagno, A. M., Varma, S., Marino, M., Green, L. J., Vora, M. I., Patel, C., Orina, J. N., Eliseeva, T. A., Singal, V., *et al.* (2011). Redefining the relevance of established cancer cell lines to the study of mechanisms of clinical anti-cancer drug resistance. Proceedings of the National Academy of Sciences of the United States of America *108*, 18708-18713.

Goardon, N., Marchi, E., Atzberger, A., Quek, L., Schuh, A., Soneji, S., Woll, P., Mead, A., Alford, K. A., Rout, R., *et al.* (2011). Coexistence of LMPP-like and GMP-like leukemia stem cells in acute myeloid leukemia. Cancer cell *19*, 138-152.

Gokbuget, N., Kneba, M., Raff, T., Trautmann, H., Bartram, C. R., Arnold, R., Fietkau, R., Freund, M., Ganser, A., Ludwig, W. D., *et al.* (2012a). Adult patients with acute lymphoblastic leukemia and molecular failure display a poor prognosis and are candidates for stem cell transplantation and targeted therapies. Blood *120*, 1868-1876.

Gokbuget, N., Stanze, D., Beck, J., Diedrich, H., Horst, H. A., Huttmann, A., Kobbe, G., Kreuzer, K. A., Leimer, L., Reichle, A., *et al.* (2012b). Outcome of relapsed adult lymphoblastic leukemia depends on response to salvage chemotherapy, prognostic factors, and performance of stem cell transplantation. Blood *120*, 2032-2041.

Goldstone, A. H., Richards, S. M., Lazarus, H. M., Tallman, M. S., Buck, G., Fielding, A. K., Burnett, A. K., Chopra, R., Wiernik, P. H., Foroni, L., *et al.* (2008). In adults with standard-risk acute lymphoblastic leukemia, the greatest benefit is achieved from a matched sibling allogeneic transplantation in first complete remission, and an autologous transplantation is less effective than conventional consolidation/maintenance chemotherapy in all patients: final results of the International ALL Trial (MRC UKALL XII/ECOG E2993). Blood *111*, 1827-1833.

Greaves, M., and Maley, C. C. (2012). Clonal evolution in cancer. Nature *481*, 306-313.

Guan, Y., Gerhard, B., and Hogge, D. E. (2003). Detection, isolation, and stimulation of quiescent primitive leukemic progenitor cells from patients with acute myeloid leukemia (AML). Blood *101*, 3142-3149.

Guenechea, G., Gan, O. I., Dorrell, C., and Dick, J. E. (2001). Distinct classes of human stem cells that differ in proliferative and self-renewal potential. Nat Immunol *2*, 75-82.

Guzman, M. L., and Allan, J. N. (2014). Concise review: Leukemia stem cells in personalized medicine. Stem cells (Dayton, Ohio) *32*, 844-851.

Hausser, H. J., and Brenner, R. E. (2005). Phenotypic instability of Saos-2 cells in long-term culture. Biochemical and biophysical research communications *333*, 216-222.

Hedley, B. D., and Keeney, M. (2013). Technical issues: flow cytometry and rare event analysis. International journal of laboratory hematology *35*, 344-350.

Hermann, P. C., Huber, S. L., Herrler, T., Aicher, A., Ellwart, J. W., Guba, M., Bruns, C. J., and Heeschen, C. (2007). Distinct populations of cancer stem cells determine tumor growth and metastatic activity in human pancreatic cancer. Cell stem cell *1*, 313-323.

Hidalgo, M., Bruckheimer, E., Rajeshkumar, N. V., Garrido-Laguna, I., De Oliveira, E., Rubio-Viqueira, B., Strawn, S., Wick, M. J., Martell, J., and Sidransky, D. (2011). A pilot clinical study of treatment guided by personalized tumorgrafts in patients with advanced cancer. Molecular cancer therapeutics *10*, 1311-1316.

Hilden, J. M., Dinndorf, P. A., Meerbaum, S. O., Sather, H., Villaluna, D., Heerema, N. A., McGlennen, R., Smith, F. O., Woods, W. G., Salzer, W. L., *et al.* (2006). Analysis of prognostic factors of acute lymphoblastic leukemia in infants: report on CCG 1953 from the Children's Oncology Group. Blood *108*, 441-451.

Hope, K. J., Jin, L., and Dick, J. E. (2003). Human acute myeloid leukemia stem cells. Archives of medical research *34*, 507-514.

Hu, Y., and Smyth, G. K. (2009). ELDA: Extreme limiting dilution analysis for comparing depleted and enriched populations in stem cell and other assays. Journal of immunological methods *347*, 70-78.

Hunger, S. P., and Mullighan, C. G. (2015). Acute Lymphoblastic Leukemia in Children. New England Journal of Medicine *373*, 1541-1552.

Huntly, B. J., and Gilliland, D. G. (2005). Leukaemia stem cells and the evolution of cancer-stem-cell research. Nature reviews Cancer *5*, 311-321.

Hutter, G., Nickenig, C., Garritsen, H., Hellenkamp, F., Hoerning, A., Hiddemann, W., and Dreyling, M. (2004). Use of polymorphisms in the noncoding region of the human mitochondrial genome to identify potential contamination of human leukemia-lymphoma cell lines. Hematol J *5*, 61-68.

Iacobucci, I., Li, Y., Roberts, K. G., Dobson, S. M., Kim, J. C., Payne-Turner, D., Harvey, R. C., Valentine, M., McCastlain, K., Easton, J.*, et al.* (2016). Truncating Erythropoietin Receptor Rearrangements in Acute Lymphoblastic Leukemia. Cancer cell *29*, 186-200.

Inaba, H., Greaves, M., and Mullighan, C. G. (2013). Acute lymphoblastic leukaemia. The Lancet *381*, 1943-1955.

Inaba, H., and Pui, C. H. (2010). Glucocorticoid use in acute lymphoblastic leukaemia. The Lancet Oncology *11*, 1096-1106.

Ishikawa, F., Yoshida, S., Saito, Y., Hijikata, A., Kitamura, H., Tanaka, S., Nakamura, R., Tanaka, T., Tomiyama, H., Saito, N.*, et al.* (2007). Chemotherapy-resistant human AML stem cells home to and engraft within the bone-marrow endosteal region. Nat Biotech *25*, 1315-1321.

Jacoby, E., Chien, C. D., and Fry, T. J. (2014). Murine models of acute leukemia: important tools in current pediatric leukemia research. Frontiers in oncology *4*, 95.

Jamieson, C. H., Ailles, L. E., Dylla, S. J., Muijtjens, M., Jones, C., Zehnder, J. L., Gotlib, J., Li, K., Manz, M. G., Keating, A.*, et al.* (2004). Granulocyte-macrophage progenitors as candidate leukemic stem cells in blast-crisis CML. The New England journal of medicine *351*, 657-667.

Jones, L., Richmond, J., Evans, K., Carol, H., Jing, D., Kurmasheva, R. T., Billups, C. A., Houghton, P. J., Smith, M. A., and Lock, R. B. (2017). Bioluminescence Imaging Enhances Analysis of Drug Responses in a Patient-Derived Xenograft Model of Pediatric ALL. Clinical cancer research : an official journal of the American Association for Cancer Research.

Jordan, C. T., Guzman, M. L., and Noble, M. (2006). Cancer Stem Cells. New England Journal of Medicine *355*, 1253-1261.

Kamb, A. (2005). What's wrong with our cancer models? Nature reviews Drug discovery *4*, 161-165.

Kamel-Reid, S., Letarte, M., Sirard, C., Doedens, M., Grunberger, T., Fulop, G., Freedman, M., Phillips, R., and Dick, J. (1989). A model of human acute lymphoblastic leukemia in immune-deficient SCID mice. Science (New York, NY) *246*, 1597-1600.

Kee, N., Sivalingam, S., Boonstra, R., and Wojtowicz, J. M. (2002). The utility of Ki-67 and BrdU as proliferative markers of adult neurogenesis. Journal of neuroscience methods *115*, 97-105.

Keysar, S. B., Astling, D. P., Anderson, R. T., Vogler, B. W., Bowles, D. W., Morton, J. J., Paylor, J. J., Glogowska, M. J., Le, P. N., Eagles-Soukup, J. R.*, et al.* (2013). A patient tumor transplant model of squamous cell cancer identifies PI3K inhibitors as candidate therapeutics in defined molecular bins. Molecular oncology *7*, 776-790.

Kiel, M. J., and Morrison, S. J. (2008). Uncertainty in the niches that maintain haematopoietic stem cells. Nature reviews Immunology *8*, 290-301.

Kim, J. E., Kalimuthu, S., and Ahn, B. C. (2015). In vivo cell tracking with bioluminescence imaging. Nuclear medicine and molecular imaging *49*, 3-10.

Kong, Y., Yoshida, S., Saito, Y., Doi, T., Nagatoshi, Y., Fukata, M., Saito, N., Yang, S. M., Iwamoto, C., Okamura, J.*, et al.* (2008). CD34+CD38+CD19+ as well as CD34+CD38-CD19+ cells are leukemia-initiating cells with self-renewal capacity in human B-precursor ALL. Leukemia *22*, 1207-1213.

Kreso, A., and Dick, J. E. (2014). Evolution of the cancer stem cell model. Cell stem cell *14*, 275-291.

Kreso, A., O'Brien, C. A., van Galen, P., Gan, O. I., Notta, F., Brown, A. M., Ng, K., Ma, J., Wienholds, E., Dunant, C.*, et al.* (2013). Variable clonal repopulation dynamics influence chemotherapy response in colorectal cancer. Science (New York, NY) *339*, 543-548.

Kuhne, M. R., Mulvey, T., Belanger, B., Chen, S., Pan, C., Chong, C., Cao, F., Niekro, W., Kempe, T., Henning, K. A.*, et al.* (2013). BMS-936564/MDX-1338: a fully human anti-CXCR4 antibody induces apoptosis in vitro and shows antitumor activity in vivo in hematologic malignancies. Clinical cancer research : an official journal of the American Association for Cancer Research *19*, 357-366.

Kunz, J. B., Rausch, T., Bandapalli, O. R., Eilers, J., Pechanska, P., Schuessele, S., Assenov, Y., Stutz, A. M., Kirschner-Schwabe, R., Hof, J.*, et al.* (2015). Pediatric T-cell lymphoblastic leukemia evolves into relapse by clonal selection, acquisition of mutations and promoter hypomethylation. Haematologica *100*, 1442-1450.

Labi, V., and Erlacher, M. (2015). How cell death shapes cancer. Cell death & disease *6*, e1675.

Lane, S. W., Scadden, D. T., and Gilliland, D. G. (2009). The leukemic stem cell niche: current concepts and therapeutic opportunities. Blood *114*, 1150-1157.

Lapidot, T., Sirard, C., Vormoor, J., Murdoch, B., Hoang, T., Caceres-Cortes, J., Minden, M., Paterson, B., Caligiuri, M. A., and Dick, J. E. (1994). A cell initiating human acute myeloid leukaemia after transplantation into SCID mice. Nature *367*, 645-648.

le Viseur, C., Hotfilder, M., Bomken, S., Wilson, K., Röttgers, S., Schrauder, A., Rosemann, A., Irving, J., Stam, R. W., Shultz, L. D.*, et al.* (2008). In Childhood Acute Lymphoblastic Leukemia, Blasts at Different Stages of Immunophenotypic Maturation Have Stem Cell Properties. Cancer cell *14*, 47-58.

Lee, E. M., Bachmann, P. S., and Lock, R. B. (2007). Xenograft models for the preclinical evaluation of new therapies in acute leukemia. Leukemia & lymphoma *48*, 659-668.

Leoni, V., and Biondi, A. (2015). Tyrosine kinase inhibitors in BCR-ABL positive acute lymphoblastic leukemia. Haematologica *100*, 295-299.

Liem, N. L. M., Papa, R. A., Milross, C. G., Schmid, M. A., Tajbakhsh, M., Choi, S., Ramirez, C. D., Rice, A. M., Haber, M., Norris, M. D.*, et al.* (2004). Characterization of childhood acute lymphoblastic leukemia xenograft models for the preclinical evaluation of new therapies. Blood *103*, 3905-3914.

Locatelli, F., Moretta, F., and Rutella, S. (2013). Management of relapsed acute lymphoblastic leukemia in childhood with conventional and innovative approaches. Current opinion in oncology *25*, 707-715.

Lock, R. B., Liem, N., Farnsworth, M. L., Milross, C. G., Xue, C., Tajbakhsh, M., Haber, M., Norris, M. D., Marshall, G. M., and Rice, A. M. (2002). The nonobese diabetic/severe combined immunodeficient (NOD/SCID) mouse model of childhood acute lymphoblastic leukemia reveals intrinsic differences in biologic characteristics at diagnosis and relapse. Blood *99*, 4100-4108.

Lock, R. B., Liem, N. L., and Papa, R. A. (2005). Preclinical Testing of Antileukemic Drugs Using an In Vivo Model of Systemic Disease. In, pp. 323-334.

Lokody, I. (2014). Drug resistance: Overcoming resistance in acute myeloid leukaemia treatment. Nature reviews Cancer *14*, 452-453.

Lutz, C., Woll, P. S., Hall, G., Castor, A., Dreau, H., Cazzaniga, G., Zuna, J., Jensen, C., Clark, S. A., Biondi, A.*, et al.* (2013). Quiescent leukaemic cells account for minimal residual disease in childhood lymphoblastic leukaemia. Leukemia *27*, 1204-1207.

Lyons, A. B., and Parish, C. R. (1994). Determination of lymphocyte division by flow cytometry. Journal of immunological methods *171*, 131-137.

Malhotra, S., and Kincade, P. W. (2009). Canonical Wnt pathway signaling suppresses VCAM-1 expression by marrow stromal and hematopoietic cells. Experimental hematology *37*, 19-30.

Marusyk, A., Almendro, V., and Polyak, K. (2012). Intra-tumour heterogeneity: a looking glass for cancer? Nature reviews Cancer *12*, 323-334.

Matsushita, H., Yahata, T., Sheng, Y., Nakamura, Y., Muguruma, Y., Matsuzawa, H., Tanaka, M., Hayashi, H., Sato, T., Damdinsuren, A.*, et al.* (2014). Establishment of a humanized APL model via the transplantation of PML-RARA-transduced human common myeloid progenitors into immunodeficient mice. PloS one *9*, e111082.

Maude, S. L., Teachey, D. T., Porter, D. L., and Grupp, S. A. (2015). CD19-targeted chimeric antigen receptor T-cell therapy for acute lymphoblastic leukemia. Blood *125*, 4017-4023.

Metzeler, K. H., and Herold, T. (2016). Spectrum and prognostic relevance of driver gene mutations in acute myeloid leukemia. *128*, 686-698.

Meyer, L. H., and Debatin, K.-M. (2011). Diversity of Human Leukemia Xenograft Mouse Models: Implications for Disease Biology. Cancer Research *71*, 7141-7144.

Meyer, L. H., Eckhoff, S. M., Queudeville, M., Kraus, J. M., Giordan, M., Stursberg, J., Zangrando, A., Vendramini, E., Moricke, A., Zimmermann, M.*, et al.* (2011). Early relapse in ALL is identified by time to leukemia in NOD/SCID mice and is characterized by a gene signature involving survival pathways. Cancer cell *19*, 206-217.

Mitra, A., Mishra, L., and Li, S. (2013). Technologies for deriving primary tumor cells for use in personalized cancer therapy. Trends in biotechnology *31*, 347-354.

Modlich, U., Navarro, S., Zychlinski, D., Maetzig, T., Knoess, S., Brugman, M. H., Schambach, A., Charrier, S., Galy, A., Thrasher, A. J.*, et al.* (2009). Insertional transformation of hematopoietic cells by self-inactivating lentiviral and gammaretroviral vectors. Molecular therapy : the journal of the American Society of Gene Therapy *17*, 1919-1928.

Moore, N., Houghton, J., and Lyle, S. (2012). Slow-cycling therapy-resistant cancer cells. Stem cells and development *21*, 1822-1830.

Morisot, S., Wayne, A. S., Bohana-Kashtan, O., Kaplan, I. M., Gocke, C. D., Hildreth, R., Stetler-Stevenson, M., Walker, R. L., Davis, S., Meltzer, P. S.*, et al.* (2010). High frequencies of leukemia stem cells in poor-outcome childhood precursor-B acute lymphoblastic leukemias. Leukemia *24*, 1859-1866.

Morrison, S. J., and Spradling, A. C. (2008). Stem Cells and Niches: Mechanisms That Promote Stem Cell Maintenance throughout Life. Cell *132*, 598-611.

Morrison, S. J., Wright, D. E., and Weissman, I. L. (1997). Cyclophosphamide/granulocyte colony-stimulating factor induces hematopoietic stem cells to proliferate prior to mobilization. Proceedings of the National Academy of Sciences of the United States of America *94*, 1908-1913.

Mullighan, C. G. (2013). Genomic characterization of childhood acute lymphoblastic leukemia. Seminars in hematology *50*, 314-324.

Nakamura, S., Takeda, Y., Kanno, M., Yoshida, T., Ohtake, S., Kobayashi, K., Okabe, Y., and Matsuda, T. (1991). Application of bromodeoxyuridine (BrdU) and anti-BrdU monoclonal antibody for the in vivo analysis of proliferative characteristics of human leukemia cells in bone marrows. Oncology *48*, 285-289.

Nervi, B., Ramirez, P., Rettig, M. P., Uy, G. L., Holt, M. S., Ritchey, J. K., Prior, J. L., Piwnica-Worms, D., Bridger, G., Ley, T. J., and DiPersio, J. F. (2009). Chemosensitization of acute myeloid leukemia (AML) following mobilization by the CXCR4 antagonist AMD3100. Blood *113*, 6206-6214.

Ninomiya, M., Abe, A., Katsumi, A., Xu, J., Ito, M., Arai, F., Suda, T., Ito, M., Kiyoi, H., Kinoshita, T., and Naoe, T. (2007). Homing, proliferation and survival sites of human leukemia cells in vivo in immunodeficient mice. Leukemia *21*, 136-142.

Nombela-Arrieta, C., and Manz, M. G. (2017). Quantification and three-dimensional microanatomical organization of the bone marrow. Blood Advances *1*, 407-416.

Nombela-Arrieta, C., Pivarnik, G., Winkel, B., Canty, K. J., Harley, B., Mahoney, J. E., Park, S. Y., Lu, J., Protopopov, A., and Silberstein, L. E. (2013). Quantitative imaging of haematopoietic stem and progenitor cell localization and hypoxic status in the bone marrow microenvironment. Nature cell biology *15*, 533-543.

Notta, F., Mullighan, C. G., Wang, J. C., Poeppl, A., Doulatov, S., Phillips, L. A., Ma, J., Minden, M. D., Downing, J. R., and Dick, J. E. (2011). Evolution of human BCR-ABL1 lymphoblastic leukaemia-initiating cells. Nature *469*, 362-367.

O'Brien, C. A., Pollett, A., Gallinger, S., and Dick, J. E. (2007). A human colon cancer cell capable of initiating tumour growth in immunodeficient mice. Nature *445*, 106-110.

Ommen, H. B. (2016). Monitoring minimal residual disease in acute myeloid leukaemia: a review of the current evolving strategies. Therapeutic advances in hematology *7*, 3-16.

Orford, K. W., and Scadden, D. T. (2008). Deconstructing stem cell self-renewal: genetic insights into cell-cycle regulation. Nature reviews Genetics *9*, 115-128.

Özdemir, E. Z. (2017) Characterization of dormant and chemotherapy-resistant ALL cells in PDX mouse models, Ludwig Maximilans Universität, München.

Paietta, E. (2015). Should minimal residual disease guide therapy in AML? Best practice & research Clinical haematology *28*, 98-105.

Pan, C., Kumar, C., Bohl, S., Klingmueller, U., and Mann, M. (2009). Comparative proteomic phenotyping of cell lines and primary cells to assess preservation of cell type-specific functions. Molecular & cellular proteomics : MCP *8*, 443-450.

Parameswaran, R., Yu, M., Lim, M., Groffen, J., and Heisterkamp, N. (2011). Combination of drug therapy in acute lymphoblastic leukemia with a CXCR4 antagonist. Leukemia *25*, 1314-1323.

Parish, C. R. (1999). Fluorescent dyes for lymphocyte migration and proliferation studies. Immunology and cell biology *77*, 499-508.

Passegue, E., Wagers, A. J., Giuriato, S., Anderson, W. C., and Weissman, I. L. (2005). Global analysis of proliferation and cell cycle gene expression in the regulation of hematopoietic stem and progenitor cell fates. The Journal of experimental medicine *202*, 1599-1611.

Patel, C., Stenke, L., Varma, S., Lindberg, M. L., Bjorkholm, M., Sjoberg, J., Viktorsson, K., Lewensohn, R., Landgren, O., Gottesman, M. M., and Gillet, J. P. (2013). Multidrug resistance in relapsed acute myeloid leukemia: evidence of biological heterogeneity. Cancer *119*, 3076-3083.

Pemovska, T., Yadav, B., Majumder, M. M., Kontro, M., Porkka, K., Kallioniemi, O., Aittokallio, T., Wennerberg, K., and Heckman, C. A. (2013). Stromal Cell Supported High-Throughput Drug Testing Of Primary Leukemia Cells For Comprehensive Assessment Of Sensitivity To Novel Therapies. Blood *122*, 1668-1668.

Pettit, K., Stock, W., and Walter, R. B. (2016). Incorporating measurable ('minimal') residual disease-directed treatment strategies to optimize outcomes in adults with acute myeloid leukemia. Leukemia & lymphoma *57*, 1527-1533.

Pitt, L. A., Tikhonova, A. N., Hu, H., Trimarchi, T., King, B., Gong, Y., Sanchez-Martin, M., Tsirigos, A., Littman, D. R., Ferrando, A. A.*, et al.* (2015). CXCL12-Producing Vascular Endothelial Niches Control Acute T Cell Leukemia Maintenance. Cancer cell *27*, 755-768.

Pollyea, D. A., Gutman, J. A., Gore, L., Smith, C. A., and Jordan, C. T. (2014). Targeting acute myeloid leukemia stem cells: a review and principles for the development of clinical trials. Haematologica *99*, 1277-1284.

Pui, C.-H., and Evans, W. E. (2006). Treatment of Acute Lymphoblastic Leukemia. New England Journal of Medicine *354*, 166-178.

Pui, C.-H., Mullighan, C. G., Evans, W. E., and Relling, M. V. (2012). Pediatric acute lymphoblastic leukemia: where are we going and how do we get there? Blood *120*, 1165-1174.

Pui, C.-H., Robison, L. L., and Look, A. T. (2008). Acute lymphoblastic leukaemia. The Lancet *371*, 1030-1043.

Pui, C. H., and Evans, W. E. (2013). A 50-year journey to cure childhood acute lymphoblastic leukemia. Seminars in hematology *50*, 185-196.

Pui, C. H., Yang, J. J., Hunger, S. P., Pieters, R., Schrappe, M., Biondi, A., Vora, A., Baruchel, A., Silverman, L. B., Schmiegelow, K.*, et al.* (2015). Childhood Acute Lymphoblastic Leukemia: Progress Through Collaboration. Journal of clinical oncology : official journal of the American Society of Clinical Oncology *33*, 2938-2948.

Raaijmakers, M. H. (2011). Niche contributions to oncogenesis: emerging concepts and implications for the hematopoietic system. Haematologica *96*, 1041-1048.

Rabinovich, B. A., Ye, Y., Etto, T., Chen, J. Q., Levitsky, H. I., Overwijk, W. W., Cooper, L. J., Gelovani, J., and Hwu, P. (2008). Visualizing fewer than 10 mouse T cells with an enhanced firefly luciferase in immunocompetent mouse models of cancer. Proceedings of the National Academy of Sciences of the United States of America *105*, 14342-14346.

Rajeshkumar, N. V., Tan, A. C., De Oliveira, E., Womack, C., Wombwell, H., Morgan, S., Warren, M. V., Walker, J., Green, T. P., Jimeno, A.*, et al.* (2009). Antitumor effects and biomarkers of activity of AZD0530, a Src inhibitor, in pancreatic cancer. Clinical cancer research : an official journal of the American Association for Cancer Research *15*, 4138-4146.

Rehe, K., Wilson, K., Bomken, S., Williamson, D., Irving, J., den Boer, M. L., Stanulla, M., Schrappe, M., Hall, A. G., Heidenreich, O., and Vormoor, J. (2013). Acute B lymphoblastic leukaemia-propagating cells are present at high frequency in diverse lymphoblast populations. EMBO molecular medicine *5*, 38-51.

Rettig, M. P., Ansstas, G., and DiPersio, J. F. (2012). Mobilization of hematopoietic stem and progenitor cells using inhibitors of CXCR4 and VLA-4. Leukemia *26*, 34-53.

Reya, T., Morrison, S. J., Clarke, M. F., and Weissman, I. L. (2001). Stem cells, cancer, and cancer stem cells. Nature *414*, 105-111.

Roboz, G. J. (2012). Current treatment of acute myeloid leukemia. Current opinion in oncology *24*, 711-719.

Rosfjord, E., Lucas, J., Li, G., and Gerber, H. P. (2014). Advances in patient-derived tumor xenografts: from target identification to predicting clinical response rates in oncology. Biochemical pharmacology *91*, 135-143.

Saito, Y., Kitamura, H., Hijikata, A., Tomizawa-Murasawa, M., Tanaka, S., Takagi, S., Uchida, N., Suzuki, N., Sone, A., Najima, Y.*, et al.* (2010a). Identification of Therapeutic Targets for Quiescent, Chemotherapy-Resistant Human Leukemia Stem Cells. Science Translational Medicine *2*, 17ra19.

Saito, Y., Uchida, N., Tanaka, S., Suzuki, N., Tomizawa-Murasawa, M., Sone, A., Najima, Y., Takagi, S., Aoki, Y., Wake, A.*, et al.* (2010b). Induction of cell cycle entry eliminates human leukemia stem cells in a mouse model of AML. Nat Biotech *28*, 275-280.

Samuels, A. L., Peeva, V. K., Papa, R. A., Firth, M. J., Francis, R. W., Beesley, A. H., Lock, R. B., and Kees, U. R. (2010). Validation of a mouse xenograft model system for gene expression analysis of human acute lymphoblastic leukaemia. BMC genomics *11*, 256.

Sanchez, P. V., Perry, R. L., Sarry, J. E., Perl, A. E., Murphy, K., Swider, C. R., Bagg, A., Choi, J. K., Biegel, J. A., Danet-Desnoyers, G., and Carroll, M. (2009). A robust xenotransplantation model for acute myeloid leukemia. Leukemia *23*, 2109-2117.

Sarry, J. E., Murphy, K., Perry, R., Sanchez, P. V., Secreto, A., Keefer, C., Swider, C. R., Strzelecki, A. C., Cavelier, C., Recher, C., *et al.* (2011). Human acute myelogenous leukemia stem cells are rare and heterogeneous when assayed in NOD/SCID/IL2Rgammac-deficient mice. The Journal of clinical investigation *121*, 384-395.

Sato, T., Issa, J. J., and Kropf, P. (2017). DNA Hypomethylating Drugs in Cancer Therapy. Cold Spring Harbor perspectives in medicine.

Schacht, R. M. (1980). Two models of population growth. American Anthropologist *82*, 782-798.

Schiffman, J. D. (2016). Applying molecular epidemiology in pediatric leukemia. Journal of investigative medicine : the official publication of the American Federation for Clinical Research *64*, 355-360.

Schillert, A., Trumpp, A., and Sprick, M. R. (2013). Label retaining cells in cancer – The dormant root of evil? Cancer Letters *341*, 73-79.

Schmitz, M., Breithaupt, P., Scheidegger, N., Cario, G., Bonapace, L., Meissner, B., Mirkowska, P., Tchinda, J., Niggli, F. K., Stanulla, M., *et al.* (2011). Xenografts of highly resistant leukemia recapitulate the clonal composition of the leukemogenic compartment. Blood *118*, 1854-1864.

Schrappe, M., Reiter, A., Zimmermann, M., Harbott, J., Ludwig, W. D., Henze, G., Gadner, H., Odenwald, E., and Riehm, H. (2000). Long-term results of four consecutive trials in childhood ALL performed by the ALL-BFM study group from 1981 to 1995. Berlin-Frankfurt-Munster. Leukemia *14*, 2205-2222.

Sharma, V., and McNeill, J. H. (2009). To scale or not to scale: the principles of dose extrapolation. British journal of pharmacology *157*, 907-921.

Shultz, L. D., Lyons, B. L., Burzenski, L. M., Gott, B., Chen, X., Chaleff, S., Kotb, M., Gillies, S. D., King, M., Mangada, J., *et al.* (2005). Human lymphoid and myeloid cell development in NOD/LtSz-scid IL2R gamma null mice engrafted with mobilized human hemopoietic stem cells. Journal of immunology (Baltimore, Md : 1950) *174*, 6477-6489.

Shultz, L. D., Schweitzer, P. A., Christianson, S. W., Gott, B., Schweitzer, I. B., Tennent, B., McKenna, S., Mobraaten, L., Rajan, T. V., Greiner, D. L., and et al. (1995). Multiple defects in innate and adaptive immunologic function in NOD/LtSz-scid mice. Journal of immunology (Baltimore, Md : 1950) *154*, 180-191.

Siegel, R. L., Miller, K. D., and Jemal, A. (2016). Cancer statistics, 2016. CA: a cancer journal for clinicians *66*, 7-30.

Siolas, D., and Hannon, G. J. (2013). Patient-derived tumor xenografts: transforming clinical samples into mouse models. Cancer Res *73*, 5315-5319.

Sison, E. A., Rau, R. E., McIntyre, E., Li, L., Small, D., and Brown, P. (2013). MLL-rearranged acute lymphoblastic leukaemia stem cell interactions with bone marrow stroma promote survival and therapeutic resistance that can be overcome with CXCR4 antagonism. British journal of haematology *160*, 785-797.

Staal, F. J., de Ridder, D., Szczepanski, T., Schonewille, T., van der Linden, E. C., van Wering, E. R., van der Velden, V. H., and van Dongen, J. J. (2010). Genome-wide expression analysis of paired diagnosis-relapse samples in ALL indicates involvement of pathways related to DNA replication, cell cycle and DNA repair, independent of immune phenotype. Leukemia *24*, 491-499.

Sun, T., Jackson, S., Haycock, J. W., and MacNeil, S. (2006). Culture of skin cells in 3D rather than 2D improves their ability to survive exposure to cytotoxic agents. Journal of biotechnology *122*, 372-381.

Suryani, S., Carol, H., Chonghaile, T. N., Frismantas, V., Sarmah, C., High, L., Bornhauser, B., Cowley, M. J., Szymanska, B., Evans, K., *et al.* (2014). Cell and molecular determinants of in vivo efficacy of the BH3 mimetic ABT-263 against pediatric acute lymphoblastic leukemia xenografts. Clinical cancer research : an official journal of the American Association for Cancer Research *20*, 4520-4531.

Tabe, Y., and Konopleva, M. (2014). Advances in understanding the leukaemia microenvironment. British journal of haematology *164*, 767-778.

Takizawa, H., Regoes, R. R., Boddupalli, C. S., Bonhoeffer, S., and Manz, M. G. (2011). Dynamic variation in cycling of hematopoietic stem cells in steady state and inflammation. The Journal of experimental medicine *208*, 273-284.

Tan, B. T., Park, C. Y., Ailles, L. E., and Weissman, I. L. (2006). The cancer stem cell hypothesis: a work in progress. Laboratory investigation; a journal of technical methods and pathology *86*, 1203-1207.

Taussig, D. C., Vargaftig, J., Miraki-Moud, F., Griessinger, E., Sharrock, K., Luke, T., Lillington, D., Oakervee, H., Cavenagh, J., Agrawal, S. G.*, et al.* (2010). Leukemia-initiating cells from some acute myeloid leukemia patients with mutated nucleophosmin reside in the CD34(-) fraction. Blood *115*, 1976-1984.

Terwilliger, T., and Abdul-Hay, M. (2017). Acute lymphoblastic leukemia: a comprehensive review and 2017 update. Blood cancer journal *7*, e577.

Terziyska, N., Alves, C. C., Groiss, V., Schneider, K., Farkasova, K., Ogris, M., Wagner, E., Ehrhardt, H., Brentjens, R. J., zur Stadt, U.*, et al.* (2012). In Vivo Imaging Enables High Resolution Preclinical Trials on Patients' Leukemia Cells Growing in Mice. PloS one *7*, e52798.

Thol, F., Schlenk, R. F., Heuser, M., and Ganser, A. (2015). How I treat refractory and early relapsed acute myeloid leukemia. Blood *126*, 319-327.

Tiedt, S. (2014) Eine seltene und sich langsam teilende Fraktion von Zellen der akuten lymphatischen Leukämie im Knochenmark von NSG-Mäusen ist chemoresistent, Ludwig-Maximilians-Universität München, München.

Townsend, E. C., Murakami, M. A., Christodoulou, A., Christie, A. L., Koster, J., DeSouza, T. A., Morgan, E. A., Kallgren, S. P., Liu, H., Wu, S. C.*, et al.* (2016). The Public Repository of Xenografts Enables Discovery and Randomized Phase II-like Trials in Mice. Cancer cell *29*, 574-586.

Trahair, T. N., Lock, R. B., Sutton, R., Sia, K. C., Evans, K., Richmond, J., Law, T., Venn, N. C., Irving, J. A., Moore, S.*, et al.* (2016). Xenograft-directed personalized therapy for a patient with post-transplant relapse of ALL. Bone marrow transplantation *51*, 1279-1282.

Trumpp, A., Essers, M., and Wilson, A. (2010). Awakening dormant haematopoietic stem cells. Nature reviews Immunology *10*, 201-209.

Ugarte, F., and Forsberg, E. C. (2013). Haematopoietic stem cell niches: new insights inspire new questions. The EMBO journal *32*, 2535-2547.

Vaidya, V. G., and Alexandro, F. J., Jr. (1982). Evaluation of some mathematical models for tumor growth. International journal of bio-medical computing *13*, 19-36.

van der Wath, R. C., Wilson, A., Laurenti, E., Trumpp, A., and Lio, P. (2009). Estimating dormant and active hematopoietic stem cell kinetics through extensive modeling of bromodeoxyuridine label-retaining cell dynamics. PloS one *4*, e6972.

van Dongen, J. J. M., van der Velden, V. H. J., Brüggemann, M., and Orfao, A. (2015). Minimal residual disease diagnostics in acute lymphoblastic leukemia: need for sensitive, fast, and standardized technologies. Blood *125*, 3996-4009.

Viale, A., De Franco, F., Orleth, A., Cambiaghi, V., Giuliani, V., Bossi, D., Ronchini, C., Ronzoni, S., Muradore, I., Monestiroli, S.*, et al.* (2009). Cell-cycle restriction limits DNA damage and maintains self-renewal of leukaemia stem cells. Nature *457*, 51-56.

Vick, B., Rothenberg, M., Sandhofer, N., Carlet, M., Finkenzeller, C., Krupka, C., Grunert, M., Trumpp, A., Corbacioglu, S., Ebinger, M.*, et al.* (2015). An advanced preclinical mouse model for acute myeloid leukemia using patients' cells of various genetic subgroups and in vivo bioluminescence imaging. PloS one *10*, e0120925.

Visvader, J. E., and Lindeman, G. J. (2008). Cancer stem cells in solid tumours: accumulating evidence and unresolved questions. Nature reviews Cancer *8*, 755-768.

Wang, J. C. (2007). Evaluating therapeutic efficacy against cancer stem cells: new challenges posed by a new paradigm. Cell stem cell *1*, 497-501.

Wang, J. C., and Dick, J. E. (2005). Cancer stem cells: lessons from leukemia. Trends Cell Biol *15*, 494-501.

Wang, K., Sanchez-Martin, M., Wang, X., Knapp, K. M., Koche, R., Vu, L., Nahas, M. K., He, J., Hadler, M., Stein, E. M.*, et al.* (2017). Patient-derived xenotransplants can recapitulate the genetic driver landscape of acute leukemias. Leukemia *31*, 151-158.

Welschinger, R., Liedtke, F., Basnett, J., Dela Pena, A., Juarez, J. G., Bradstock, K. F., and Bendall, L. J. (2013). Plerixafor (AMD3100) induces prolonged mobilization of acute lymphoblastic leukemia cells and increases the proportion of cycling cells in the blood in mice. Experimental hematology *41*, 293-302.e291.

Wilson, A., Laurenti, E., Oser, G., van der Wath, R. C., Blanco-Bose, W., Jaworski, M., Offner, S., Dunant, C. F., Eshkind, L., Bockamp, E.*, et al.* (2008). Hematopoietic Stem Cells Reversibly Switch from Dormancy to Self-Renewal during Homeostasis and Repair. Cell *135*, 1118-1129.

Wilson, A., Oser, G. M., Jaworski, M., Blanco-Bose, W. E., Laurenti, E., Adolphe, C., Essers, M. A., Macdonald, H. R., and Trumpp, A. (2007). Dormant and self-renewing hematopoietic stem cells and their niches. Annals of the New York Academy of Sciences *1106*, 64-75.

Wilson, A., and Trumpp, A. (2006). Bone-marrow haematopoietic-stem-cell niches. Nature reviews Immunology *6*, 93-106.

Woiterski, J., Ebinger, M., Witte, K. E., Goecke, B., Heininger, V., Philippek, M., Bonin, M., Schrauder, A., Rottgers, S., Herr, W.*, et al.* (2013). Engraftment of low numbers of pediatric acute lymphoid and myeloid leukemias into NOD/SCID/IL2Rcgammanull mice reflects individual leukemogenecity and highly correlates with clinical outcome. International journal of cancer *133*, 1547-1556.

Wu, M. H., Huang, S. B., and Lee, G. B. (2010). Microfluidic cell culture systems for drug research. Lab on a chip *10*, 939-956.

Yoshihara, H., Arai, F., Hosokawa, K., Hagiwara, T., Takubo, K., Nakamura, Y., Gomei, Y., Iwasaki, H., Matsuoka, S., Miyamoto, K.*, et al.* (2007). Thrombopoietin/MPL signaling regulates hematopoietic stem cell quiescence and interaction with the osteoblastic niche. Cell stem cell *1*, 685-697.

Zeng, Z., Shi, Y. X., Samudio, I. J., Wang, R. Y., Ling, X., Frolova, O., Levis, M., Rubin, J. B., Negrin, R. R., Estey, E. H.*, et al.* (2009). Targeting the leukemia microenvironment by CXCR4 inhibition overcomes resistance to kinase inhibitors and chemotherapy in AML. Blood *113*, 6215-6224.

Zhang, J., Ding, L., Holmfeldt, L., Wu, G., Heatley, S. L., Payne-Turner, D., Easton, J., Chen, X., Wang, J., Rusch, M.*, et al.* (2012). The genetic basis of early T-cell precursor acute lymphoblastic leukaemia. Nature *481*, 157-163.

Zhou, B.-B. S., Zhang, H., Damelin, M., Geles, K. G., Grindley, J. C., and Dirks, P. B. (2009). Tumour-initiating cells: challenges and opportunities for anticancer drug discovery. Nature reviews Drug discovery *8*, 806-823.

Zufferey, R., Donello, J. E., Trono, D., and Hope, T. J. (1999). Woodchuck hepatitis virus posttranscriptional regulatory element enhances expression of transgenes delivered by retroviral vectors. Journal of virology *73*, 2886-2892.

8 Appendix

8.1 Supplementary data

Table S 1, related to Table 5: Clinical data of AML patients and sample characteristics

sample	ELN classification	disease stage*	age* [years]	sex	cytogenetics	xeno-graft established in	passaging time§ [days]	transgenic for
AML-346	adverse	1st relapse	1	f	complex karyotype	Tübingen	47	mCherry, luciferase, NGFR
AML-356	not available	1st relapse	5	m	not determined	Tübingen	40	-
AML-358	not available	2st relapse	9	m	not determined	Tübingen	68	-
AML-361	intermediate I (CN, mutated NPM1 and FLT3-ITD)	initial diagnosis	40	f	normal karyotype	our lab	55	-
AML-372	adverse (complex karyotype)	1st relapse	42	m	complex karyotype	our lab	87	mCherry, luciferase, NGFR
AML-388	adverse (MLL rearranged)	initial diagnosis	57	m	not determined	our lab	43	mCherry, luciferase

*when the primary AML sample was obtained; §time of passaging through mice refers to the time from injection of the sample until mice had to be sacrificed due to end stage leukemia; ELN = European Leukemia Net; MLL = mixed lineage leukemia; CN = cytogenetically normal; f = female; m = male

Table S 1 continued

sample	ELN classification	disease stage*	age* [years]	sex	cytogenetics	xeno-graft established in	passaging time§ [days]	transgenic for
AML-393	adverse (MLL rearranged)	1st relapse	47	f	46, XX, ins(10;11) (p12;q23q23) MLL-AF10	our lab	39	mCherry, luciferase
AML-415	intermediate I (CN, mutated NPM1 and FLT3-ITD)	2nd relapse	69	f	normal karyotype	our lab	116	-
AML-491	cytogenetic abnormalities not classified as favorable or adverse	1st relapse	53	f	46, XX, del(7) (q21)	our lab	47	mCherry, luciferase
AML-538	not available	1st relapse	68	f	not determined	our lab	88	-
AML-579	intermediate I (CN, mutated NPM1 and FLT3-ITD)	initial diagnosis	51	m	normal karyotype	our lab	98	mCherry, luciferase

Table S 2, related to Table 6: Clinical data of ALL patients and sample characteristics

sample	type of ALL	disease stage*	age* [years]	sex	cyto-genetics	xeno-graft estab-lished in	passag-ing time§ [days]	trans-genic for
ALL-50	BCP-ALL pediatric	initial diagno-sis	7	f	BCR/ABL positive	our lab	45	mCherry, luciferase
ALL-177	BCP-ALL pediatric	initial diagno-sis	8	f	TEL/AML1 positive	our lab	130	-
ALL-199	BCP-ALL pediatric	2nd relapse	8	f	somatic trisomy 21; leukemic homo-zygous 9p deletion	our lab	42	mCherry, luciferase, NGFR
ALL-230	T-ALL pediatric	initial diagno-sis	4	m	t(11;14)(p32; q11); rearrange-ment of TAL1-gene with the T-cell receptor locus	our lab	35	-
ALL-256	BCP-ALL adult	initial diagno-sis	41	f	trisomy 8; BCR/ABL positive t(9;22)(q34;q 11)	Rostock	75	-
ALL-265	BCP-ALL pediatric	1st relapse	5	f	hyperploidy with additional 6, 13, 14, 17, 18, 21, X chromo-some	Zürich	30	mCherry, luciferase, NGFR
ALL-363	BCP-ALL adult	initial diagno-sis	65	m	BCR-ABL positive t(9;22)(q34,q 11)	our lab	60	-
ALL-435	BCP-ALL pediatric	initial diagno-sis	<1	m	MLL-ENL, t(11;19)	Hamburg	40	mCherry, luciferase

*when the primary ALL sample was obtained; §time of passaging through mice refers to the time from injection of the sample until mice had to be sacrificed due to end stage leukemia; BCP = B-cell precursor; f = female; m = male;

Table S 3, related to Figure 23: LRC and non-LRC harbor similar numbers of leukemia initiating cells

cell type	AML-393				AML-491			
	injected cells	number of mice	engrafted mice	LIC frequency	injected cells	number of mice	engrafted mice	LIC frequency
non-LRC	2885	1	1		2000	1	1	
	1000	1	1		600	1	0	
	300	2	2	1/127	-	-	-	1/1364
	100	3	1		-	-	-	
	30	3	1		-	-	-	
LRC	900	2	2		2000	1	1	
	300	3	2		600	2	1	
	100	2	2	1/172	200	1	0	1/853
	30	3	0		-	-	-	

8.2 Acknowledgment

First I like to special thank *Prof. Dr. Irmela Jeremias* for giving me the opportunity to perform my PhD thesis in her lab and her supervision of my PhD project. Thank you for all your support and assistance with my projects, for all the good inspiration and advises, for your belief and trust in me, and for all the things I learned during my time in the lab and especially from you.

I am very thankful to *Prof. Dr. Dirk Eick* for the official supervision of my PhD thesis and his interest in my projects. Thank you for your scientific support, the helpful discussions about my projects, and for all the support, advice and ideas for writing my PhD thesis.

A big thank you to my Thesis Advice Committee, including *Prof. Dr. Dirk Eick, Prof. Dr. Olivier Gires, PD Dr. Ursula Zimber-Strobl,* and *Prof. Dr. Irmela Jeremias* for the productive discussion rounds about my projects in a friendly atmosphere, for the input, ideas, and all the inspiriting advice and confidence regarding our data and publication.

A special thank you goes to my PhD collaborating partner *Erbey Özdemir*. Thank you so much for being so uncomplicated and reliable, for the good and successful teamwork, and for all the nice and funny work together!

I thank my *whole working group* "*Jeremias"*, all current and alumni members. For their introduction and teaching in all techniques, and for the friendly and great working atmosphere. A special thanks to all the TAs for all the help with the mice work, without your support the complex experiments for the present study would not have been possible! I am very grateful of all the help especially from *Maike Fritschle* and *Fabian Klein*. Thank you *Dr. Binje Vick* for answering all questions, your help, ideas, and the review of my thesis! I thank *Dr. Catarina Castro-Alves* for her support, helpful input, and her scientific and human advises. Thank you all for being great colleagues, becoming new friends, and for all the great time spending together in the lab and during free time!

Thanks to all members of the animal facility for taking care and pay attention of my mice.

And finally I thank my family for all the distraction during free time and their motivation, support, and admirations for what I do.

8.3 Publications

Sarah Ebinger, Erbey Ziya Özdemir, Christoph Ziegenhain, Sebastian Tiedt, Catarina Castro Alves, Michaela Grunert, Michael Dworzak, Christoph Lutz, Virginia A. Turati, Tariq Enver, Hans-Peter Horny, Karl Sotlar, Swati Parekh, Karsten Spiekermann, Wolfgang Hiddemann, Aloys Schepers, Bernhard Polzer, Stefan Kirsch, Martin Hoffmann, Bettina Knapp, Jan Hasenauer, Heike Pfeifer, Renate Panzer-Grümayer, Wolfgang Enard, Olivier Gires, Irmela Jeremias (2016) „Characterization of Rare, Dormant, and Therapy-Resistant Cells in Acute Lymphoblastic Leukemia"
Cancer Cell 30.6, 849-862;http://dx.doi.org/10.1016/j.ccell.2016.11.002

Sarah Ebinger, Binje Vick, Christina Zeller, Karsten Spiekermann, Wolfgang Hiddemann, Irmela Jeremias „Patients' AML stem cells growing in mice display heterogeneous proliferation features"
Manuscript in preparation